

63-3-4

404 488

AFOSR 2981

404488

CORNELL UNIVERSITY



GRADUATE SCHOOL OF AEROSPACE ENGINEERING

STAGNATION POINT OF FLOW OF A VARIABLE
PROPERTY FLUID AT LOW REYNOLDS NUMBERS

by

Michael Lenard

JUNE, 1962

Ithaca, New York

STAGNATION POINT FLOW OF A VARIABLE PROPERTY FLUID
AT LOW REYNOLDS NUMBERS

Michael Lenard

Submitted to the Office of Scientific
Research of the Air Research and
Development Command, in partial
fulfillment of contract number
AF 49(638)-544.


W. R. Sears

BIBLIOGRAPHICAL CONTROL SHEET

1. Originating agency and/or monitoring agency
O.A.: Graduate School of Aerospace Engineering, Cornell University,
Ithaca, New York
M.A.: Mechanics Division, Office of Scientific Research
2. Originating agency and/or monitoring agency report number
O.A.: None
M.A.: AFOSR 2981
3. Title and classification of title: "Stagnation Point Flow of a Variable
Property Fluid at Low Reynolds Numbers" (Unclassified)
4. Personal author: Michael Lenard
5. Date of Report: June, 1962
6. Pages: 170
7. Illustrative Material: Figures and Tables included in text
8. Prepared for Contract No: AF 49(638)-544
9. Prepared for Project Code and/or No: None
10. Security Classification: Unclassified
11. Distribution limitations: None
12. Abstract: See page 1.

FOREWORD

The present report is a part of the research program on boundary layer problems being pursued at the Graduate School of Aeronautical Engineering under the provisions of contract AF 49(638)-544. This contract is financed by the United States Air Force Office of Scientific Research and is monitored by the Mechanics Division. The intent of this investigation has been to cast light on some details of boundary layer flow at stagnation points in flow of air at high speeds.

This investigation was proposed by Professor Nicholas Rott and the investigator, Mr. Lenard, has worked under the direction of Professor Rott and Professor S. H. Lam. The research carried out under this contract is under the general direction of Professor W. R. Sears, Director of the School.

ERRATA.

P. 16, Equation (1.23):

Add factor of $(1+n)$ on right-hand side of equation, viz.:

$$V = -A(1+n) y \left[1 + \left(\frac{nV}{2} - \frac{n+3}{2R} \right) y + \dots \right]$$

P. 21, Equation (2.8):

6th line; omit R^2 in denominator of 1st and 2nd terms; change R^2 to R in denominator of 3rd and 5th terms:

$$-\frac{\Psi_{xx}\mu_x}{(1+\frac{x}{R})^2} + \frac{\Psi_{xx}\mu_x}{(1+\frac{x}{R})^2} \frac{s_x}{S} + \frac{n \cos \frac{x}{R}}{R \sin \frac{x}{R}} \frac{\Psi_{xx}\mu}{(1+\frac{x}{R})^2} - \frac{n \cos \frac{x}{R}}{R^2 (\sin \frac{x}{R})^2} \frac{\Psi_{xx}\mu}{(1+\frac{x}{R})^2} - \frac{n \cos \frac{x}{R}}{R \sin \frac{x}{R}} \frac{\Psi_{xx}\mu}{(1+\frac{x}{R})^2} \frac{s_x}{S}$$

7th line; omit R^2 in denominator of 1st, 2nd, 4th and 5th terms, viz.:

$$-\frac{\Psi_{xxx}\mu}{(1+\frac{x}{R})^2} + \frac{2\Psi_{xxx}\mu}{(1+\frac{x}{R})^2} \frac{s_x}{S} - \frac{n}{R^2} \frac{\Psi_{xx}\mu}{(1+\frac{x}{R})^2} + \frac{\Psi_{xx}\mu}{(1+\frac{x}{R})^2} \frac{s_{xx}}{S} - \frac{2\Psi_{xx}\mu}{(1+\frac{x}{R})^2} \left(\frac{s_x}{S} \right)^2 - \Psi_{xyy}\mu +$$

8th line; change density derivative in last term:

$$+ \frac{n-1}{R} \frac{\Psi_{xyy}\mu}{1+\frac{x}{R}} + \Psi_{yy}\mu \frac{s_x}{S} + \Psi_{xy}\mu \frac{s_y}{S} + \Psi_y\mu \frac{s_{xy}}{S} \}$$

P. 22, Equation (2.13):

2nd line; change 2nd term from x to y derivative:

$$-\Psi_y^2 \frac{s_x}{S} + \Psi_y \Psi_{xy} - \frac{n \cos \frac{x}{R}}{R \sin \frac{x}{R}} \Psi_y^2 \} + \frac{S P_x}{1+\frac{x}{R}} =$$

P. 65, 4th line from bottom:

Insert j , viz.:

..... terms with the j subscript

P. 65, 2nd line from bottom:

Insert K_1 and K_2 , viz.:

..... of proportionality K_1 and K_2 . The

P. 95, Equation (F.11):

In right-hand side of 2nd and 3rd expressions, replace h (enthalpy) by μ (viscosity), viz.:

$$f_1'(0) = K_1 \frac{AR}{\sqrt{RT_s}} \frac{\mu_w}{\mu_s} \sqrt{W} f_0''(0)$$

$$f_{h_1}(0) = K_2 \frac{AR}{\sqrt{RT_s}} \frac{\mu_w}{\mu_s} \sqrt{W} f_{h_1}'(0)$$

P. 95, Equation (F.12):

Last line refers to function f_{1c}' , viz.:

$$\eta \rightarrow \infty \quad f_{1c}'(\eta) \rightarrow (n-1)\eta$$

P. 103, Equation (H.2):

Re on right-hand side has subscript 1, viz.:

$$\dots\dots\dots = \frac{\hat{U}_c'(0) Re_1}{4} (1 + 2 M_{\text{max}}^2)^{1.7}$$

P. 105. In line above equation (H.7), reference is made to (H.3) instead of (h.3), viz.:

(H.3), are presented

P. 108. In definition of τ , replace h and v by μ and U , viz.:

$$\tau \quad \text{shear parallel to surface} \quad \tau = \mu \frac{\partial U}{\partial y}$$

ABSTRACT

Steady, viscous, two-dimensional and axially symmetric stagnation-point flows of a gas are considered for the case when the Reynolds number is too low for the applicability of the classical boundary-layer theory. It is assumed that the low-density gas is still a continuous fluid, permitting the use of the Navier-Stokes and associated equations as the basis of the problem. The effects of low Reynolds number are determined by applying an expansion procedure (similar to Lagerstrom and Cole's⁽²⁰⁾) in terms of a parameter, essentially $1/\sqrt{Re}$, to the fluid-dynamical equations. The highest-order equations in this expansion are the boundary-layer equations; the next-order equations, which therefore involve first-order low-Reynolds-number correction terms to the boundary-layer quantities, are presented and discussed in detail, together with the appropriate boundary conditions. The boundary conditions are of two types; at the wall they are derived from the kinetic theory of gases, far from the wall the flow must "merge" into the inviscid solution.

It is shown that the following quantities are necessary to define the inviscid flow near the stagnation point: the stagnation properties of the gas, a velocity gradient, a nose radius, and a vorticity parameter. The latter is present in the axially symmetric case only; it defines the slope of the inviscid shear flow near the stagnation point of the axially symmetric body. It is shown that further generalization of the inviscid flow by considering additional

parameters necessary to define the flow over larger regions in the vicinity of the stagnation point is not necessary, because any additional parameters will not affect the first-order corrections considered in the analysis of the viscous flow.

The result of the analysis is that the following correction effects to boundary-layer theory are defined: curvature effect, displacement effect, velocity slip and temperature-jump effect, vorticity effect (this last one for the axially symmetric case only). The magnitude of these effects depends on the following parameters, respectively: the ratio of the boundary-layer thickness to nose radius, the change in stagnation-point velocity gradient from the inviscid value due to the displacement effect of the boundary layer around the body, the ratio of the mean free path to the boundary-layer thickness, and finally the ratio of the slope of the inviscid shear-flow profile (in axially symmetric flow only) to the average slope of the boundary-layer velocity profile.

Some applications are discussed, in particular the case of a blunt body flying through the atmosphere is considered in detail. Real-gas properties are used to calculate the expansion parameters for this case; the results are plotted in chart form. The region of best applicability of the expansion procedure is where the expansion parameters are less than 1 and are about the same order of magnitude. This occurs in the flight-speed range of Mach 2 to 7.

Numerical solutions of the equations are then presented using the properties of undissociated air corresponding to this speed range (perfect gas, constant Prandtl number, variation of specific heat, viscosity, heat conductivity with powers of absolute temperature).

Results are tabulated for five values of wall-to-free-stream temperature ratio; examples of low-Reynolds-number velocity and temperature profiles are given. The effect of temperature ratio on wall shear and wall heat-transfer rates are shown in both table and graph forms. The behavior of the shear and heat-transfer corrections due to velocity slip and temperature jump is especially significant; the results clearly indicate that, in spite of the much smaller mean free path at the wall for strongly cooled boundary layers, the reduction in heat transfer due to this effect is determined by the mean free path in the (hot) inviscid flow at the stagnation point. This conclusion is the result of including the effects of variable fluid properties in the analysis.

The predicted stagnation-point heat-transfer reductions for a cylinder in a supersonic airstream at low Reynolds numbers are compared to the experimental results of Tewfik and Giedt^{(40), (41)}. Both theory and experiment indicate reductions in heat transfer at low Reynolds numbers; but the measured reductions, while agreeing in trend, are considerably larger than the predictions.

INTRODUCTION

The flow in the vicinity of forward stagnation points has long been of special interest to aerodynamicists. The reasons for this interest are both theoretical and practical. Theoretically, the flow impinging on an "infinite" flat plate provides one of the few exact solutions of the Navier-Stokes equations; furthermore the solution of boundary-layer flow around bodies always "begins" at the stagnation point. Practically, heat-transfer rates are usually at a maximum in the stagnation region; furthermore, stagnation properties of the flow are often the easiest to measure by means of various probes and measuring instruments. In addition, in recent times, the reentry problem has generated renewed interest in this problem, especially in the low-Reynolds-Number flow regime. The purpose of the present investigation is to reexamine this problem in this low-Reynolds-number flow regime for the steady-flow case and for the plane two-dimensional and axially symmetric flow patterns; due to their similarities a unified treatment of the two types of flow will be possible.

Implicit in the aerodynamicist's solution of flow problems is the assumption of a continuous fluid. The classical equations of Navier-Stokes, together with the continuity and energy equations, and additional equations, which relate the thermodynamic and transport properties of the fluid, form the basis of continuum aerodynamics. This approach will be maintained in the present investigation; though it must be duly noted that it imposes a very definite limitation on the applicability of the results on gases (which are principally of interest) in terms of a Knudsen number, which cannot exceed a "reasonably small" value. What this limitation means can be inferred from the kinetic

theory of gases. It is well known that the properties of a fluid flow field for a gas can be obtained if the (molecular) velocity distribution function is given, by taking the appropriate statistical averages. Solutions of the Maxwell-Boltzmann equation, which is the conservation equation for this distribution function, can be obtained in terms of an iteration procedure, which results in successive sets of "continuum" differential equations; i.e., equations in terms of the "locally average" quantities. It has been pointed out by a number of authors (e.g. Sherman⁽³⁹⁾, Schaaf and Chambre⁽³⁶⁾, etc.) that this iteration procedure is roughly equivalent to an expansion in terms of the mean free path between molecules. The successive sets of equations are: Euler's (inviscid) equations, the Navier-Stokes and associated equations (which will be used in the present work), the Burnett equations, and equations of still higher order. It can be seen then that the present analysis neglects the Burnett and higher-order terms, which implies that only "small" changes in local flow quantities are permissible over distances equal to the mean free path. Actually it has been found (Schaaf and Chambre⁽³⁶⁾) that even for some specially simple and well understood problems in gasdynamics, such as the structure of normal shocks and the propagation of high-frequency sound waves, where the Burnett terms were clearly non-negligible, their inclusion in the theory gave less satisfactory agreement with experimental results than the theory based on the Navier-Stokes equations only. Furthermore, the Burnett terms include derivatives of higher order than are present in the Navier-Stokes equations, which indicates the necessity for additional boundary conditions. There is no agreement at the present as to what, if any, these additional boundary conditions should be. A

more detailed discussion of these and other difficulties involved in the use of the Burnett equations can be found in reference 36.

The present work is then an application of the Navier-Stokes equations to the stagnation-point problem for a gas with known thermodynamic and transport properties. A perfect gas will be assumed, with the specific heat, viscosity, and heat conductivity proportional to arbitrary powers of the absolute temperature. (These assumptions regarding the properties of the gas will be justified in another section.) The classical solution of this problem for very large Reynolds numbers has two phases: first, the solution of the inviscid-flow problem with slip around a given body is obtained; this gives the location of the stagnation point and the velocity gradient there. The second phase completes the calculation of the flow by applying these results to the well known solutions of the stagnation-point boundary-layer equations in the two-dimensional and axially symmetric cases respectively (e.g. Cohen and Reshotko⁽⁵⁾, Brown and Donoughe⁽³⁾, Howe and Mersman⁽¹⁶⁾, etc.). It is shown by Lagerstrom and Cole⁽²⁰⁾ that these two steps can be looked upon as the first steps in an expansion procedure for obtaining approximations to the solution of the Navier-Stokes equations for high Reynolds numbers. This procedure consists of expanding the stream function in powers of a Reynolds-number parameter, (in this case $\frac{1}{\sqrt{Re}}$) in terms of two parallel series, the so-called "inner" and "outer" expansions. Successive terms in the two series are solved for alternately. In this manner first the inviscid flow around the body is obtained (the first term in the "outer" expansion), then the complete boundary-layer problem solved (the first term in the inner expansion), then a correction to the external-flow follows (usually due only to the

displacement effect of the boundary layer); and then a correction to the boundary-layer solution, etc. It is apparent from physical considerations that the formal mathematical procedure developed in this reference is rigorously applicable only to certain very special types of problems. It entirely fails to account for such universally present phenomena as turbulence, and the possibility of separation, for example.

In the following, a treatment of this second approximation to the "inner" flow for these two types of stagnation-point flows is presented. The formal mathematical procedure of reference 20 will not be followed; still the above comments indicate that a complete treatment of this second approximation, which is essentially an improvement of boundary-layer theory for low Reynolds numbers, would require a solution of the second approximation to the "outer" flow. This implies that in addition to a superimposed external velocity gradient of arbitrary magnitude (which is the result of the solution of the first approximation to the "outer" flow, i.e., the inviscid flow) one should have an additional arbitrary external-flow parameter, which influences the second "inner"-flow approximation, and which should properly be the result of calculating the improvement to the outer flow due to the displacement effect of the boundary layer. Obviously such a calculation cannot be made within the framework of calculating the flow at the stagnation point only. Thus one has to accept the presence of an additional arbitrary parameter in the problem, due to an undetermined "displacement" effect.

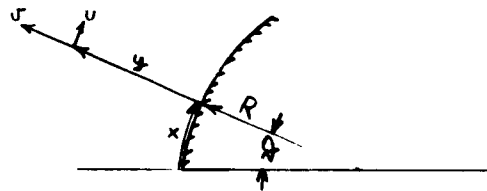
CHAPTER I

Inviscid Flow near the Stagnation Point

Let R be the radius of curvature of the body near the stagnation point. Then the "polar" coordinate system of Appendix A (A.6) can be transformed into the conventional boundary-layer coordinate system by the transformation:

$$\begin{aligned} y &= r - R \\ x &= R\theta \end{aligned} \tag{1.1}$$

where $y = 0$ defines the body contour, as shown in the sketch.



Using transformation (1.1) in (A.8) and (A.9) the inviscid momentum equations can now be written down. In the y direction;

$$\begin{aligned} & \frac{1}{(1 + \frac{y}{R})^{2n}} \frac{1}{R^{2n} (\sin \frac{x}{R})^{2n}} \left\{ \frac{1}{(1 + \frac{y}{R})^2} \psi_y \psi_x \frac{s_x}{s} - \frac{1}{1 + \frac{y}{R}} \frac{\psi_y^2}{R} - \frac{1}{(1 + \frac{y}{R})^2} \psi_y \psi_{xx} + \right. \\ & + \frac{n \cos \frac{x}{R}}{\sin \frac{x}{R}} \frac{1}{(1 + \frac{y}{R})^2} \frac{\psi_y \psi_x}{R} - \frac{1}{(1 + \frac{y}{R})^2} \psi_x^2 \frac{s_y}{s} + \frac{1}{(1 + \frac{y}{R})^2} \psi_x \psi_{xy} - \\ & \left. - \frac{1+n}{(1 + \frac{y}{R})^3} \frac{\psi_x^2}{R} \right\} + s p_y = 0 \end{aligned} \tag{1.2}$$

Similarly, in the x direction

$$\frac{1}{(1+\frac{\gamma}{R})^{2n} R^{2n} (\sin \frac{\alpha}{R})^{2n}} \left\{ \Psi_y \Psi_y \frac{g_y}{g} + \frac{n-1}{1+\frac{\gamma}{R}} \frac{\Psi_x \Psi_y}{R} - \Psi_x \Psi_{yy} - \right. \\ \left. - \Psi_y^2 \frac{g_x}{g} + \Psi_x \Psi_{xy} - \frac{n \cos \frac{\alpha}{R}}{\sin \frac{\alpha}{R}} \frac{\Psi_y^2}{R} \right\} + g P_x = 0 \quad (1.3)$$

The velocities can be related to the compressible stream function by using (A.6) and (1.1) in (A.3):

$$u = \frac{1}{(1+\frac{\gamma}{R})^n R^n (\sin \frac{\alpha}{R})^n} \frac{\Psi_y}{g} \\ v = -\frac{1}{(1+\frac{\gamma}{R})^{1+n} R^n (\sin \frac{\alpha}{R})^n} \frac{\Psi_x}{g} \quad (1.4)$$

Since flow in the free stream is uniform, and the flow is steady, the "iso-energeticity" condition can be written as:

$$\frac{u^2 + v^2}{2} + h - h_s = \frac{\Psi_y^2 + \frac{1}{(1+\frac{\gamma}{R})^2} \Psi_x^2}{2 g^2 (1+\frac{\gamma}{R})^{2n} R^{2n} (\sin \frac{\alpha}{R})^{2n}} + h - h_s = 0 \quad (1.5)$$

where the subscript s refers to stagnation conditions. For the assumption of temperature-dependent specific heat the enthalpy can be expanded about the stagnation condition in a Taylor series, as follows:

$$h - h_s = c_{p_s} (T - T_s) + \dot{c}_{p_s} \frac{(T - T_s)^2}{2} + \ddot{c}_{p_s} \frac{(T - T_s)^3}{6} + \dots \quad (1.6)$$

where the dots signify derivatives with respect to temperature.

The symmetry of the problem, and the boundary condition that $\psi = 0$ on the body $y = 0$ can be used to write down the following expansions for the various quantities:

$$\psi = \rho_s A x^{1+n} [y + a_1 y^2 + a_2 y^3 + \dots + b_1 x^2 y + b_2 x^2 y^2 + \dots]$$

$$\rho = \rho_s [1 + a_{r1} y + a_{r2} y^2 + \dots + b_{r1} x^2 + b_{r2} x^2 y + \dots]$$

$$T = T_s [1 + a_{T1} y + a_{T2} y^2 + \dots + b_{T1} x^2 + b_{T2} x^2 y + \dots]$$

$$p = p_s [1 + a_{p1} y + a_{p2} y^2 + \dots + b_{p1} x^2 + b_{p2} x^2 y + \dots]$$

(1.7)

The perfect-gas law can be used to relate the pressure, density, and temperature expansions:

$$\frac{p_s}{\rho_s} = \rho_s T_s$$

$$a_{p1} = a_{T1} + a_{r1}$$

$$a_{p2} = a_{T2} + a_{r2} + a_{T1} a_{r1}$$

$$b_{p1} = b_{r1} + b_{T1}$$

$$b_{p2} = b_{r2} + b_{T2} + a_{r1} b_{T1} + a_{T1} b_{r1}$$

(1.8)

Now expansions (1.6) and (1.7) will be substituted into equations (1.2), (1.3), and (1.5). Coefficients of like powers of the independent variables will then be equated, giving a succession of additional relations, similar to (1.8). The results of this procedure will be that many of the coefficients in expansions (1.7) will be expressed in terms of a smaller number of independent ones. This will show the truly significant independent parameters necessary to describe the inviscid stagnation-point flow that we are considering. The details of the procedure follow. Substituting the expansions (1.6) and (1.7) into the energy equation (1.5), coefficients of the y term give:

$$2 g_s^2 c_p T_s a_{T1} = 0$$

thus

$$a_{T1} = 0 \quad (1.9)$$

Using this result, the x^2 , y^2 , and $x^2 y$ terms give:

$$g_s^2 A^2 + 2 g_s^2 c_p T_s k_{T1} = 0$$

$$(1+n)^2 g_s^2 A^2 + 2 g_s^2 c_p T_s a_{T2} = 0$$

$$-\frac{2n}{R} g_s^2 A^2 + 4 g_s^2 A^2 a_1 + 4 g_s^2 c_p T_s k_{T1} a_{r1} + 2 g_s^2 c_p T_s k_{T2} = 0$$

from which

$$k_{T1} = -\frac{A^2}{2 c_p T_s} \quad (1.10)$$

$$a_{T2} = -\frac{(1+n)^2 A^2}{2 \rho_s T_s} \quad (1.11)$$

$$\frac{n}{\epsilon R} a_1 = -\frac{a_{r1}}{2} + \frac{\rho_s T_s}{2 A^2} b_{T2} \quad (1.12)$$

A similar substitution into the y momentum equation (1.2), and grouping coefficients of the constant, x , and x^2 terms gives:

$$S_s P_s a_{p1} = 0$$

$$(1+n)^2 A^2 S_s^2 + 2 S_s P_s a_{p2} + S_s P_s a_{r1} a_{p1} = 0$$

$$-\frac{S_s^2 A^2}{R} + S_s P_s (b_{p2} + b_{r1} a_{p1}) = 0$$

from which

$$a_{p1} = 0 \quad (1.13)$$

$$a_{p2} = -S_s \frac{A^2 (1+n)^2}{2 P_s} \quad (1.14)$$

$$b_{p2} = \frac{S_s A^2}{P_s R} \quad (1.15)$$

Finally the x momentum equation (1.3) is used in a similar way, grouping coefficients of the constant and y terms:

$$\frac{S_s^2 A^2}{2} + S_s P_s b_{p1} = 0$$

$$S_s^2 A^2 \left[(1+n) a_{r1} + \frac{n-1}{R} - 2(1+n) a_1 + 4a_1 - \frac{2n}{R} \right] + 2 P_s S_s [b_{r1} a_{r1} + b_{r2}] = 0$$

hence,

$$b_{r1} = - \frac{\rho_s A^2}{2 \rho_s} \quad (1.16)$$

Now use (1.8) together with (1.9), (1.10), (1.11), (1.13), (1.14), and (1.16) to get:

$$a_{r1} = 0$$

$$a_{r2} = - \frac{A^2}{2 \rho_s T_s} (1+n)^2 \frac{\rho_s - R}{R}$$

$$b_{r1} = - \frac{A^2}{2 \rho_s T_s} \frac{\rho_s - R}{R} \quad (1.17)$$

These results make it possible to determine the coefficient of the second term in the expansion for the stream function, a_1 :

$$\rho_s^2 A^2 \left[2(1-n)a_1 + \frac{n^2 - 2n - 1}{R} + \frac{2}{R} \right] = \rho_s^2 A^2 (1-n) \left[2a_1 + \frac{1-n}{R} \right] = 0$$

Thus:

$$\text{for } n=0 \quad a_1 = - \frac{1}{2R}$$

$$\text{for } n=1 \quad a_1 \text{ is arbitrary}$$

An expression for the vorticity near the stagnation point can be found by using (1.1) in (A.13):

$$\begin{aligned} \Omega = & - \frac{1}{\rho_s^2 R^n \left(1 + \frac{r}{R}\right)^n \left(\sin \frac{\theta}{R}\right)^n} \left[\Psi_{,2} \rho_{,2} + \frac{\Psi_{,n} \rho_{,n}}{\left(1 + \frac{r}{R}\right)^2} - \frac{\rho_{,n} \Psi_{,n}}{\left(1 + \frac{r}{R}\right)^2} + \right. \\ & \left. + \frac{n \cos \frac{\theta}{R}}{\left(1 + \frac{r}{R}\right)^2 R \sin \frac{\theta}{R}} \rho_{,n} \Psi_{,n} + \rho_{,2} \Psi_{,2} + (1-n) \frac{\rho_{,2}}{R \left(1 + \frac{r}{R}\right)} \right] \end{aligned} \quad (1.18)$$

Substituting expansion (1.7) into (1.18) the expression for the vorticity is:

$$\Omega = -A \times \left[2a_1 + \frac{1-n}{R} \right] + \dots$$

Thus, for the two types of stagnation-point flow:

$$\text{for } n = 0 \quad \Omega = \sigma(x, y)$$

$$\text{for } n = 1 \quad \Omega = -A \times [2a_1 + \sigma(x, y)] = -A \times [V + \dots]$$

(1.19)

where the above expression defines a vorticity parameter V .

Coefficient a_1 can then be written as

$$a_1 = \frac{n-1}{2R} + \frac{nV}{2} \quad (1.20)$$

This result can now be used, together with (1.8), (1.12), (1.15) and (1.17) to determine

$$k_{Tz} = -\frac{A^2}{\rho_s T_s} \left[nV - \frac{1}{R} \right]$$

$$k_{rz} = \frac{A^2}{\rho_s T_s} \left[nV + \frac{1}{R} \frac{\rho_s - \rho}{\rho} \right] \quad (1.21)$$

The above intermediate results can be summarized by writing expansions (1.7), using the derived values of the coefficients:

$$\psi = g_s A x^{1+n} \left[\frac{y}{2} + \left(\frac{n-1}{R} + nV \right) \frac{y^2}{2} + \dots \right] \quad (1.22)$$

$$g = g_s - \frac{g_s A^2}{c_p T_s} \left[\frac{c_p - R}{R} (1+n)^2 \frac{y^2}{2} + \frac{c_p - R}{R} \frac{x^2}{2} - \left(\frac{c_p - R}{R} + nV \right) x^2 y + \dots \right] \quad (1.23)$$

$$T = T_s - \frac{A^2}{c_p} \left[(1+n)^2 \frac{y^2}{2} + \frac{x^2}{2} - \left(\frac{1}{R} - nV \right) x^2 y + \dots \right] \quad (1.24)$$

$$p = p_s - g_s A^2 \left[(1+n)^2 \frac{y^2}{2} + \frac{x^2}{2} - \frac{x^2 y}{R} + \dots \right] \quad (1.25)$$

From these expressions the parameters for the symmetrical inviscid stagnation-point flow can be ascertained. Velocity gradient A is a fundamental parameter; it is determined by solving the inviscid flow around the entire body. It will be of the order of magnitude of free-stream velocity, U , divided by a "significant body size," L , perpendicular to the flow direction. Two more parameters appear in the stream function; nose radius R , and vorticity parameter V . It has been pointed out previously (e.g. Rott and Leonard⁽³⁵⁾) that there is an important difference in this respect between two-dimensional and axially symmetric stagnation-point flows; the latter admitting a vortical term but showing no effect of nose curvature to the order of terms that are considered here (i.e., y^2), whereas the two-dimensional flow is irrotational, but has a curvature term. Stagnation thermodynamic properties, p_s , g_s , T_s , and c_p are the additional arbitrary parameters. Had

subsequent terms in the expansion (i.e., higher-order terms in x^2 and y than included in (1.22) through (1.25)) been considered, additional parameters would have appeared. These parameters will be arbitrary, or identifiable as the rate of change of the nose radius with x^2 , etc. The possible effect such additional arbitrary parameters may have on the viscous flow near the stagnation point will be discussed in the latter part of Chapter II.

As expected, the expansions for the thermodynamic properties exhibit Crocco's relation. On the stagnation streamline the flow is isentropic; isentropicity is maintained off the stagnation streamline also, with the exception of the rotational term ∇ . The pressure term shows no effect of rotationality; the $x^2 y$ term is the centrifugal pressure gradient due to curvature.

To complete the treatment of the inviscid flow, the velocities can be written down by substituting (1.22) into (1.4)

$$u = A x \left[1 + \left(nV - \frac{1}{R} \right) y + \dots \right]$$

$$v = -A y \left[1 + \left(\frac{nV}{2} - \frac{n+3}{2R} \right) y + \dots \right]$$

(1.23)

CHAPTER II

Viscous Flow near the Stagnation Point

General Considerations

The basis of considering the viscous flow near the stagnation point is Lagerstrom and Cole's expansion procedure (reference 20), as described briefly in the Introduction. The essence of this procedure is a magnification of both the independent coordinate and the velocity component perpendicular to the solid surface in inverse proportion to a "significant viscous length" (i.e., the boundary-layer thickness) and a velocity based on it. As the limit of very large Reynolds number is taken, viscous effects will be limited to a very thin layer near the body surface, and these magnifications then permit an analytic investigation of the structure of this very thin layer. This layer is of course the classical boundary layer of Prandtl; and Lagerstrom and Cole's⁽²⁰⁾ procedure consists of improving the boundary-layer result by expanding all flow quantities in powers of the inverse square root of a Reynolds number based on some significant length. Thus, immediately as this improvement is considered the question has to be raised what this significant length should be. There is no such length inherent in the classical boundary-layer solution itself. Another way to formulate this same question is: what length should the boundary-layer thickness at the stagnation point be compared to in order to decide whether or not a correction term to the boundary-layer solution is necessary, when considering the viscous flow near the stagnation point. This is a crucial question, which will affect the formulation of the entire problem.

One such length that suggests itself is the radius of curvature at the nose. That this may be a suitable length can be seen by considering a stagnation point located on a curved nose. For very large Reynolds numbers the boundary-layer thickness becomes negligibly small compared to the nose radius, which, (by geometric intuition) is equivalent to taking the "infinite" radius limit. In this limit then the classical solution of flow impinging on an "infinite" plate is recovered. On the other hand it is easy to see (relying again on intuition) that, as the Reynolds number becomes smaller, and hence the boundary-layer thickness larger when compared to the nose radius, it may become necessary to consider a correction to the classical result due to the curvature of the boundary layer near the stagnation point. (Subsequent analysis will show later that these intuitive considerations are essentially correct.) If, however, the nose radius is taken as the sole length which could be of significance in the problem, then no correction terms whatsoever can be admitted for a flat-nosed body. This is certainly contrary to expectation, and in direct contradiction to the presence of a "boundary-layer displacement effect," as discussed in the introduction. Actually, it is not necessary, or even possible, to decide beforehand what the proper reference length should be. It is clear that the proposed procedure could be applied with the reference length left arbitrary, and whatever the important reference length or lengths may be they will appear in the solution upon proper expansion of the equations of motion and proper application of the boundary conditions. In the subsequent analysis, the nose radius will be used as the reference length; in the light of the above remarks, this choice is one of convenience only and cannot affect the validity

of the outcome of the analysis. At the end of this chapter, it will be possible to identify all the low-Reynolds-number effects in terms of several reference lengths to which the boundary-layer thickness has to be compared when considering the necessity of a low-Reynolds-number correction to the boundary-layer result.

Development of Theory

The procedure for investigating the viscous flow near the stagnation point will then consist of writing the full viscous equations of motion, as derived in Appendix A, in the curvilinear boundary-layer coordinate system of equation (1.1). Magnification of the independent coordinate y is accomplished by replacing it with the boundary-layer variable:

$$\eta = y \sqrt{\frac{A}{y_s}} \quad (2.1)$$

Magnification of velocity U , and the desired expansion of the velocities is accomplished by writing the stream function in terms of the following expansion:

$$\psi = \rho_s \sqrt{y_s A} x^{1+n} \left[f_0(\eta) + \frac{1}{R} \sqrt{\frac{y_s}{A}} f_1(\eta) + \dots + x^2 g_0(\eta) + \frac{x^2}{R} \sqrt{\frac{y_s}{A}} g_1(\eta) + \dots \right] \quad (2.2)$$

Using the symmetry of the problem analogous expansions can be written down for the thermodynamic properties:

$$T = T_s \left[H_0(\eta) + \frac{1}{R} \sqrt{\frac{y_s}{A}} H_1(\eta) + \dots + x^2 g_{t_0}(\eta) + \frac{x^2}{R} \sqrt{\frac{y_s}{A}} g_{t_1}(\eta) + \dots \right] \quad (2.3)$$

$$\beta = \beta_s \left[\beta_0(\eta) + \frac{1}{R} \sqrt{\frac{\beta_s}{A}} \beta_1(\eta) + \dots + x^2 g_{\beta_0}(\eta) + \frac{x^2}{R} \sqrt{\frac{\beta_s}{A}} g_{\beta_1}(\eta) + \dots \right] \quad (2.4)$$

$$P = P_s \left[\beta_0(\eta) + \frac{1}{R} \sqrt{\frac{\beta_s}{A}} \beta_1(\eta) + \dots + x^2 g_{P_0}(\eta) + \frac{x^2}{R} \sqrt{\frac{\beta_s}{A}} g_{P_1}(\eta) + \dots \right] \quad (2.5)$$

As in (1.6), the fluid properties are assumed to be temperature dependent, and can be expanded in a Taylor series about the leading term in expansion (2.3). The dots again signify derivatives with respect to temperature; the subscript 0 indicates evaluation at infinite Reynolds number and $x = 0$;

$$c_p = c_{p_0} + \dot{c}_{p_0} (T - T_s H_0) + \frac{\ddot{c}_{p_0}}{2} (T - T_s H_0)^2 + \dots$$

$$\mu = \mu_0 + \dot{\mu}_0 (T - T_s H_0) + \frac{\ddot{\mu}_0}{2} (T - T_s H_0)^2 + \dots$$

$$k = k_0 + \dot{k}_0 (T - T_s H_0) + \frac{\ddot{k}_0}{2} (T - T_s H_0)^2 + \dots$$

(2.6)

Using expansion (2.3) these expressions can be written:

$$c_p = c_{p_0} + \frac{1}{R} \sqrt{\frac{\beta_s}{A}} T_s \dot{c}_{p_0} H_1(\eta) + \dots + x^2 T_s \dot{c}_{p_0} g_{c_p}(\eta) + \frac{x^2}{R} \sqrt{\frac{\beta_s}{A}} \left[T_s \dot{c}_{p_0} g_{c_p}(\eta) + T_s^2 \frac{\ddot{c}_{p_0}}{2} H_1(\eta) g_{c_p}(\eta) \right] + \dots$$

$$\mu = \mu_0 + \frac{1}{R} \sqrt{\frac{\beta_s}{A}} T_s \dot{\mu}_0 H_1(\eta) + \dots + x^2 T_s \dot{\mu}_0 g_{\mu}(\eta) + \frac{x^2}{R} \sqrt{\frac{\beta_s}{A}} \left[T_s \dot{\mu}_0 g_{\mu}(\eta) + T_s^2 \frac{\ddot{\mu}_0}{2} H_1(\eta) g_{\mu}(\eta) \right] + \dots$$

$$k = k_0 + \frac{1}{R} \sqrt{\frac{\beta_s}{A}} T_s \dot{k}_0 H_1(\eta) + \dots + x^2 T_s \dot{k}_0 g_k(\eta) + \frac{x^2}{R} \sqrt{\frac{\beta_s}{A}} \left[T_s \dot{k}_0 g_k(\eta) + T_s^2 \frac{\ddot{k}_0}{2} H_1(\eta) g_k(\eta) \right] + \dots$$

(2.7)

The y momentum equation can be written down by considering (1.1) in (A.7)

$$\begin{aligned}
 & \frac{1}{(1+\frac{x}{R})^{2n} R^{2n} (\sin \frac{x}{R})^{2n}} \left\{ \frac{1}{(1+\frac{x}{R})^2} \Psi_2 \Psi_x \frac{S_x}{S} - \frac{1}{1+\frac{x}{R}} \frac{\Psi_2^2}{R} - \frac{\Psi_2 \Psi_{xx}}{(1+\frac{x}{R})^2} + \right. \\
 & \left. + \frac{n \cos \frac{x}{R}}{R \sin \frac{x}{R}} \frac{\Psi_2 \Psi_x}{(1+\frac{x}{R})^2} - \frac{\Psi_x^2}{1+\frac{x}{R}} \frac{S_x}{S} + \frac{\Psi_x \Psi_{xx}}{(1+\frac{x}{R})^2} - \frac{(1+n) \Psi_x^2}{R(1+\frac{x}{R})^3} \right\} + S P_y = \\
 & = \frac{1}{(1+\frac{x}{R})^{n+1} R^n (\sin \frac{x}{R})^n} \left\{ \frac{4}{3} \Psi_x \mu_y \frac{S_x}{S} - \frac{8}{3} \Psi_x \mu \frac{S_x^2}{S^2} - \frac{4}{3} \frac{(1+n) \Psi_x \mu}{R(1+\frac{x}{R})} \frac{S_x}{S} + \right. \\
 & \left. + \frac{2}{3} \Psi_y \mu_y \frac{S_x}{S} + \frac{2}{3} \Psi_y \mu \frac{S_x S_x}{S^2} + \frac{7+n}{3R} \frac{\Psi_x \mu}{1+\frac{x}{R}} \frac{S_x}{S} + \frac{2(1+n)}{R} \frac{\Psi_x \mu_y}{(1+\frac{x}{R})} - \right. \\
 & \left. - \Psi_y \mu_x \frac{S_x}{S} - \frac{(1+n)}{R} \frac{\Psi_y \mu_x}{(1+\frac{x}{R})} + \Psi_{y2} \mu_x - 2 \Psi_{xy} \mu_y + \frac{n \cos \frac{x}{R}}{R \sin \frac{x}{R}} \Psi_y \mu_x - \right. \\
 & \left. - \frac{\Psi_{xx} \mu_x}{R^2 (1+\frac{x}{R})^2} + \frac{\Psi_x \mu_{xx}}{R(1+\frac{x}{R})^2} \frac{S_x}{S} + \frac{n \cos \frac{x}{R}}{R^2 \sin \frac{x}{R}} \frac{\Psi_{xx} \mu}{(1+\frac{x}{R})^2} - \frac{n \cos \frac{x}{R}}{R (\sin \frac{x}{R})^2} \frac{\Psi_x \mu}{(1+\frac{x}{R})^2} - \frac{n \cos \frac{x}{R}}{R^2 \sin \frac{x}{R}} \frac{\Psi_x \mu}{(1+\frac{x}{R})^2} \frac{S_x}{S} - \right. \\
 & \left. - \frac{\Psi_{xxx} \mu}{R^2 (1+\frac{x}{R})^2} + \frac{2 \Psi_{xx} \mu}{R^2 (1+\frac{x}{R})^2} \frac{S_x}{S} - \frac{n}{R^2} \frac{\Psi_x \mu}{(1+\frac{x}{R})^2} + \frac{\Psi_x \mu_{xx}}{R(1+\frac{x}{R})^2} \frac{S_{xx}}{S} - \frac{2 \Psi_{xx} \mu}{R^2 (1+\frac{x}{R})^2} \left(\frac{S_x}{S} \right)^2 - \Psi_{xy2} \mu + \right. \\
 & \left. + \frac{n-1}{R} \frac{\Psi_{xy} \mu}{1+\frac{x}{R}} + \Psi_{y2} \mu \frac{S_x}{S} + \Psi_{xy} \mu \frac{S_x^2}{S} + \Psi_y \mu \frac{S_x}{S} \right\} \quad (2.8)
 \end{aligned}$$

Now expansions (2.2) through (2.5) and (2.7) can be substituted into this equation, and the results grouped according to powers of x^2 and $\frac{1}{R} \sqrt{\frac{A}{A}}$. The coefficients of the $R \sqrt{\frac{A}{A}}$, constant, $x^2 R \sqrt{\frac{A}{A}}$, and x^2 terms are

$$S_5 P_5 (t_0 t_{p_0}') = 0$$

$$S_5 P_3 (t_1 t_{p_0}' + t_0 t_{p_1}') = 0$$

$$S_5 P_2 (t_1 t_{p_1}' + t_0 t_{p_2}') = 0$$

$$S_5 P_1 (t_1 t_{p_2}' + t_0 t_{p_3}' + t_0 t_{p_1}' + t_1 t_{p_0}') - S_5^2 A^2 t_0'^2 = 0$$

hence:

$$\psi'_0 = 0 \quad (2.9)$$

$$\psi'_1 = 0 \quad (2.10)$$

$$\psi'_0 = 0 \quad (2.11)$$

$$\frac{P_2}{S_1 A^2} \psi'_1 = \frac{t_0'^2}{t_0} \quad (2.12)$$

The \times momentum equation is obtained by using (1.1)

in (A.8);

$$\begin{aligned} & \frac{1}{\left(1 + \frac{\nu}{R}\right)^{2n+1} R^{2n} (\sin \frac{\pi}{R})^{2n}} \left\{ \psi_x \psi_y \frac{s_x}{s} + \frac{n-1}{R} \frac{\psi_x \psi_y}{1 + \frac{\nu}{R}} - \psi_x \psi_{yy} - \right. \\ & \left. - \psi_y^2 \frac{s_x}{s} + \psi_x \psi_{xy} - \frac{n}{R} \frac{\cos \frac{\pi}{R}}{\sin \frac{\pi}{R}} \psi_y^2 \right\} + \frac{3 P_x}{1 + \frac{\nu}{R}} = \\ & = \frac{1}{\left(1 + \frac{\nu}{R}\right)^n R^n (\sin \frac{\pi}{R})^n} \left\{ \frac{4}{3} \frac{\psi_x \mu_x}{\left(1 + \frac{\nu}{R}\right)^2} \frac{s_x}{s} - \frac{5}{3} \frac{\psi_x \mu_x}{\left(1 + \frac{\nu}{R}\right)^2} \frac{s_x s_y}{s^2} - \frac{n \cos \frac{\pi}{R}}{3 R \sin \frac{\pi}{R}} \frac{\psi_x \mu_x}{\left(1 + \frac{\nu}{R}\right)^2} \frac{s_x}{s} - \right. \\ & - \frac{10}{3} \frac{\psi_y \mu_x}{\left(1 + \frac{\nu}{R}\right)^2} \frac{s_x}{s} + \frac{8}{3} \frac{\psi_y \mu_x}{\left(1 + \frac{\nu}{R}\right)^2} \frac{s_x^2}{s^2} + \frac{4}{3} \frac{n \cos \frac{\pi}{R}}{R \sin \frac{\pi}{R}} \frac{\psi_y \mu_x}{\left(1 + \frac{\nu}{R}\right)^2} \frac{s_x}{s} + \frac{1}{3} \frac{\psi_{xx} \mu_x}{\left(1 + \frac{\nu}{R}\right)^2} \frac{s_x}{s} + \\ & + \frac{1}{3} \frac{\psi_x \mu_x}{\left(1 + \frac{\nu}{R}\right)^2} \frac{s_{xx}}{s} - \frac{7}{3} \frac{\psi_{xy} \mu_x}{\left(1 + \frac{\nu}{R}\right)^2} \frac{s_x}{s} - \frac{4}{3} \frac{\psi_y \mu_x}{\left(1 + \frac{\nu}{R}\right)^2} \frac{s_{xx}}{s} - \frac{\psi_x \mu_x}{\left(1 + \frac{\nu}{R}\right)^2} \frac{s_x}{s} + \\ & + \frac{n \cos \frac{\pi}{R}}{R \sin \frac{\pi}{R}} \frac{\psi_x \mu_x}{\left(1 + \frac{\nu}{R}\right)^2} - \frac{2n \cos \frac{\pi}{R}}{R \sin \frac{\pi}{R}} \frac{\psi_y \mu_x}{\left(1 + \frac{\nu}{R}\right)^2} + \frac{2 \psi_{xy} \mu_x}{\left(1 + \frac{\nu}{R}\right)^2} - \frac{\psi_{xx} \mu_x}{\left(1 + \frac{\nu}{R}\right)^2} - \\ & - \frac{(1+n)}{R} \frac{\psi_y \mu_x}{1 + \frac{\nu}{R}} + \psi_{yy} \mu_x - \psi_y \mu_y \frac{s_y}{s} - \frac{2 \psi_x \mu_x}{R \left(1 + \frac{\nu}{R}\right)^2} + \frac{\psi_{xy} \mu_x}{\left(1 + \frac{\nu}{R}\right)^2} - \\ & - \frac{2 \psi_{xx} \mu_x}{R \left(1 + \frac{\nu}{R}\right)^2} - \frac{n \cos \frac{\pi}{R}}{R \sin \frac{\pi}{R}} \frac{\psi_{xy} \mu_x}{\left(1 + \frac{\nu}{R}\right)^2} + \frac{2n \cos \frac{\pi}{R}}{R^2 \sin \frac{\pi}{R}} \frac{\psi_x \mu_x}{\left(1 + \frac{\nu}{R}\right)^2} + \frac{2 \psi_{xx} \mu_x}{R \left(1 + \frac{\nu}{R}\right)^2} \frac{s_x}{s} + \\ & + \psi_{yyy} \mu_x - 2 \psi_{yy} \mu_y \frac{s_y}{s} + \frac{1-n}{R} \frac{\psi_{yy} \mu_x}{1 + \frac{\nu}{R}} - \frac{(1-n)}{R} \frac{\psi_y \mu_x}{1 + \frac{\nu}{R}} \frac{s_y}{s} - \\ & \left. - \frac{(1-n)}{R^2} \frac{\psi_y \mu_x}{\left(1 + \frac{\nu}{R}\right)^2} - \frac{\psi_y \mu_x s_{yy}}{s} + 2 \psi_y \mu_x \frac{s_y^2}{s^2} \right\} \quad (2.13) \end{aligned}$$

Repeating the former procedure, coefficients of the \times term give the following equation:

$$(1+n) t_0 t_0' \frac{t_0'}{t_0} - (1+n) t_0 t_0'' + t_0'^2 + \frac{\rho_s}{s_s A^2} 2 t_0 g p_0 = \frac{\mu_0}{\mu_s} T_s H_0' (t_0'' - t_0' \frac{t_0'}{t_0}) +$$

$$+ \frac{\mu_0}{\mu_s} \left[t_0''' - 2 t_0'' \frac{t_0'}{t_0} - t_0' \frac{t_0''}{t_0} + 2 t_0' \left(\frac{t_0'}{t_0} \right)^2 \right] \quad (2.14)$$

Terms $\frac{\mu_0}{\mu_s} T_s$ and $\frac{\mu_0}{\mu_s}$ in the above expression are functions of $H_0(\eta)$ only, the exact functional form depending on the viscosity vs. temperature law that is assumed.

The next equation is obtained by collecting coefficients of the $\frac{\times}{R} \sqrt{\frac{\rho_s}{A}}$ term in the \times momentum equation (2.13):

$$-\eta \left\{ (2n+1) \left[(1+n) t_0 t_0' \frac{t_0'}{t_0} - (1+n) t_0 t_0'' + t_0'^2 \right] + \frac{\rho_s}{s_s A^2} 2 t_0 g p_0 \right\} +$$

$$+ (n^2-1) t_0 t_0' + (1+n) \frac{t_0 t_0'}{t_0} t_1' - (1+n) t_0 t_0' \frac{t_0'}{t_0^2} t_1 + (1+n) t_0 \frac{t_0'}{t_0} t_1' +$$

$$+ (1+n) t_0 \frac{t_0'}{t_0} t_1 - (1+n) t_0 t_1'' - (1+n) t_0'' t_1 + 2 t_0' t_1' + \frac{\rho_s}{s_s A^2} 2 (g p_0 t_1 + t_0 g p_1) =$$

$$= \frac{\mu_0}{\mu_s} T_s^2 H_0' (t_0'' - t_0' \frac{t_0'}{t_0}) H_1 + \frac{\mu_0}{\mu_s} T_s \left[(t_0'' - t_0' \frac{t_0'}{t_0}) H_1' + (t_0''' - \right.$$

$$\left. - 2 t_0'' \frac{t_0'}{t_0} - t_0' \frac{t_0''}{t_0} + 2 t_0' \frac{t_0'^2}{t_0^2} \right) H_1 + H_0' t_1'' - H_0' \frac{t_0'}{t_0} t_1' - H_0' \frac{t_0'}{t_0} t_1' +$$

$$+ H_0' t_0 \frac{t_0'}{t_0^2} t_1 \left. \right] + \frac{\mu_0}{\mu_s} \left[t_1''' - 2 \frac{t_0'}{t_0} t_1'' - 2 \frac{t_0''}{t_0} t_1' + 2 t_0'' \frac{t_0'}{t_0} t_1 - \right.$$

$$\left. - \frac{t_0''}{t_0} t_1' - \frac{t_0'}{t_0} t_1'' + t_0' \frac{t_0''}{t_0} t_1 + 2 \frac{t_0'^2}{t_0^2} t_1' + 4 t_0' \frac{t_0'}{t_0} t_1' - 4 t_0' \frac{t_0'^2}{t_0^2} t_1 \right] -$$

$$- \frac{\mu_0}{\mu_s} T_s H_0' \left\{ \eta n \left[t_0'' - t_0' \frac{t_0'}{t_0} \right] + (1+n) t_0' \right\} - \frac{\mu_0}{\mu_s} \left\{ \eta n \left[t_0'' - 2 t_0' \frac{t_0'}{t_0} - \right. \right.$$

$$\left. \left. - t_0' \frac{t_0''}{t_0} + 2 t_0' \frac{t_0'^2}{t_0^2} \right] + (n-1) t_0'' + (1-n) t_0' \frac{t_0'}{t_0} \right\} \quad (2.15)$$

Finally, the energy equation (A.11) is written down in coordinates (1.1):

$$\begin{aligned} & \frac{1}{R^n (\sin \frac{x}{R})^n} \left[c_p (\psi_y T_x - \psi_x T_y) + \frac{1}{5} (\psi_x p_y - \psi_y p_x) \right] = \left(1 + \frac{y}{R}\right)^{(1+n)} k T_{yy} + \\ & + \left(1 + \frac{y}{R}\right)^{(1+n)} k_y T_y + \frac{1+n}{R} \left(1 + \frac{y}{R}\right)^n k T_y + \left(1 + \frac{y}{R}\right)^{(n-1)} k T_{xx} + \\ & + \left(1 + \frac{y}{R}\right)^{(n-1)} k_x T_x + \frac{n \cos \frac{x}{R}}{R \sin \frac{x}{R}} \left(1 + \frac{y}{R}\right)^{(n-1)} k T_x + \mu \bar{\Phi} \end{aligned} \quad (2.16)$$

The dissipation function $\bar{\Phi}$ in the above expression has not been expanded, because, to the order of terms considered, it will not contribute to the equations. In order to ascertain this, one has to consider the form of the dissipation function given in (A.10) in terms of the general coordinate system. Each term will be of the form of the stream function occurring twice, and four derivatives occurring in like pairs. In order to contribute to the stagnation-point term, at least two of these derivatives have to be \times derivatives (otherwise the term will be of order x^2). Since ψ is of order \sqrt{x} and ψ derivatives of order $\frac{1}{\sqrt{x}}$, the largest term in the dissipation function will be of order viscosity times two stream functions and two ψ derivatives, which is altogether of order $\frac{1}{x}$. But only terms of order 1 and order \sqrt{x} are of interest.

Now (2.1) through (2.7) can be substituted into energy equation (2.16), and terms grouped in powers of $\frac{1}{R} \sqrt{\frac{x}{A}}$ and x^2 . The leading term is

$$-\frac{c_{p0}}{c_{ps}}(1+n) t_0 H_0' + \frac{P_2}{c_{ps} T_s S_s} (1+n) t_0 t_{p0}' = \frac{k_s}{\mu_s c_{ps}} \left[\frac{k_0}{k_s} H_0'' + \frac{k_0}{k_s} T_s H_0'^2 \right] \tag{2.17}$$

Collecting the $\frac{1}{R} \sqrt{\frac{\rho_s}{A}}$ terms gives

$$\begin{aligned} -\frac{c_{p0}}{c_{ps}} T_s (1+n) t_0 H_0' H_1 - \frac{c_{p0}}{c_{ps}} (1+n) (t_0 H_1' + H_0' t_1) + \frac{P_2}{c_{ps} T_s S_s} (1+n) (t_0 t_{p1}' + \\ + t_{p0}' t_1) = \frac{k_s}{\mu_s c_{ps}} \left\{ \frac{k_0}{k_s} H_1'' + \frac{k_0}{k_s} T_s (H_0'' H_1 + 2 H_0' H_1') + \right. \\ \left. + \frac{k_0}{k_s} T_s^2 H_0'^2 H_1 + \frac{k_0}{k_s} (1+n) [\eta H_0'' + H_0'] + \frac{k_0}{k_s} T_s (1+n) \eta H_0'^2 \right\} \end{aligned} \tag{2.18}$$

where the terms $\frac{k_0}{k_s}$ etc., are again given, but as yet unspecified function of $f_0(\eta)$. An additional relation between the variables is given by the perfect-gas law, which was assumed

$$t_{p0} = H_0 t_{r0}$$

$$t_{p1} = H_0 t_{r1} + t_{r0} H_1$$

etc.

$$\tag{2.19}$$

Now the formulation of the differential equations is complete. Equations (2.9) through (2.12), (2.14), (2.15), and (2.17) through (2.19) define two coupled sets of ordinary differential equations, in the zero-th and first-order variables respectively. The zeroth-order set is nonlinear; it is essentially the boundary-layer equation at the stagnation point. The first-order set is linear, with the coefficients and inhomogeneous terms composed of the known boundary-layer solution.

In order to proceed with the solution of these equations suitable boundary conditions have to be specified. Two types of boundary conditions are available; at the solid-fluid interface (i.e., the "wall") and in the inviscid flow, where the viscous solution has to "merge" into the inviscid solution specified earlier. The boundary conditions at the wall are derived in Appendix B, and are repeated here.

$$\begin{aligned} f_0(0) &= 0 \\ f_0'(0) &= 0 \\ H_0(0) &= W \end{aligned} \tag{2.20}$$

and

$$\begin{aligned} f_1(0) &= 0 \\ f_1'(0) &= \frac{2-\delta}{\delta} \sqrt{\frac{\pi}{2}} \frac{AR}{\sqrt{RT_s}} \frac{\mu_w}{\mu_s} \frac{1}{\sqrt{W}} \frac{f_0''(0)}{f_0'(0)} \equiv K_1 \frac{AR}{\sqrt{RT_s}} \frac{\mu_w}{\mu_s} \frac{1}{\sqrt{W}} \frac{f_0''(0)}{f_0'(0)} \\ H_1(0) &= \frac{2-\alpha_w}{\alpha_w} \sqrt{\frac{\pi}{2}} \frac{2\tau_w}{\tau_w+1} \frac{1}{Re_w} \frac{AR}{\sqrt{RT_s}} \frac{\mu_w}{\mu_s} \frac{1}{\sqrt{W}} \frac{H_0'(0)}{f_0'(0)} \equiv K_2 \frac{AR}{\sqrt{RT_s}} \frac{\mu_w}{\mu_s} \frac{1}{\sqrt{W}} \frac{H_0'(0)}{f_0'(0)} \end{aligned} \tag{2.21}$$

where constants K_1 and K_2 are defined by the above expressions. In order to determine the boundary conditions in the inviscid flow, one can use "the inner-flow" independent variable (2.1) in the expressions for the inviscid flow given by (1.22) through (1.25). Furthermore, as explained in the introduction, a correction will be necessary in the inviscid ("outer")-flow parameters, due to the displacement effect of the boundary layer around the body. This effect will change the velocity gradient A , which is a

fundamental parameter of the problem, by an unknown amount. This change can be expressed as follows:

$$A\left(\frac{1}{R}\sqrt{\frac{\nu_s}{A}}\right) = A\left[1 + \frac{1}{R}\sqrt{\frac{\nu_s}{A}} C_D + \dots\right] \quad (2.22)$$

The other parameters of the inviscid flow will not be changed to the order of terms considered here. (A more detailed discussion of these correction terms, and their significance will be given in a later section). The inviscid stream function can now be written in terms of the viscous (i.e., "inner") expansion as

$$\Psi = \rho_s \sqrt{\nu_s A} x^{1+n} \left\{ \eta + \frac{1}{R} \sqrt{\frac{\nu_s}{A}} \left[C_D \eta + \frac{n-1+nRV}{2} \eta^2 \right] + \dots \right\} \quad (2.23)$$

Similarly, the expansions for the thermodynamic properties in the inviscid flow become ;

$$S = S_s \left[1 + O\left(\frac{\nu_s}{R^2 A}\right) + O(x^2) + \dots \right]$$

$$T = T_s \left[1 + O\left(\frac{\nu_s}{R^2 A}\right) + O(x^2) + \dots \right]$$

$$P = P_s \left\{ 1 + O\left(\frac{\nu_s}{R A}\right) + x^2 \left[-\frac{\rho_s A^2}{2 P_s} + \frac{1}{R} \sqrt{\frac{\nu_s}{A}} \frac{\rho_s A^2}{P_s} (\eta - C_D) \right] + \dots \right\} \quad (2.24)$$

Expressions (2.23) and (2.24) in conjunction with (2.2) through (2.5) can now be used to define the boundary conditions necessary for the proper "mergence" of the viscous "inner" flow into the inviscid "outer" flow. As η becomes very large

$$\begin{aligned}
 & f_0(\eta) \rightarrow \eta \\
 & H_0(\eta) \rightarrow 1 \\
 \eta \rightarrow \infty & \quad f_{r_0}(\eta) \rightarrow 1 \\
 & \quad f_{p_0}(\eta) \rightarrow 1 \\
 & \quad \frac{2 p_s}{s_s A^2} g_{p_0}(\eta) \rightarrow -1
 \end{aligned} \tag{2.25}$$

and

$$\begin{aligned}
 & f_1(\eta) \rightarrow C_3 \eta + \frac{n-1+nRV}{2} \eta^2 \\
 & H_1(\eta) \rightarrow 0 \\
 \eta \rightarrow \infty & \quad f_{r_1}(\eta) \rightarrow 0 \\
 & \quad f_{p_1}(\eta) \rightarrow 0 \\
 & \quad \frac{p_s}{s_s A^2} g_{p_1}(\eta) \rightarrow \eta - C_3
 \end{aligned} \tag{2.26}$$

Using these boundary conditions three of the differential equations, namely (2.9) through (2.11), can be integrated immediately

$$f_{p_0}(\eta) = 1$$

$$f_{p_1}(\eta) = 0$$

$$\frac{2 p_s}{s_s A^2} g_{p_0}(\eta) = -1 \tag{2.27}$$

These results can be combined with the perfect-gas law

(2.19) to obtain

$$t_0 = \frac{1}{\mu_0}$$

$$t_1 = -\frac{\mu_1}{\mu_0^2}$$

(2.28)

The remaining differential equations can now be simplified by using the above intermediate results. Using (2.27) and (2.28) equation (2.14) becomes

$$(1+n) t_0 t_0' \frac{\mu_0'}{\mu_0} + (1+n) t_0 t_0'' - t_0'^2 + \frac{1}{\mu_0} + \frac{\mu_0}{\mu_s} T_s \left[t_0'' \mu_0' + t_0' \frac{\mu_0'^2}{\mu_0} \right] + \frac{\mu_0}{\mu_s} \left[t_0''' + 2 t_0'' \frac{\mu_0'}{\mu_0} + t_0' \frac{\mu_0''}{\mu_0} \right] = 0$$

(2.29)

The x momentum equation for the correction term, (2.15), is similarly modified. Grouping homogeneous and inhomogeneous terms on the left- and right-hand sides respectively, the equation becomes

$$\begin{aligned} & \left[(1+n) t_0' \frac{\mu_0'}{\mu_0} + (1+n) t_0'' \right] t_1 + \left[(1+n) t_0 \frac{\mu_0'}{\mu_0} - 2 t_0' \right] t_1' + (1+n) t_0 t_1'' - \\ & - \left[(1+n) t_0 t_0' \frac{\mu_0'}{\mu_0^2} + \frac{1}{\mu_0^2} \right] \mu_1 + (1+n) \frac{t_0 t_0'}{\mu_0} \mu_1' - \frac{1}{\mu_0} \frac{2 p_2}{g_s A^2} g p_1 + \\ & + \frac{\mu_0}{\mu_s} T_s^2 \left[t_0'' \mu_0' + t_0' \frac{\mu_0'^2}{\mu_0} \right] \mu_1 + \frac{\mu_0}{\mu_s} T_s \left[(t_0'' + 2 t_0' \frac{\mu_0'}{\mu_0}) \mu_1' + \right. \\ & \left. + (t_0''' + 2 t_0'' \frac{\mu_0'}{\mu_0} + t_0' \frac{\mu_0''}{\mu_0} - t_0' \frac{\mu_0'^2}{\mu_0^2}) \mu_1 + \mu_0' t_1'' + \frac{\mu_0'}{\mu_1} t_1' \right] + \\ & + \frac{\mu_0}{\mu_s} \left[t_1''' + 2 \frac{\mu_0'}{\mu_0} t_1'' + \frac{\mu_0''}{\mu_0} t_1' + \frac{t_0'}{\mu_0} \mu_1'' + 2 \frac{t_0''}{\mu_0} \mu_1' - \right. \\ & \left. - (2 t_0'' \frac{\mu_0'}{\mu_0^2} + t_0' \frac{\mu_0''}{\mu_0^2}) \mu_1 \right] = \eta \left\{ (2n+1) \left[(1+n) t_0 t_0' \frac{\mu_0'}{\mu_0} + \right. \right. \end{aligned}$$

$$\begin{aligned}
& + (1+n) \left\{ \ddot{t}_0 \left[\dot{t}_0'' - \dot{t}_0'^2 \right] + \frac{1}{k_0} \right\} + (n^2-1) \dot{t}_0 \dot{t}_0' + \frac{k_0}{k_s} T_s \left\{ \eta n \left[\dot{H}_0' \dot{t}_0'' + \right. \right. \\
& + \dot{t}_0' \frac{\dot{H}_0'^2}{k_0} \left. \right] + (1+n) \dot{t}_0' \dot{H}_0' \left. \right\} + \frac{k_0}{k_s} \left\{ \eta n \left[\dot{t}_0''' + 2 \dot{t}_0'' \frac{\dot{H}_0'}{k_0} + \right. \right. \\
& + \dot{t}_0' \frac{\dot{H}_0''}{k_0} + 2(1-n) \dot{t}_0' \frac{\dot{H}_0'^2}{k_0^2} \left. \right] + (n-1) \dot{t}_0'' + (n-1) \dot{t}_0' \frac{\dot{H}_0'}{k_0} \left. \right\} \quad (2.30)
\end{aligned}$$

The same substitutions can be made in the energy equations;

(2.17) becomes

$$\rho_r \frac{c_p}{c_p} (1+n) \dot{t}_0 \dot{H}_0' + \frac{k_0}{k_s} \dot{H}_0'' + \frac{k_0}{k_s} T_s \dot{H}_0'^2 = 0 \quad (2.31)$$

Similarly, grouping homogeneous and inhomogeneous terms

(2.18) becomes

$$\begin{aligned}
& \rho_r \left[\frac{c_p}{c_p} T_s (1+n) \dot{t}_0 \dot{H}_0' \dot{H}_1 + \frac{c_p}{c_p} (1+n) (\dot{t}_0 \dot{H}_1' + \dot{H}_0' \dot{t}_1) \right] + \\
& + \frac{k_0}{k_s} T_s^2 \dot{H}_0'^2 \dot{H}_1 + \frac{k_0}{k_s} T_s (\dot{H}_0'' \dot{H}_1 + 2 \dot{H}_0' \dot{H}_1') + \frac{k_0}{k_s} \dot{H}_1'' = \\
& = - \frac{k_0}{k_s} T_s (1+n) \eta \dot{H}_0'^2 - \frac{k_0}{k_s} (1+n) [\eta \dot{H}_0'' + \dot{H}_0'] \quad (2.32)
\end{aligned}$$

Equations (2.29) and (2.31) now constitute a system of two coupled non linear differential equations in the two variables \dot{t}_0 and \dot{H}_0 . The order of the combined system is 5, thus 5 boundary conditions are needed. Equations (2.20) give 3 at the wall;

thus two more are needed "at infinity." The proper boundary conditions are then from (2.25)

$$\eta \rightarrow \infty \quad \begin{aligned} f_0'(\eta) &\rightarrow 1 \\ f_0(\eta) &\rightarrow 1 \end{aligned} \quad (2.33)$$

These are the boundary-layer equations; their solutions can be obtained (numerically) as soon as the dependence of fluid properties upon temperature is specified. The wall-to-free-stream stagnation-temperature ratio, W , will be a parameter of the solution. After these results are obtained the solution of coupled equations (2.30) and (2.32) can be considered. Variable \mathfrak{P}_1 in equation (2.30) can be eliminated by integrating equation (2.12), which can be done directly because, using (2.29)

$$\frac{P_s}{S_s A^2} \mathfrak{P}_1' = f_0'^2 f_0 = \frac{1}{2+n} \frac{d}{d\eta} \left[(1+n) f_0 f_0' f_0 + \gamma + \frac{k_0}{\mu_s} (f_0' f_0' + f_0'' f_0) \right]$$

The boundary condition for \mathfrak{P}_1 , as given in (2.26), can be used to determine the unknown constant of integration. Let the behavior of f_0 far from the wall be described by

$$\eta \rightarrow \infty \quad f_0(\eta) \rightarrow \eta - \eta^* \quad (2.34)$$

where η^* is determined from the solution of the boundary-layer equations. Then, far from the wall

$$\eta \rightarrow \infty$$

$$\frac{P_s}{S_s A^2} \mathfrak{P}_1 = \frac{1}{2+n} \left[(1+n) f_0 f_0' f_0 + \gamma + \frac{k_0}{\mu_s} (f_0' f_0' + f_0'' f_0) \right] + K \rightarrow \eta - \frac{1+n}{2+n} \eta^* + K$$

Hence, using (2.26)

$$K = \frac{1+n}{2+n} \eta^* - C_D \quad (2.35)$$

and the expression

$$\frac{P_s}{s_s A^2} g p_1 = \frac{1}{2+n} \left[(1+n) f_0' f_0'' H_0 + (1+n) \eta^* + \eta + \frac{K_2}{K_1} (f_0' H_0' + f_0'' H_0'') \right] - C_D \quad (2.36)$$

can now be used in (2.30).

Before proceeding with the discussion of the solution of equations (2.30) and (2.32), result (2.28) can be used to modify the boundary conditions at the wall for ψ_1 and H_1 as given in (2.21)

$$\psi_1(0) = 0$$

$$\psi_1'(0) = K_1 \frac{AR}{\sqrt{2} T_s} \frac{\mu_w}{\mu_s} \sqrt{W} \psi_0''(0)$$

$$H_1(0) = K_2 \frac{AR}{\sqrt{2} T_s} \frac{\mu_w}{\mu_s} \sqrt{W} H_0'(0)$$

(2.37)

The two constants (or rather combination of constants) that appear in the above boundary conditions are arbitrary in magnitude; their ratio K_1/K_2 is also arbitrary, depending partly on empirically determined solid-gas interaction properties σ and α_a . Additional arbitrary constants appear in the boundary conditions for ψ_1 "at infinity" as given in (2.26), namely C_D and V (this latter only for the $n=1$ case). The linearity of the equations

suggests that it will be possible to construct a solution of the equations for any combination of the above arbitrary constants in terms of a sum, where the arbitrary constants appear as coefficients. Each of the functions, associated with any one of the arbitrary constants, can be solved for once and for all. The solutions of the equations could then be written in the form

$$\begin{aligned} f_1 &= f_{1c} + \frac{AR}{\sqrt{Re_s}} \frac{k_2}{k_1} \sqrt{W} \left[K_1 f_0''(0) f_{11} + K_2 H_0'(0) f_{12} \right] + C_D f_{1D} + nRV f_{1V} \\ H_1 &= H_{1c} + \frac{AR}{\sqrt{Re_s}} \frac{k_2}{k_1} \sqrt{W} \left[K_1 f_0''(0) f_{11} + K_2 H_0'(0) f_{12} \right] + C_D H_{1D} + nRV H_{1V} \end{aligned} \quad (2.38)$$

where the functions with subscript c are associated with the solution of the inhomogeneous equation, subject to the boundary conditions with all arbitrary constants vanishing; whereas the other functions represent solutions of the homogeneous equations, subject to boundary conditions associated with the respective constants. Result (2.36), above, then implies the existence of 5 different pairs of functions (4 pairs for $n = 0$), each pair being a solution of two coupled linear equations, and subject to the respective boundary conditions. A simplification is possible if one observes that the pair of functions f_0' and H_0' identically satisfies the homogeneous equations (2.30) and (2.32), (because the left-hand sides become merely the derivatives of the corresponding boundary-layer equations (2.29) and (2.31)). This pair of functions, multiplied by an arbitrary constant, also satisfies the slip and temperature-jump boundary conditions at the wall, (2.37) provided the two constants K_1 and K_2 are equal. This solution is completely equivalent to

Lin and Schaeff's⁽²³⁾ boundary-layer perturbation solution due to slip, or the alternate method used by Mangler⁽²⁴⁾ of "depressing" the position of the solid-fluid interface in the boundary layer by a length proportional to the mean free path, in order to account for the slip. Howdler⁽²⁷⁾ pointed out that depressing the true position of the wall in order to account for the slip, will not, in general, account correctly for the effect of the temperature jump. Only if this "depression" times the local temperature gradient is equal to the temperature jump will this approximation be correct; this case is equivalent to the special case $K_1 = K_2$ in the terminology of the present analysis. For the general case, $K_1 \neq K_2$, a correction function can then be determined, which accounts for the fact that the two constants are not equal. Expressions (2.38) can then be rewritten as follows

$$\begin{aligned}
 f_1 &= f_{1c} + \frac{AR}{\sqrt{Re}_s} \frac{\mu_w}{\mu_s} \sqrt{W} \left[K_1 f_0' + (K_2 - K_1) f_0'(0) f_{1M} \right] + C_D f_{1D} + nRV f_{1V} \\
 H_1 &= H_{1c} + \frac{AR}{\sqrt{Re}_s} \frac{\mu_w}{\mu_s} \sqrt{W} \left[K_1 H_0' + (K_2 - K_1) H_0'(0) H_{1M} \right] + C_D H_{1D} + nRV H_{1V}
 \end{aligned} \tag{2.39}$$

Thus, to determine the effect of slip and temperature jump, only one pair of functions, f_{1M} and H_{1M} , has to be determined, instead of the two pairs in (2.38).

The differential equations and boundary conditions for each of the functions appearing in (2.39) can now be summarized. First of all, the governing differential equations (2.30) and (2.32) can be modified and written in shortened operator notation as follows:

$$M(t_1, H_1) = M_c(t_0, H_0, \eta) - 2 \frac{k_s}{k_0} \frac{c_0}{H_0}$$

$$E(t_1, H_1) = E_c(t_0, H_0, \eta) \quad (2.40)$$

where the symbols M and E denote the respective differential operators for the momentum and energy equations; and M_c and E_c denote the respective inhomogeneous terms appearing on the right-hand sides of the equation. From (2.30) and (2.32), the above operators are:

$$\begin{aligned} M(t_1, H_1) \equiv & \frac{k_s}{k_0} [(1+n)t_0' \frac{H_0'}{H_0} + (1+n)t_0''] t_1 + \left\{ \frac{k_s}{k_0} [(1+n)t_0' \frac{H_0'}{H_0} - 2t_0'] + \right. \\ & + \frac{k_0}{k_0} T_s \left[\frac{H_0'^2}{H_0} + \frac{H_0''}{H_0} \right] t_1' + \left\{ \frac{k_s}{k_0} (1+n)t_0' + \frac{k_0}{k_0} T_s \frac{H_0'}{H_0} + 2 \frac{H_0'}{H_0} \right\} t_1'' + t_1''' \\ & + \left\{ - \frac{k_s}{k_0} \left[\frac{1}{H_0^2} + (1+n)t_0' t_0' \frac{H_0'}{H_0^2} \right] + \frac{k_0}{k_0} T_s^2 \left[t_0'' \frac{H_0'}{H_0} + t_0' \frac{H_0'^2}{H_0^2} \right] + \frac{k_0}{k_0} T_s \left[t_0''' + \right. \right. \\ & + 2t_0'' \frac{H_0'}{H_0} + t_0' \frac{H_0''}{H_0} - t_0' \frac{H_0'^2}{H_0^2} \left. \right] - 2t_0'' \frac{H_0'}{H_0^2} - t_0' \frac{H_0''}{H_0^2} \left. \right\} H_1 + \\ & + \left\{ \frac{k_s}{k_0} (1+n) \frac{t_0' t_0'}{H_0} + \frac{k_0}{k_0} T_s \left[t_0'' + 2t_0' \frac{H_0'}{H_0} \right] + 2 \frac{t_0''}{H_0} \right\} H_1' + \frac{t_0'}{H_0} H_1'' \end{aligned} \quad (2.41)$$

and

$$\begin{aligned} E(t_1, H_1) \equiv & P_{r_s} \frac{c_0}{c_s} \frac{k_s}{k_0} (1+n) H_0' t_1 + \left[P_{r_s} \frac{c_0}{c_s} T_s \frac{k_0}{k_0} (1+n) t_0' H_0' + \right. \\ & + \frac{k_0}{k_0} T_s^2 \frac{H_0'^2}{H_0} + \frac{k_0}{k_0} T_s \frac{H_0''}{H_0} \left. \right] H_1 + \left[P_{r_s} \frac{c_0}{c_s} \frac{k_s}{k_0} (1+n) t_0' + \right. \\ & + \frac{k_0}{k_0} T_s \left. 2 \frac{H_0'}{H_0} \right] H_1' + H_1'' \end{aligned} \quad (2.42)$$

Also

$$\begin{aligned}
 M_c(f_0, H_0, \eta) - 2 \frac{c_D}{\mu_0} \frac{\mu_s}{\mu_0} &\equiv \eta \frac{\mu_s}{\mu_0} \left\{ (1+n) \left[(1+n) f_0' \frac{H_0'}{\mu_0} + (1+n) (f_0'' - f_0'^2) \right] + \right. \\
 &+ \left. \frac{1}{\mu_0} \left(1-n + \frac{c}{2+n} \right) \right\} + \frac{\mu_s}{\mu_0} \left\{ \left[(n-1) + \frac{2(1+n)}{2+n} \right] f_0' f_0' + \left[\frac{2(1+n)}{2+n} \eta^2 \right] \frac{1}{\mu_0} \right\} + \\
 &+ \left[(n-1) + \frac{c}{2+n} \right] (f_0'' + f_0' \frac{H_0'}{\mu_0}) + \frac{\mu_0}{\mu_0} T_s (1+n) f_0' H_0' - 2 \frac{c_D}{\mu_0} \frac{\mu_s}{\mu_0}
 \end{aligned} \tag{2.43}$$

and

$$E_c(f_0, H_0, \eta) \equiv - (1+n) \left[\eta \left(H_0'' + \frac{c}{\mu_0} T_s H_0'^2 \right) + H_0' \right] \tag{2.44}$$

Now let all the arbitrary parameters in (2.39) vanish.

Then the differential equations to be solved are

$$M(f_{1c}, H_{1c}) = M_c(f_0, H_0, \eta)$$

$$E(f_{1c}, H_{1c}) = E_c(f_0, H_0, \eta)$$

(2.45)

The boundary conditions at the wall are

$$f_{1c}(0) = 0$$

$$f_{1c}'(0) = 0$$

$$H_{1c}(0) = 0$$

(2.46)

while, very far from the wall

$$H_{1c}(\eta) \rightarrow 0 \quad (2.47)$$

$$\eta \rightarrow \infty \quad \text{for } n=0 \quad f_{1c}''(\eta) \rightarrow -1$$

$$\text{for } n=1 \quad f_{1c}'(\eta) \rightarrow 0$$

Now the correction terms due to the slip and temperature-jump effects can be considered. The equations are

$$M(f_{1m}, H_{1m}) = 0$$

$$E(f_{1m}, H_{1m}) = 0$$

(2.48)

In agreement with (2.37) and (2.39), the boundary conditions at the wall are

$$f_{1m}(0) = 0$$

$$f_{1m}'(0) = 0$$

$$H_{1m}(0) = 1$$

(2.49)

The "outer" boundary conditions are

$$\eta \rightarrow \infty \quad H_{1m}(\eta) \rightarrow 0$$

$$f_{1m}'(\eta) \rightarrow 0$$

(2.50)

Using (2.45) the equations for the terms multiplied by C_D are

$$M(f_{1D}, H_{1D}) = -2 \frac{\mu_{\infty}}{\mu_0} \frac{1}{H_0}$$

$$E(f_{1D}, H_{1D}) = 0$$

(2.51)

The boundary conditions at the wall are homogeneous

$$f_{1D}(0) = 0$$

$$f'_{1D}(0) = 0$$

$$H_{1D}(0) = 0$$

(2.52)

At "infinity", using (2.26)

$$\begin{aligned} \eta \rightarrow \infty \quad H_{1D}(\eta) &\rightarrow 0 \\ f'_{1D}(\eta) &\rightarrow 1 \end{aligned}$$

(2.53)

Correction functions f_{1D} and H_{1D} can be written down in terms of the boundary-layer solutions f_0 and H_0 directly. To obtain these expressions one has to observe that coefficient C_D appeared in the inviscid boundary conditions because velocity gradient A was expanded, as shown in (2.22). This very same expansion of A can be applied to the original expressions for the stream-function and temperature, as given in (2.1) through

(2.3). Not considering terms with subscript 1, the expansion of A yields the following expressions

$$\psi = s_s \sqrt{\frac{1}{3}A} x^{1+n} \left\{ f_0(\eta) + \frac{1}{2} \frac{1}{R} \sqrt{\frac{1}{3}A} \zeta f_0(\eta) + \frac{1}{2} \frac{1}{R} \sqrt{\frac{1}{3}A} \zeta \eta f_0'(\eta) + \dots \right\}$$

$$T = T_s \left[H_0(\eta) + \frac{1}{2} \frac{1}{R} \sqrt{\frac{1}{3}A} \zeta \eta H_0'(\eta) \dots \right]$$

(2.54)

Comparing with (2.39), one can immediately identify

$$f_{10} = \frac{1}{2} [f_0 + \eta f_0']$$

$$H_{10} = \frac{1}{2} \eta H_0'$$

(2.55)

Substitution into (2.51) through (2.53) verifies these solutions. Expressions (2.39) can now be written

$$f_1 = f_{1c} + \frac{AR}{12T_s} \frac{k_w}{k_s} \sqrt{W} \left[K_1 f_0' + (K_2 - K_1) H_0'(0) f_{1w} \right] + \frac{\zeta}{2} (f_0 + \eta f_0') + nRV f_{1w}$$

$$H_1 = H_{1c} + \frac{AR}{12T_s} \frac{k_w}{k_s} \sqrt{W} \left[K_1 H_0' + (K_2 - K_1) H_0'(0) H_{1w} \right] + \frac{\zeta}{2} \eta H_0' + nRV H_{1w}$$

(2.56)

Finally, the equations for the terms proportional to V are

$$M(f_{1w}, H_{1w}) = 0$$

$$E(f_{1w}, H_{1w}) = 0$$

(2.57)

The boundary conditions at the wall are again homogeneous

$$\begin{aligned} f_{IV}(0) &= 0 \\ f'_{IV}(0) &= 0 \\ f''_{IV}(0) &= 0 \end{aligned} \tag{2.58}$$

while far from the wall

$$\begin{aligned} \eta \rightarrow \infty \quad f_{IV}(\eta) &\rightarrow 0 \\ f''_{IV}(\eta) &\rightarrow 1 \end{aligned} \tag{2.59}$$

Expressions (2.45) through (2.50) and (2.57) through (2.59) give the differential equations and the associated boundary conditions that are necessary to determine the five pairs of functions (two for $n = 0$ and three for $n = 1$) that occur in expressions (2.56) for the boundary-layer correction terms that are under consideration in the present investigation. The solution of these equations is contingent upon solution of the stagnation-point boundary-layer equations (2.29) and (2.31) subject to boundary conditions (2.20) and (2.33). In order to complete formulation of the theory, it is only necessary now to specify the dependence of fluid properties upon temperature. This dependence can now be stipulated as follows (cf. Chapter III)

$$\begin{aligned} \mu &\propto T^\omega \\ k &\propto T^\epsilon \\ \rho &\propto T^\alpha \end{aligned} \tag{2.60}$$

Hence, using the definitions of (2.6)

$$\begin{aligned}\frac{h_0}{\mu_s} &= f_0^\omega \\ \frac{k_0}{k_s} &= f_0^\varepsilon \\ \frac{q_0}{\omega_s} &= f_0^\alpha\end{aligned}\quad (2.61)$$

The temperature derivatives occurring in the equations then become

$$\begin{aligned}\frac{h_0}{\mu_s} T_s &= \omega f_0^{\omega-1} \\ \frac{k_0}{k_s} T_s^2 &= \omega(\omega-1) f_0^{\omega-2} \\ &\text{etc.}\end{aligned}\quad (2.62)$$

Using (2.61) and (2.62), the boundary-layer equations and the operators occurring in the equations for the correction terms can now be written down explicitly. In order to isolate the highest-order derivatives the expressions will all be divided by the appropriate powers of f_0 . Boundary-layer equations (2.29) and (2.31) become

$$(1+n) f_0 \frac{f_0'}{f_0^{1+n}} + (1+n) \frac{f_0 f_0''}{f_0^{1+n}} - \frac{f_0'^2}{f_0} + \frac{1}{f_0^{1+\omega}} + f_0''' + (\omega+2) f_0'' \frac{f_0'}{f_0} + \omega f_0' \frac{f_0'^2}{f_0} + f_0' \frac{f_0''}{f_0} = 0$$

$$Pr_s (1+n) f_0 f_0^{\alpha-\varepsilon} f_0' + f_0'' + \varepsilon \frac{f_0'^2}{f_0} = 0$$

$$f_0(0) = 0$$

$$f_0'(0) = 0$$

$$f_0(0) = W$$

$$\eta \rightarrow \infty \quad \begin{aligned} f_0'(\eta) &\rightarrow 1 \\ f_0(\eta) &\rightarrow 1 \end{aligned}$$

(2.63)

where unchanged boundary conditions (2.20) and (2.33) have been appended for the sake of convenient reference. These equations are completely equivalent to those originally presented by Brown (2), and then solved for the two-dimensional case by Brown and Donough (3), Brown and Livingood (4), and for the axially symmetric case by Howe and Mersman (16). The apparent differences are due to the slightly different normalizations of the temperature and stream functions.

For the correction terms f_1 and h_1 operators (2.41) through (2.44) can now be written down

$$\begin{aligned}
 M(f_1, h_1) \equiv & \left[(1+n) f_0' \frac{h_0'}{h_0^{1+\omega}} + (1+n) \frac{f_0''}{h_0^\omega} \right] f_1 + \left[(1+n) f_0 \frac{h_0'}{h_0^{1+\omega}} - \right. \\
 & \left. - 2 \frac{f_0'}{h_0^\omega} + \omega \frac{h_0'^2}{h_0^2} + \frac{h_0''}{h_0} \right] f_1' + \left[(1+n) \frac{f_0}{h_0^\omega} + (\omega+2) \frac{h_0'}{h_0} \right] f_1'' + f_1''' + \\
 & + \left[-\frac{1}{h_0^{\omega+2}} - (1+n) f_0 f_0' \frac{h_0'}{h_0^{\omega+2}} + \omega \frac{f_0''}{h_0} + (\omega^2 + \omega - 2) f_0' \frac{h_0'}{h_0} + \right. \\
 & \left. + (\omega-1) f_0' \frac{h_0''}{h_0^2} + (\omega^2 - 2\omega) f_0' \frac{h_0'^2}{h_0^3} \right] h_1 + \left[(1+n) \frac{f_0 f_0'}{h_0^{1+\omega}} + (\omega+2) \frac{f_0'}{h_0} + \right. \\
 & \left. + 2\omega f_0' \frac{h_0'}{h_0^2} \right] h_1' + \frac{f_0}{h_0} h_1''
 \end{aligned}$$

$$\begin{aligned}
 E(f_1, h_1) \equiv & P_{r_2} (1+n) h_0^{\alpha-2} h_0' f_1 + \left[P_{r_2} (1+n) \alpha f_0 h_0^{\alpha-2} f_1' + \right. \\
 & \left. + \varepsilon (\varepsilon-1) \frac{h_0'^2}{h_0^2} + \varepsilon \frac{h_0''}{h_0} \right] h_1 + \left[P_{r_2} (1+n) f_0 h_0^{\alpha-2} + \right. \\
 & \left. + 2\varepsilon \frac{h_0'}{h_0} \right] h_1' + h_1''
 \end{aligned} \tag{2.68}$$

and

$$\begin{aligned}
 M_c(t_0, \mu_0, \gamma) &\equiv \gamma \left\{ (n+1) \left[(n+1) t_0' \frac{\mu_0'}{\mu_0^{1+n}} + (n+1) \frac{t_0' t_0''}{\mu_0^{1+n}} - \frac{t_0'^2}{\mu_0^{1+n}} \right] + \right. \\
 &+ \left. \left[1 - n + \frac{2}{2+n} \right] \frac{t_0'}{\mu_0^{1+n}} \right\} + \left[n-1 + \frac{2(n+1)}{2+n} \right] \frac{t_0' t_0''}{\mu_0^{1+n}} + \left[n-1 + \frac{2}{2+n} \right] t_0'' + \\
 &+ \left[n-1 + \frac{2}{2+n} + \omega + \omega n \right] t_0' \frac{\mu_0'}{\mu_0} + \frac{2(1+n)}{2+n} \gamma^* \frac{1}{\mu_0^{1+n}} \\
 E_c(t_0, \mu_0, \gamma) &\equiv -(1+n) \left[\gamma \left(\varepsilon \frac{t_0'^2}{\mu_0} + t_0'' \right) + t_0' \right] \tag{2.65}
 \end{aligned}$$

Discussion of Theory

This completes the presentation of all the differential equations and associated boundary conditions that are necessary for obtaining the boundary-layer and first-order boundary-layer correction terms for stagnation-point flow. The consequences of arbitrarily choosing nose radius R as the reference length in the Reynolds number that forms the basis of the asymptotic expansions for all the flow and thermodynamic quantities in the problem, can now be discussed. Let the viscous length, $\sqrt{\frac{\nu_0}{A}}$, which is indicative of the boundary-layer thickness at the stagnation point, be denoted by δ . The expansion parameter that was used in the above analysis is then $\frac{\delta}{R}$; the ratio of the boundary-layer thickness to the nose radius. As R becomes very large compared to δ , the first of the correction terms in (2.56), the term without any coefficient and labelled by subscript C

will become negligibly small compared to the boundary-layer term. This term is then indeed due to the curvature of the nose; it will not be present for a flat-nosed body, for instance.

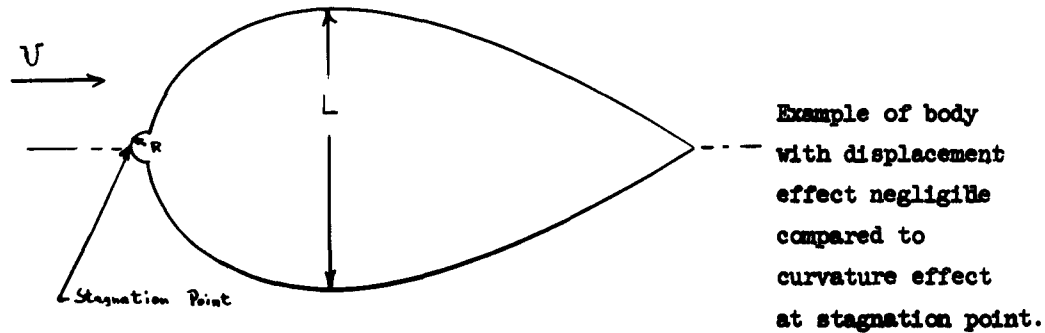
In order to investigate the physical significance of the remaining correction terms, the expansion parameter $\frac{\delta}{R}$ has to be considered together with the coefficients of the respective terms. For the slip and temperature-jump terms, the parameter that is significant is

$$\frac{\delta}{R} \frac{AR}{\sqrt{RT_s}} \frac{\mu_w}{\mu_s} \sqrt{W} = \frac{A\delta}{\sqrt{RT_s}} \frac{\mu_w}{\mu_s} \frac{s_s}{s_w} \frac{a_s}{a_w} = A \sqrt{\frac{s_s}{s_w}} \frac{a_s}{\sqrt{RT_s}} \frac{1}{s_w a_w} = \text{constant} \frac{\lambda_w}{\delta}$$

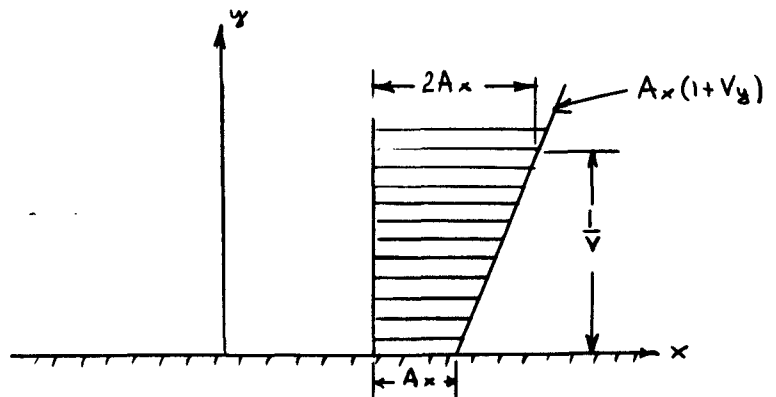
where the constant is of order 1. The above shows that this correction arises when the mean free path at the wall becomes significant compared to the boundary-layer thickness. Since δ here is in the denominator the behavior of this term is quite different from the former one.

The displacement effect arises due to a change in velocity gradient "A" at small Reynolds numbers. Therefore, the length that will be significant in this Reynolds number is the length that plays a determining role in establishing the magnitude of "A". This reference length L could be the "size" of the body perpendicular to the free stream for the case of the body in a steady subsonic stream. Or, for a blunt body in hypersonic flow, it is actually the nose radius, as will be shown in a later section. The correction to "A" arises when the boundary-layer thickness δ is large enough compared to this reference length L . Unknown constant C_D is then of the order of the ratio of R to L , which

could be quite insignificant if, for example, the stagnation point is located on a "small bump" on a much larger body. This shows that the curvature and displacement effects can arise independently from each other. (See sketch below.)



Finally, the last term in (2.56), due to the vorticity effect in axially symmetric flow, can be considered. It is clear from inspecting the coefficient of this term that radius R cancels out; instead δ is compared to length $1/\nu$. A physical interpretation of this length can be obtained from the linear velocity profile in the inviscid flow given in (1.23), as indicated in the sketch below.



The ratio of the boundary-layer thickness to this length is actually identical to Kemp's⁽¹⁹⁾ vorticity parameter; the ratio of the vorticity in the inviscid flow to the "average" vorticity in the boundary layer.

These considerations show that the first-order correction terms to the stagnation-point boundary-layer solution, which are discussed in the present investigation, arise due to four different effects; namely the curvature, velocity slip and temperature jump, displacement, and vorticity effects. Each of these effects is associated with a different low-Reynolds-number flow parameter. Three of the parameters arise from a comparison of the boundary-layer thickness with three different, and in general, independent, significant lengths; nose radius R , length L (indicative of body size) which determines velocity gradient A , and length $1/\sqrt{v}$ which is associated with the slope of the uniform inviscid shear flow that can be present in axially symmetric stagnation-point flows. The fourth parameter is essentially a Knudsen number based on the mean free path near the wall and the boundary-layer thickness. In order that the expansion procedure of the above analysis be applicable to a practical problem it is necessary then that all four independent parameters described above be an order of magnitude smaller than one. This implies then that the smallest one of the three reference lengths be considerably larger than the boundary-layer thickness. It also implies that the mean free path near the wall be considerably smaller than the boundary-layer thickness. This last requirement is actually implicit in the use of the

Navier-Stokes equations, because, as pointed out in the introduction, these equations do not permit large changes in flow properties (such as occur across a boundary layer) to take place within distances of only a few mean free paths long. This shows that the use of the slip and temperature-jump boundary conditions as first-order corrections to the boundary-layer equations is consistent with the use of the Navier-Stokes equations. If λ_w/δ is of order 1, the expansion procedure of the present analysis and the Navier-Stokes equations break down simultaneously.

If all four of the expansion parameters are sufficiently small (i.e., smaller than of order 1), so that it is meaningful to apply the Reynolds-number-expansion procedure described in the above analysis, it is interesting to consider what type of terms may arise if the next term in the expansion is considered. The energy and momentum equations are again used, as in (2.8) through (2.18) now terms to the second power of expansion variable $\frac{1}{R} \sqrt{\frac{\nu_2}{A}}$ are collected. On the left-hand side of the equations, terms involving the new (second-order) variables $\psi_2, \psi_2', \psi_2''$, etc. will appear. These terms will all be linear, with the coefficients composed of the zero-th-order (i.e., boundary-layer) terms. The linearity of the equations again permits splitting the second-order correction terms into a number of separate, mutually independent effects. These effects will arise due to various parameters that appear in the inhomogeneous terms and in the boundary conditions.

The inhomogeneous terms will be composed of various combinations of the zero-th and first-order terms. At most two first-order functions can be combined in each term. Since the

first-order functions can have either of three arbitrary coefficients or no coefficient at all, the second-order terms that arise can be associated with combinations of any two of the three arbitrary coefficients or no coefficient at all, the second-order terms that arise can be associated with combinations of any two of the three arbitrary coefficients, or any one of the coefficients, or no coefficient at all (thereby giving rise to seven different effects for the axially symmetric and five for the plane flow cases). Another new effect will also appear among the inhomogeneous terms due to the presence of boundary-layer terms that are one order higher in the x^2 expansion about the $x = 0$ point than the stagnation-point boundary-layer terms (i.e., terms like q_0 , q_1 , etc.). Thus, to this second order, the description of the body has to include, in addition to the nose radius and nose wall temperature, also the rate of change of these quantities with x^2 in order to specify the stagnation-point flow (implying the appearance of two more arbitrary parameters). As mentioned in Chapter I, additional arbitrary parameters will undoubtedly appear in the "outer" (i.e., inviscid-flow) boundary conditions to the second-order correction terms. These considerations show that a full treatment of the second-order correction terms would be very laborious and complicated indeed. These correction terms will not be considered in the present analysis, except a word of caution has to be added. It is possible that coefficients of some of the new second-order terms are so large that the expansion procedure of the present analysis (which is based

on the nose radius as the significant length) is not applicable, even though the first-order correction terms are all sufficiently small. This implies that there are new physical parameters, which show up only in the second (or possibly higher)-order terms in an expansion procedure based on nose radius, but which are of the same order as the boundary-layer term itself, thereby precluding the possibility of this type of asymptotic-expansion procedure. For example, the rate of change of curvature at the stagnation point could be so large that this effect dominates the viscous flow near the stagnation point, even though the curvature itself is not large.

For those cases when one of the expansion parameters is so large that the expansion procedure outlined in this chapter is not applicable any more, yet the Navier-Stokes equations are still applicable, different methods of solution have to be considered. One method, which is feasible under certain circumstances, is solution of the full Navier-Stokes equations, with the Reynolds number based on radius as a parameter. Such solutions have been obtained for hypersonic flow around a sphere, with a constant-density fluid and concentric shock wave, by Probstein and Kemp⁽³¹⁾, and Hoshizaki⁽¹³⁾. Later Hoshizaki⁽¹⁴⁾ included the slip effect for this case, as a separate parameter. Another method is solution of the boundary-layer equations, with the particular strong low-Reynolds-number effect as a parameter. The vorticity effect for incompressible fluid is considered in this manner by Kemp⁽¹⁹⁾. A somewhat different approach, again for the axially symmetric hypersonic-flow case, is used by Oguchi⁽²⁸⁾ and Herring⁽¹¹⁾. Their method consists of using the bow shock wave as an "outer" boundary condition for the boundary-layer

equations, thereby accounting for both the vorticity and displacement effects; the former for a $\rho = \text{constant}$, the latter for a $\mu = \text{constant}$ fluid. More recently Oguchi⁽²⁹⁾ presented an analytic solution for this same axially symmetric constant-density hypersonic-flow case, in terms of an expansion in shock density ratio e . This analysis includes the curvature, displacement, and vorticity effects simultaneously. Finally, the method of Probstein and Kemp⁽³¹⁾ has also been applied to a variable-property fluid by Probstein and Ho⁽³²⁾, again, for the case of a sphere in hypersonic flow.

In the present analysis the restriction to small values of the parameters was accepted, as this disadvantage was compensated by the possibility of identifying the four first-order low-Reynolds-number effects and comparing them on an equal footing. The validity of the present approach can be extended by constructing "hybrid" or "composite" solutions, including only the largest of the above effects in the nonlinear solution, and accounting for the remaining low-Reynolds-number effects by the perturbation procedure of the present analysis. For example, Kemp's⁽¹⁹⁾ parametric solution of the boundary-layer equations subject to a vortical outer boundary condition could be "perturbed" with respect to slip and or curvature; etc. Such a solution could be useful in a flow regime with large vorticity interaction effect but comparatively small slip and curvature parameters. The most useful approach will be different for each problem, and can be determined by estimating the orders of magnitude of the various low-Reynolds-number flow parameters.

CHAPTER III

Examples of Stagnation-Point Flows

In order to apply the results of the foregoing theory to flows around specific bodies, the flow parameters that are inherent in the stagnation-point flow problem have to be determined for the specific flow example. Some simple examples and applications will be considered in the following paragraphs. In some cases, it may be more appropriate to use experimental results to determine the parameters under consideration.

Subsonic flow around circular cylinder and sphere.

At low Mach numbers, the results of incompressible flow around these bodies can be used. The stream functions are given for the cylinder

$$\psi = S_1 U \left(r - \frac{R^2}{r} \right) \sin \theta \quad (3.1)$$

and for the sphere

$$\psi = S_2 \frac{U}{2} \left(r^2 - \frac{R^3}{r} \right) \sin^2 \theta$$

Using the boundary-layer coordinate system of (1.1) and expanding about the stagnation point, these expressions become

$$\psi = S_1 \frac{U}{R} x \left[y - \frac{y^2}{2R} + \dots \right]$$

$$\psi = S_2 \frac{3U}{2R} x^2 \left[y + O(y^3) \dots \right]$$

(3.2)

for the cylinder and sphere respectively. Comparing with (1.22),
for the cylinder

$$A = \frac{2U}{R} \quad (3.3a)$$

and for the sphere

$$A = \frac{3U}{2R}$$

$$V = 0 \quad (3.3b)$$

Due to the presence of turbulence and the possibility of separation, displacement constant C_D has to be left undetermined for this type of flow. The remaining parameters are essentially arbitrary thermodynamic properties.

Hypersonic flow around circular cylinder and sphere.

Inviscid solutions for hypersonic flow around circular cylinder and sphere were given by Whitham⁽⁴³⁾ and also Hayes and Probstein⁽⁹⁾ for the cylinder, and Lighthill⁽²²⁾ for the sphere. Both of these solutions are predicated upon three assumptions; shock shape that is concentric with the body, incompressible fluid behind the shock, density ratio across shock is a constant. The stream functions are, for the cylinder

$$\begin{aligned} \psi &= g_s U R_{shk} \sin \theta \left\{ \left[K_1 \left(\frac{1-\epsilon}{\epsilon} \right) - (1-\epsilon) K_1 \left(\frac{1-\epsilon}{\epsilon} \right) \right] I_1 \left(\frac{\epsilon-1}{\epsilon} \frac{r}{R_{shk}} \right) - \left[I_1 \left(\frac{\epsilon-1}{\epsilon} \right) - (1-\epsilon) \right] K_1 \left(\frac{\epsilon-1}{\epsilon} \frac{r}{R_{shk}} \right) \right\} = \\ &= g_s U R_{shk} \sin \theta \left\{ C_I(\epsilon) I_1 \left(\frac{\epsilon-1}{\epsilon} \frac{r}{R_{shk}} \right) - C_K(\epsilon) K_1 \left(\frac{\epsilon-1}{\epsilon} \frac{r}{R_{shk}} \right) \right\} \end{aligned} \quad (3.4a)$$

which defines $C_I(\epsilon)$ and $C_K(\epsilon)$; and for the sphere

$$\psi = \rho_s U \sin^2 \theta r^2 \left\{ \frac{e}{2} + \frac{(1-e)(1-6e)}{15e} \left(\frac{R_{shock}^3}{r^3} - 1 \right) - \frac{(1-e)^2}{10e} \left(1 - \frac{r^2}{R_{shock}^2} \right) \right\} \quad (3.4b)$$

where e is the density ratio across the shock $\frac{\rho_\infty}{\rho_{shock}}$, and R_{shock} the radius of the shock. Let the inviscid shock stand-off distance be Δ , so that

$$R_{shock} = R + \Delta \quad (3.5)$$

In the boundary-layer coordinate system of (1.1) then, and considering the leading power in x only, the expressions for the respective stream functions become, for the cylinder:

$$\psi = \rho_s U x \left(1 + \frac{\Delta}{R} \right) \left\{ C_I I_1 \left(\frac{e-1}{e} \frac{1 + \frac{x}{R}}{1 + \frac{\Delta}{R}} \right) - C_K K_1 \left(\frac{e-1}{e} \frac{1 + \frac{x}{R}}{1 + \frac{\Delta}{R}} \right) \right\} \quad (3.6a)$$

and for the sphere:

$$\psi = \rho_s U x^2 \left(1 + \frac{\Delta}{R} \right) \left\{ \frac{e}{2} + \frac{(1-e)(1-6e)}{15e} \left[\left(\frac{1 + \frac{x}{R}}{1 + \frac{\Delta}{R}} \right)^3 - 1 \right] - \frac{(1-e)^2}{10e} \left[1 - \left(\frac{1 + \frac{x}{R}}{1 + \frac{\Delta}{R}} \right)^2 \right] \right\} \quad (3.6b)$$

Since the body outline is part of the stagnation streamline, the expressions in brackets in (3.6) are equal to 0 at $y = 0$. This relates $\frac{\Delta}{R}$ to e

$$C_I(e) I_1 \left[\frac{e-1}{e \left(1 + \frac{\Delta}{R} \right)} \right] - C_K(e) K_1 \left[\frac{e-1}{e \left(1 + \frac{\Delta}{R} \right)} \right] = 0 \quad (3.7a)$$

$$\frac{3(1-e)^2}{\left(1 + \frac{\Delta}{R} \right)^4} - \frac{5(1-4e)}{\left(1 + \frac{\Delta}{R} \right)^2} + 2(1-e)(1-6e) \left(1 + \frac{\Delta}{R} \right) = 0 \quad (3.7b)$$

These implicit relations can be expanded in a series form for small e (cf. Hayes and Probstein⁽⁹⁾)

$$\frac{\Delta}{R} = \frac{e}{2} \left[\ln \frac{4}{3e} + \frac{e}{2} \left(\ln \frac{4}{3e} \right)^2 + e \ln \frac{4}{3e} + \dots \right] \quad (3.8a)$$

$$\frac{\Delta}{R} = e \left[1 - \frac{2}{3} \sqrt{e} + 4e + \dots \right] \quad (3.8b)$$

Now stream functions (3.6) can be expanded in powers of y ;

$$\Psi = \beta_s \frac{U}{R} \frac{1-e}{e} \left\{ C_I I_0 \left[\frac{1-e}{e(1+\frac{e}{R})} \right] + C_K K_0 \left[\frac{1-e}{e(1+\frac{e}{R})} \right] \right\} \times \left[y - \frac{y^2}{2R} + \dots \right] \quad (3.9a)$$

$$\Psi = \beta_s \frac{U}{R} \frac{1}{2e} \left[\left(\frac{1-e}{1+\frac{e}{R}} \right)^2 - 1 + 4e \right] \times^2 \left[y + \frac{1}{1 - (1+e) \left(\frac{1+\frac{e}{R}}{1-e} \right)^2} \frac{y^2}{R} + \dots \right] \quad (3.9b)$$

Again, comparing with (1.22), the velocity gradient for the cylinder becomes

$$A = \frac{U}{R} \frac{1-e}{e} \left\{ C_I I_0 \left[\frac{1-e}{e(1+\frac{e}{R})} \right] + C_K K_0 \left[\frac{1-e}{e(1+\frac{e}{R})} \right] \right\} \quad (3.10a)$$

Similarly for the sphere

$$A = \frac{U}{R} \frac{1}{2e} \left[\left(\frac{1-e}{1+\frac{e}{R}} \right)^2 - 1 + 4e \right]$$

$$V = \frac{1}{R} \frac{2}{1 - (1+e) \left(\frac{1+\frac{e}{R}}{1-e} \right)^2} \quad (3.10b)$$

In this case, the displacement effect can also be ascertained; the shock stand-off distance will be changed from the inviscid value due to the presence of the boundary layer, without (to this order) affecting the shape of the shock surface. It will then appear as if the nose radius were increased by the boundary-layer displacement thickness δ^* . Then, in the velocity gradients in (3.10) above

$$\frac{1}{R+\delta^*} = \frac{1}{R \left[1 + \frac{1}{R} \sqrt{\frac{\rho_2}{\rho_1}} \gamma^* \right]} = \frac{1}{R} \left[1 - \frac{1}{R} \sqrt{\frac{\rho_2}{\rho_1}} \gamma^* + \dots \right]$$

Comparing with (2.22), it is apparent that

$$\zeta_D = -\gamma^* \quad (3.11)$$

the corresponding low-Reynolds-number correction to the shock stand-off distance is also of interest

$$R_{\text{shock}} - R = A + \sqrt{\frac{\rho_2}{\rho_1}} \gamma^* \quad (3.12)$$

For small e expressions (3.10) can be expanded; the leading terms are

$$A = \frac{U}{R} \left[\sqrt{\frac{\rho_2}{\rho_1}} \sqrt{e} + \dots \right] \quad (3.13a)$$

for the cylinder, and

$$A = \frac{U}{R} \left[\left[\frac{\rho_2}{\rho_1} \right]^{1/2} \sqrt{e} + O(e^{3/2}) \dots \right]$$

$$V = \frac{1}{R} \left[\left[\frac{\rho_2}{\rho_1} \right]^{1/2} e^{-1/2} + O(e^{-3/2}) \dots \right]$$

(3.13b)

for the sphere respectively. Graphs of stand-off distance d/R , velocity gradient "A", and vorticity parameter V are shown in Figures 1 and 2, for the sake of convenient reference. The corresponding numerical computations are shown in Appendix C.

Empirically determined stagnation point velocity gradient vs. free-stream Mach-number curves are given by Reshotko and Beckwith⁽³³⁾ for circular cylinders, and by Crawford and McCauley⁽⁶⁾, and Romig⁽³⁴⁾ for spheres.

Flight of a Blunt Body through the Atmosphere.

An especially interesting and practically significant application of low-Reynolds-number stagnation-point flow occurs in the case of a body flying at high altitudes. In order to determine whether any of the four correction terms described in the analysis of Chapter II are necessary or appropriate, one has to estimate the magnitude of the four respective parameters at various flight speeds and altitudes for a body of given size. In order to determine the boundary-layer thickness at the stagnation point the stagnation kinematic viscosity ν_s and velocity gradient "A" have to be known. The former can be determined unequivocally for a given altitude and flight speed. Velocity gradient "A" will be proportional to V/L , where L is some significant length, usually indicative of body size. Leaving this body length unspecified, boundary-layer thickness will be proportional to quantity $\sqrt{\frac{\nu_s}{V}}$, which is a function of altitude and flight speed only. In order to determine whether the curvature and displacement correction effects are important, the quantity $\sqrt{\frac{\nu_s}{V}}$

should be divided by the square root of the respective length. If the two lengths "R" and "L" are of different orders of magnitude $\frac{\sqrt{L}}{R} \sqrt{\frac{\nu_2}{\nu}}$ is the proper parameter to determine the significance of the curvature effect, which is then different from the displacement-effect parameter $\sqrt{\frac{\nu_2}{\nu L}}$.

To assess the significance of the slip and temperature-jump effects, the mean free path at the stagnation point has to be compared to the boundary-layer thickness. The former can be calculated from the thermodynamic properties, and thus can be determined as a function of \bar{U} and H only. Thus the ratio

$$\frac{\lambda_s}{\delta} = \frac{\lambda_s}{\sqrt{\frac{\nu_2}{\nu}} \sqrt{L}}$$

depends on a parameter, which is a function of \bar{U} and H only, divided by the square root of reference length L . (For a strongly cooled body, the mean free path at the wall may be considerably smaller than the mean free path at the stagnation condition, the effect of this will be discussed in detail in Chapter IV).

For axially symmetric blunt bodies in supersonic flow, the vorticity correction effect may have to be considered due to the presence of a curved shock wave. At high Mach numbers, Lighthill's approximation (discussed in the previous section) is reasonably accurate if the nose outline and the shock are concentric. If this is not the case, an empirically (or otherwise) determined shock radius can be used instead of the nose radius. Equation (3.10) shows, that in addition to radius R , vorticity parameter $\sqrt{\nu}$ is also dependent on shock density ratio e , which is a function of \bar{U} and H only. Thus the parameter that determines the magnitude of the vorticity effect

$$\sqrt{\nu} \delta = \sqrt{\nu} \sqrt{\frac{\nu_2}{\nu}} \sqrt{R} = \sqrt{\nu} R \sqrt{\frac{\nu_2}{\nu}} \frac{1}{\sqrt{R}}$$

is then completely dependent on V and H with the exception of a factor of \sqrt{R} .

These considerations show that it is possible to plot on a V vs. H chart families of lines showing the magnitude of all four of the significant parameters, leaving out the effect of body size as a multiplicative factor of arbitrary magnitude. Such a plot is shown in Figure 3. The following families of lines are shown

$$\lambda_s, Ft$$

$$e, \text{ therefore } \frac{A}{R} \text{ and } V$$

$$\sqrt{\frac{z}{U}}, \sqrt{Ft}$$

$$\lambda, \sqrt{\frac{U}{z}}, \sqrt{Ft}$$

$$VR \sqrt{\frac{z}{U}}, \sqrt{Ft}$$

$$\sqrt{\frac{z}{U}} \frac{R}{A}, \sqrt{Ft}$$

(3.14)

The plot is based on the ARDC model atmosphere (reference 42); real-gas effects are included in the calculations. The procedure and numerical details are given in Appendix D.

For a given size body, the lines of Figure 3 can be used to delineate the region of applicability of the expansion procedure of the present analysis. All four of the expansion parameters have to be less than 1.0 (actually unless they are less than about 0.3,

the error committed in neglecting the second-order terms may be more than 10%). Inspection of the figure shows that at low subsonic flight speeds the curvature (and displacement) correction effects become significant at a much lower altitude than the slip and temperature-jump effects. On the other hand, at hypersonic speeds the slip correction occurs at a somewhat lower altitude than the curvature and displacement corrections. For spheres at hypersonic speeds the vorticity correction effect is larger by orders of magnitude than the other terms, especially as the shock density ratio becomes small. Also, it appears, that as the boundary-layer and shock-layer thicknesses become of the same order of magnitude, the altitude is already too high (and hence the Reynolds number is too low) for the applicability of the expansion procedure. A very detailed and thorough discussion of the successive flow regimes at hypersonic flow has been given recently by Probstein and Kemp⁽³¹⁾; there is no need to reiterate these results here except to point out that the parameters plotted on figure 3 clearly indicate this succession. The expansion procedure of the present analysis is applicable near the high-Reynolds-number (i.e., low-altitude) end of this spectrum; especially for the axially symmetric case, where the vorticity "correction" becomes as large as the boundary-layer term itself at comparatively low altitudes, where the other corrections are still small. At hypersonic flow then either the "exact" solutions for a sphere by Probstein and Kemp⁽³¹⁾ or by Hoshizaki⁽¹³⁾ should be used (because the vorticity parameter is too large for the applicability of the present expansion procedure); or, at low enough altitudes,

where the expansion procedure is applicable, only the vorticity correction is significant, and therefore the "modified boundary-layer solutions" (where the vorticity boundary condition is a parameter) of Kemp⁽¹⁹⁾, Oguchi⁽²⁸⁾, and Herring⁽¹¹⁾ are equally practical (this is the "vorticity-interaction regime" of Probstein and Kemp⁽³¹⁾). Figure 3 indicates that the flow region where all four of the correction effects are about equally large occurs in the supersonic regime (between about 2000 and 6000 ft/sec). It is on this basis that the fluid properties used in the solution of the equations, as presented in the next chapter, were chosen. The procedure for obtaining these properties is shown in Appendix E. The body size will shift the flow regimes on the altitude scale, but not on the velocity scale, since all parameters are divided by the square root of the significant length.

•

CHAPTER IV

Numerical Results

Presentation of Results

The differential equations presented in Chapter II, with fluid properties given in Appendix E, were solved numerically at the Cornell Computing Center by means of a Burrows 220 electronic computer. Some details of the computing procedure are given in Appendix G. The results of the computations are determinations of "zeroth-" and first-order terms (i.e., boundary-layer and first-order ~~correction~~ terms) for the non-dimensional stream function ψ and temperature function θ . In addition to the functions, their derivatives, up to an including the highest that occur in the differential equations (i.e., the first three for ψ and the first two for θ), were also computed. The obtained solutions were then used to determine some additional quantities of practical interest. These quantities are the two velocity components, the two mass-velocity components, temperature and density profiles, and the variation of vorticity, shear (parallel to the wall), and heat-transfer rate (normal to the wall) in the viscous layer.

Recalling the definitions given in (2.2) and (2.3), one can write

$$\frac{\psi}{\frac{1}{2} \sqrt{\beta_s} A x^{1/2}} \equiv \frac{\psi}{\psi_{ref}} = \frac{\psi_0}{\psi_{ref}} + \frac{1}{R} \sqrt{\frac{\beta_s}{A}} \frac{\psi}{\psi_{ref}} = \psi_0 + \frac{1}{R} \sqrt{\frac{\beta_s}{A}} \psi_1$$

$$\frac{T}{T_s} = \frac{T_0}{T_s} + \frac{1}{R} \sqrt{\frac{\beta_s}{A}} \frac{T_1}{T_s} = \theta_0 + \frac{1}{R} \sqrt{\frac{\beta_s}{A}} \theta_1$$

(4.1)

which defines Ψ_{ref} , Ψ_0 , Ψ_1 , T_0 , T_1 .

Similar expression can be written for the density, by using result

(2.38) in (2.4)

$$\frac{\rho}{\rho_c} = \frac{\rho_0}{\rho_s} + \frac{1}{R} \sqrt{\frac{\beta_2}{\beta_1}} \frac{\rho_1}{\rho_s} = \frac{1}{M_0} - \frac{1}{R} \sqrt{\frac{\beta_2}{\beta_1}} \frac{H_1}{M_0^2} \quad (4.2)$$

All the other quantities of interest can be written down in like manner by using the above expressions and the relations developed in Appendices A and B between the stream function and the various flow quantities. Thus

$$\frac{v}{(1+n)\beta_2 A} = \frac{v}{v_{ref}} = \frac{v_0}{v_{ref}} + \frac{1}{R} \sqrt{\frac{\beta_2}{\beta_1}} \frac{v_1}{v_{ref}} = t_0 H_0 + \frac{1}{R} \sqrt{\frac{\beta_2}{\beta_1}} [H_0 t_1 + t_0 H_1 - (1+n)\eta t_0 H_0]$$

$$\frac{u}{A x} = \frac{u}{u_{ref}} = \frac{u_0}{u_{ref}} + \frac{1}{R} \sqrt{\frac{\beta_2}{\beta_1}} \frac{u_1}{u_{ref}} = t_0' H_0 + \frac{1}{R} \sqrt{\frac{\beta_2}{\beta_1}} [H_0 t_1' + t_0' H_1 - n\eta t_0' H_0]$$

$$\frac{g v}{(1+n)\beta_2 A x} = \frac{g v}{(g v)_{ref}} = \frac{(g v)_0}{(g v)_{ref}} + \frac{1}{R} \sqrt{\frac{\beta_2}{\beta_1}} \frac{(g v)_1}{(g v)_{ref}} = t_0 + \frac{1}{R} \sqrt{\frac{\beta_2}{\beta_1}} [t_1 - (1+n)\eta t_0]$$

$$\frac{g v}{\beta_2 A x} = \frac{g v}{(g v)_{ref}} = \frac{(g v)_0}{(g v)_{ref}} + \frac{1}{R} \sqrt{\frac{\beta_2}{\beta_1}} \frac{(g v)_1}{(g v)_{ref}} = t_0' + \frac{1}{R} \sqrt{\frac{\beta_2}{\beta_1}} [t_1' - n\eta t_0']$$

$$\frac{\omega \rho \bar{q}}{-A x \sqrt{\beta_2}} = \frac{\Omega}{\Omega_{ref}} = \frac{\Omega_0}{\Omega_{ref}} + \frac{1}{R} \sqrt{\frac{\beta_2}{\beta_1}} \frac{\Omega_1}{\Omega_{ref}} = t_0'' H_0 + t_0'' H_0' + \frac{1}{R} \sqrt{\frac{\beta_2}{\beta_1}} [H_0 t_1'' + H_0' t_1'' +$$

$$+ t_0' H_1' + t_0'' H_1 + (1-n) t_0'' H_0 - n\eta (t_0'' H_0 + t_0' H_0')]$$

$$\frac{A \bar{z}_0}{x \beta_2 \sqrt{\beta_2}} = \frac{z}{z_{ref}} = \frac{z_0}{z_{ref}} + \frac{1}{R} \sqrt{\frac{\beta_2}{\beta_1}} \frac{z_1}{z_{ref}} = H_0^w (t_0'' H_0 + t_0' H_0') + \frac{1}{R} \sqrt{\frac{\beta_2}{\beta_1}} H_0^w [H_0 t_1'' + H_0' t_1'' +$$

$$+ t_0' H_1' + (1+n) t_0'' H_1 + n t_0' H_1 - n t_0'' H_0 - n\eta (t_0'' H_0 + t_0' H_0')]$$

$$\frac{P_{02}^{2T}}{L_0 \beta_2 \sqrt{\beta_2}} = \frac{Q}{Q_{ref}} = \frac{Q_0}{Q_{ref}} + \frac{1}{R} \sqrt{\frac{\beta_2}{\beta_1}} \frac{Q_1}{Q_{ref}} = H_0^c H_0' + \frac{1}{R} \sqrt{\frac{\beta_2}{\beta_1}} H_0^c [H_1' + c \frac{H_0'}{H_0} H_1] \quad (4.3)$$

A further breakdown of the above expressions occurs when the different effects which make up the first-order correction term (as derived in Chapter II) are considered separately. To facilitate this process, let the terms due to velocity slip and temperature jump be redefined as follows

$$K_1 \downarrow_0' + (K_2 - K_1) \downarrow_0'(0) \downarrow_{1M} \equiv K_1 \left[\downarrow_{1SL} + \left(\frac{K_2}{K_1} - 1 \right) \downarrow_{1J} \right] \quad (4.4)$$

(It may be noted that the term marked by subscript \downarrow_{1M} is due to both the velocity-slip and temperature-jump boundary conditions, and the term marked by \downarrow_{1J} arises not due to the temperature-jump boundary condition alone, but rather due to the difference between the constants of proportionality for the velocity-slip and temperature-jump boundary conditions to the respective gradients at the wall). Using this definition and the results of Chapter II the stream function can be expanded as

$$\begin{aligned} \frac{\psi}{\psi_{ref}} &= \frac{\psi_0}{\psi_{ref}} + \frac{1}{R} \sqrt{\frac{\beta_2}{A}} \frac{\psi_{1c}}{\psi_{ref}} + \frac{C_2}{R} \sqrt{\frac{\beta_2}{A}} \frac{\psi_{1D}}{\psi_{ref}} + \frac{\sqrt{\frac{\beta_2 A}{RT_3}}}{\sqrt{RT_3}} \frac{k_w}{\mu_s} \sqrt{W} K_1 \left[\frac{\psi_{1SL}}{\psi_{ref}} + \left(\frac{K_2}{K_1} - 1 \right) \frac{\psi_{1J}}{\psi_{ref}} \right] + nV \sqrt{\frac{\beta_2}{A}} \frac{\psi_{1V}}{\psi_{ref}} = \\ &= \downarrow_0 + \frac{1}{R} \sqrt{\frac{\beta_2}{A}} \downarrow_{1c} + \frac{C_2}{R} \sqrt{\frac{\beta_2}{A}} \downarrow_{1D} + \frac{\sqrt{\frac{\beta_2 A}{RT_3}}}{\sqrt{RT_3}} \frac{k_w}{\mu_s} \sqrt{W} K_1 \left[\downarrow_{1SL} + \left(\frac{K_2}{K_1} - 1 \right) \downarrow_{1J} \right] + nV \sqrt{\frac{\beta_2}{A}} \downarrow_{1V} \end{aligned} \quad (4.5)$$

All the quantities in (4.3) can be written down in like manner. E.g.

$$\begin{aligned} \frac{U}{U_{ref}} &= \frac{U_0}{U_{ref}} + \frac{1}{R} \sqrt{\frac{\beta_2}{A}} \frac{U_{1c}}{U_{ref}} + \frac{C_2}{R} \sqrt{\frac{\beta_2}{A}} \frac{U_{1D}}{U_{ref}} + \frac{\sqrt{\frac{\beta_2 A}{RT_3}}}{\sqrt{RT_3}} \frac{k_w}{\mu_s} \sqrt{W} K_1 \left[\frac{U_{1SL}}{U_{ref}} + \right. \\ &\left. + \left(\frac{K_2}{K_1} - 1 \right) \frac{U_{1J}}{U_{ref}} \right] + nV \sqrt{\frac{\beta_2}{A}} \frac{U_{1V}}{U_{ref}} = \end{aligned}$$

$$\begin{aligned}
&= f_0' H_0 + \frac{1}{R} \sqrt{\frac{\nu_s}{A}} \left[H_0 f_{1c}' + f_0' H_{1c} - n\gamma f_0' H_0 \right] + \frac{\sigma}{R} \sqrt{\frac{\nu_s}{A}} \left[H_0 f_{1\sigma}' + f_0' H_{1\sigma} \right] + \\
&+ \sqrt{\frac{\nu_s A}{RT_s}} \frac{\mu_w}{\mu_s} \sqrt{W} k_1 \left\{ H_0 f_{1sc}' + f_0' H_{1sc} + \left(\frac{\mu_w}{\mu_s} - 1 \right) (H_0 f_{1s}' + f_0' H_{1s}) \right\} + \\
&+ nV \sqrt{\frac{\nu_s}{A}} \left[H_0 f_{1v}' + f_0' H_{1v} \right]
\end{aligned} \tag{4.6}$$

etc.

The results of the numerical calculations are given in Tables I and II. Table I gives the "incompressible" (i.e., constant-fluid-property) results; the boundary-layer term (given for reference only), curvature-correction term, displacement-correction term, velocity-slip and temperature-jump term, and the vorticity-correction term are tabulated in that order. For each term, the two-dimensional ($n=0$) and axially symmetric ($n=1$) results are tabulated subsequently, except for the vorticity correction term which exists only for the axially symmetric case. The appropriate differential equations, boundary conditions, and formulae expressing all the quantities listed in (4.3) are given as a convenient reference at the appropriate sections of the table.

A similar tabulation for the "compressible" (i.e., variable-fluid-property) case is given in Table II. Results are shown for the $W = 0.75, 0.5, 0.25,$ and 0.1 cases. The $W = 1.0$ case is identical to the "incompressible" result (cf. Appendix F). To illustrate these results, velocity and temperature profiles have been computed and are plotted in Figures 4 and 5. Shown are the uncorrected

boundary-layer profiles, boundary-layer profiles corrected due to the effect of curvature only, displacement effect only, velocity slip and temperature jump only, and vorticity effect only. For each case, the pertinent expansion parameter was assumed to be 20%; e.g., for the curvature correction only profile $U = U_0 + 0.2 U_{ic}$ etc.

For the velocity slip and temperature jump correction term the parameter was assumed to be 1.0, which is the right order of magnitude. To emphasize the effect of compressibility, cooling ratio $W = 0.1$ was chosen in these examples. The obtained curves are shown in two separate groupings. In figures 4a and 5a, the velocity and temperature profiles respectively are grouped together according to the type of correction that is (or is not) considered. Thus, separate groups are given for the boundary-layer profiles only, for boundary-layer profiles corrected for curvature only, for displacement effect only, etc. Each group of four curves then brings out the difference between the two dimensional and axially symmetric profiles for both the incompressible and compressible (i.e., constant- and variable-fluid-property) cases. In the second grouping (Figures 4b and 5b), the profiles are grouped together according to the type of flow, i.e., all two-dimensional incompressible profiles are shown in the same group, etc. This grouping then brings out the differences between the various correction effects, compares them to each other and the uncorrected (i.e., boundary-layer) profiles. The large increases in fluid velocity and temperature at the wall due to the velocity-slip and temperature-jump boundary conditions are especially noteworthy for the compressible case. This large increase is due mainly to the terms with the subscript in equation (4.4), i.e., to the terms arising from the difference between constants of proportionality and . The resulting velocity and temperature values at the wall are (according to the curves of

Figures 4, 5) nearly equal to, or slightly exceeding the free-stream values; also, the profile slopes at the wall appear to reverse sign. Such a large change cannot be expected to occur in the actual flow; it shows that for the parameters that were assumed $W = 0.1$, $\frac{k_2}{k_1} - 1 = 1$ the expansion procedure of the present analysis cannot be used any more if the velocity-slip and temperature-jump expansion parameter

$$\sqrt{\frac{\rho_\infty A}{\rho_w T_w}} \frac{k_w}{k_\infty} \sqrt{W} > 1, \quad \text{is } 20\% \text{ or larger.}$$

The quantities that are of the most practical interest are the shear and heat-transfer rate at the wall ($y = 0$). Table III gives these quantities for the range of cooling ratios that were employed in the calculations. The heat-transfer rates are expected to be very much dependent on the temperature difference between the free stream and the wall, $T_\infty - T_w$. A direct proportionality of wall heat-transfer rate to this temperature difference is usually assumed; then, in order to properly normalize the non-dimensional wall heat-transfer rates, they should be divided by the quantity $1 - W$. The heat-transfer rates are therefore given in this normalized form; they are equivalent to the usual boundary-layer-heat-transfer parameter Nu / \sqrt{Re} where Nu is the Nusselt number. A plot of shear and heat-transfer rate versus cooling ratio W is given in Figures 6 and 7 respectively. For the boundary-layer term, it is well known (e.g. Lees⁽²¹⁾) that the shear is not very sensitive to the presence or absence of cooling, and the normalized heat-transfer rate is even less so. This is true in spite of the fact that there is a sharp increase in the slopes of the velocity and temperature profiles near

the wall for the variable-property-fluid case, but there is a correspondingly large decrease in viscosity and heat conductivity in the cold-gas layer near the wall. The net effect is a moderate decrease in shear for small W (i.e., strong cooling), and an insignificantly small decrease in heat-transfer rate.

Discussion of Results

Among the correction effects that were considered, the behavior of the displacement term parallels that of the boundary-layer terms, as could be expected from the close relationship between them. Both the shear and heat-transfer rate are increased; this is in accordance with the sign convention that was adopted, which implies that the increase is due to the increase in velocity gradient A . (It may be noted that in most cases A will decrease due to the displacement effect of the boundary layer, thus the sign of the displacement coefficient will be negative, and in reality there will be a decrease in shear and heat-transfer rate. For very strongly cooled compressible boundary layers, it is, however, possible to have negative displacement thicknesses, implying an apparent "shrinkage" of the body, thereby increasing A , and the shear and heat-transfer rates likewise.)

The curvature effect tends to decrease the shear at the stagnation point; this decrease becomes smaller for small cooling ratios. The heat-transfer rate is affected differently by curvature for the two-dimensional and axially symmetric stagnation-point flows. In the former case, the heat transfer is decreased, and

almost completely unaffected by the cooling ratio. On the other hand, for the axially symmetric case the heat-transfer rate is increased by curvature; this increase becomes smaller for small cooling ratios. There is no simple explanation for these curvature effects; they arise from the inhomogeneous terms in the expanded differential equations, and also from the modified boundary conditions in the inviscid "outer" flow. For example, it is apparent by inspection of the velocity profiles of Figure 4, that the negative slope of the inviscid profile has an effect on the entire viscous layer. Another effect is the different pressure gradients experienced by adjacent layers of fluid in the viscous layer, due to the centrifugal pressure rise across the thick curved layer. There are many other terms in the Navier-Stokes equations that contribute to this effect; no attempt has been made to identify them separately since the effects always occur simultaneously.

Direct comparison of these curvature results with other theories cannot be made for the sphere, because the fully viscous shock-layer theories (references 13, and 31) include the displacement, curvature, and vorticity effects simultaneously, and for the shock density ratios employed the vorticity effect predominates. However, for cylinders, where the vorticity effect is of second order, Hoahizaki's⁽¹⁵⁾ theory shows an increase in heat-transfer rate at all Reynolds numbers, even the large ones (where presumably the second-order effects should be insignificant). This is contrary to the predictions of the present analysis, according to which the first-order corrections that were implied in the fully-viscous-layer theory,

namely the displacement and curvature effects, are both negative, i.e., they will tend to reduce the heat transfer instead of increasing it. Expansion of Hoshizaki's equations in the expansion parameter of the present analysis, $\frac{1}{\sqrt{Re}}$, resulted in the same equations that were derived in Chapter II, above. It was not possible, therefore, to resolve this discrepancy between the theories. Comparison with the experiments of Tewfik and Giedt^(40,41) seems to imply that a reduction in heat transfer due to curvature, rather than an increase, is in better agreement with experimental results. (A more detailed discussion of comparison with experiments follows in a subsequent paragraph.)

In agreement with previous reports (references 13, 19, 31, etc.), the existence of vorticity in the inviscid flow (to the first order present in the axially symmetric case only), tends to increase both the shear and heat-transfer rates. This increase is appreciably larger at small cooling ratios.

The behavior of the term due to slip and temperature jump at the wall is especially interesting. The expansion parameter for this term (cf. Chapter II) is essentially λ_w/δ , the mean free path at the wall divided by the boundary-layer thickness parameter. The term contains two separate effects; one effect arising when $K_1 = K_2$, the other arising due to the difference between these two constants. Considering the

$K_1 = K_2$ effect first it has already been noted (cf. equations (2.39) and subsequent paragraph) that this term leaves the wall heat-transfer rate unaffected. Similarly, using the known identities for the correction functions (e.g. 4.4) in the

expression for the shear correction (4.3), and comparing with boundary-layer equation (2.63) one immediately observes that $\frac{\tau_{12}}{\tau_{ref}} = -1$ at the wall irrespective of W .

The other slip and temperature-jump effect, the term proportional to $(K_2 - K_1)$, affects both the shear and the heat-transfer rates at the wall. The shear is increased; the increase varies from 0 to large values as W varies from 1 to small values. (The uncooled wall also represents the constant-property-fluid case, in this case K_2 can have obviously no effect on the shear since the momentum and energy equations are not coupled). But, as W becomes small, the mean free path near the wall, which determines the amount of slip, and which appears in the expansion parameter, also becomes small, since the cooled gas near the wall is more dense. It is of interest to find the combined effect of strong cooling on the two competing effects: the increased correction function and the decreased mean free path. Since

$\lambda \propto \frac{\mu}{\rho a}$ one may write

$$\frac{\tau_w}{\delta} \tau_{12} = \frac{\tau_s}{\delta} \frac{\tau_w}{\tau_s} \tau_{12} = \frac{\tau_s}{\delta} \frac{\mu_w}{\mu_s} \frac{\rho_s}{\rho_w} \sqrt{\frac{T_s}{T_w}} \tau_U = \frac{\tau_s}{\delta} W^{\frac{1}{2}+w} \tau_{12}$$

The quantity $W^{\frac{1}{2}+w} \tau_{12}(0)$ is plotted in Figure 6; the graph shows that as W changes from 1.0 (no cooling) to 0 (strong cooling), the quantity increases from 0 and then appears to approach a constant value for very small W . The combined effect on shear of the "slip and jump" term is then an increase for strong cooling, because as $W \rightarrow 0$, the $W^{\frac{1}{2}+w} \tau_{12}$ term dominates; whereas in the region near $W = 1$ the only significant effect is the term $\frac{\tau_{12L}}{\tau_{ref}} = -1$, and the shear is thus decreased.

The wall-heat-transfer-rate correction effect, $Q_{11}(0)$, shows a behavior similar to $\zeta_{11}(0)$. The effect tends to decrease the heat-transfer rate; as W becomes very small the decrease becomes excessively large. But if the quantity $W^{1+\omega} Q_{11}(0)$ is plotted, it remains reasonable in magnitude throughout the entire range of W . These observations indicate that for the effect that is under consideration, namely, the correction arising due to the difference in the constants of proportionality for the velocity slip and temperature jump, K_1 and K_2 , the proper parameter that determines the order of magnitude of this effect is not λ_w/δ , as was formerly supposed (e.g. references 9, 31, etc.) but rather λ_s/δ . This implies that the reduction in heat transfer at the stagnation point of a blunt body due to slip could be significant even for the case of strong cooling in hypersonic flow. Just how large this reduction may be in different flight regimes is indicated by the lines of constant λ_s/δ plotted in Figure 3.

Comparison of Results with Experiments

It is finally of interest to compare the numerical results presented in this chapter to experimentally determined properties of low-Reynolds-number stagnation-point flow. For a particular experiment, it is necessary that the appropriate flow parameters, Reynolds number, stagnation-point velocity gradient, mean free path, etc., be known, and then the results of the present analysis can be applied to predict the flow properties. In one series of experiments Neice, Rutowski, and Chan⁽²⁶⁾ measured heat-transfer rates at the

blunt nose of a hemisphere cylinder placed into a low-density hypersonic shock tunnel. But these experimental results are not too well suited for comparison with the present analysis. The reason for this is partly the difference between the fluid properties of the present analysis and those of the high temperature dissociated air of the shock tunnel. This difficulty could be overcome by taking ratios of the theoretical low-Reynolds-number and boundary-layer results, and then applying this ratio to available dissociated-air boundary-layer solutions to obtain a reasonable theoretical prediction, which could then be compared to the experimental results. (This was the scheme used by the authors of the experiments, who compared their results with the constant-fluid-property, "exact," viscous shock-layer solution of reference 13.) A more serious difficulty in using these experiments as a basis of comparison is the predominance of a very large vorticity effect, which puts the results beyond the reasonable validity of the expansion procedure of the present analysis.

For cylinders, an extensive series of low-Reynolds-number flow measurements were performed by Tewfik and Giedt^{(40), (41)}. These experiments were performed in the Mach-number range of 1.3 to 5.7, and with low temperature (and therefore non-dissociated) air. Thus the fluid properties that were used in the present analysis are exactly those that are applicable to these experimental conditions. Furthermore, for the range of flow parameters that were employed in these tests, all significant low-Reynolds-number effects are about equally large, sufficiently large to be important, yet not large enough to preclude reasonable applicability of the expansion procedure of the present analysis. For these reasons, a comparison of

the experimental results with the present theory seemed especially appropriate, and was undertaken in detail. The pertinent calculation procedure is described in Appendix H; the results of the calculations are presented in Table IV.

The free-stream Mach number M_∞ , Reynolds number Re_∞ (ranging from 37 to 4100), and the wall-to-stagnation-temperature ratio W (ranging from 0.24 to 0.74) are the independent parameters which are the input necessary for application of the theory. In addition, the stagnation-point velocity gradients were also measured and recorded; from these the significant Reynolds number, $\frac{A R^2}{\nu}$ (based on stagnation fluid properties) could be calculated. The inverse square root of this quantity is the expansion parameter of the present theory; it determines the size of the curvature correction. Both of these quantities are tabulated in the table, the former ranging from 25 to 930, the latter from 3.3% to 20%. The quantity that is significant for the velocity-slip and temperature-jump effect, $\frac{\lambda w}{\sqrt{\nu} k}$, is also tabulated; it ranges from 1.8% to 14%.

Based on the above information, the theoretical results discussed earlier in this chapter were used to predict stagnation-point heat-transfer rates. Predictions were based both on the constant-fluid-property and the variable-fluid-property theories. Curvature and velocity-slip-temperature-jump corrections were considered. No other low-Reynolds-number effects occur since there is no first-order vorticity correction for cylinders, and the effect of boundary-layer displacement on the external flow has already been

accounted for by using the experimentally measured velocity gradients. The predictions are presented in terms of a comparison to the heat-transfer rate based on uncorrected constant-fluid-property boundary-layer theory, viz.

$$\frac{Q_{\text{conc}}(0)}{(1-w)k_s T_s / \sqrt{\frac{\mu_s}{\rho_s}}} = 0.5123$$

All the corrections that were calculated, are shown in Table IV, as a fraction of the above number, in the following order: incompressible curvature correction, incompressible temperature-jump correction, total incompressible correction, compressible boundary-layer correction, compressible curvature, temperature-jump, and total compressible corrections. The experimental results are presented on the same basis, as a deviation from the prediction of incompressible boundary-layer theory.

The tabulated predictions indicate a reduction in heat transfer due to all the effects that were considered; the reduction is larger in the compressible case, especially for the temperature-jump term. However, the experimentally measured heat-transfer rates uniformly differ from the incompressible boundary-layer prediction by significantly larger amounts than either combination of correction terms predict. In order to investigate the possibility of a relation between this discrepancy and the displacement effect, displacement coefficients C_D were calculated for all the points. The calculations were based on comparing the experimentally obtained velocity gradients with the high-Reynolds-number velocity gradients given by Reshotko and Beckwith⁽³³⁾ (cf. Appendix H.) There appears to be no relation, nor do the observed discrepancies show any

other obvious regularity. The discrepancies then remain unexplained, pending further comparison with other experimental results. Nevertheless, it can at least be ascertained that the predictions of the theory show the same trend as the experimental results; namely a reduction in heat transfer. This is significant when compared to the predictions of references 15 and 31, which show an increase in stagnation-point heat-transfer rate for a cylinder at low Reynolds numbers (these calculations neglected the decrease due to velocity slip and temperature jump.)

APPENDIX A

Derivation of the Equations of Motion

The Navier-Stokes (momentum) equations for steady flow can be written down in vector form

$$\rho \left[(\text{curl } \vec{q}) \times \vec{q} + \frac{1}{2} \text{grad } q^2 \right] + \text{grad } p = \frac{4}{3} \text{grad } (\mu \text{div } \vec{q}) + \text{grad } (\vec{q} \cdot \text{grad } \mu) - \vec{q} \nabla^2 \mu + \text{grad } \mu \times \text{curl } \vec{q} - \text{div } \vec{q} \text{ grad } \mu - \text{curl } \text{curl } \mu \vec{q} \quad (\text{A.1})$$

A general orthogonal coordinate system can be defined by the directions

$$\vec{e}_1, \vec{e}_2, \vec{e}_3$$

with coordinates

$$x_1, x_2, x_3 \quad (\text{A.2})$$

and metric functions

$$h_1, h_2, h_3$$

Let $x_1 = \text{constant}$ define the planes of symmetry of the flow field, so that the derivatives $\frac{\partial}{\partial x_1}$ of all quantities vanish. For this case, a compressible stream function can be defined by

$$\vec{q} = \text{curl } \vec{e}_2 \frac{\psi}{h_2} = \left[-\frac{\vec{e}_1}{h_2 h_3} \frac{\partial \psi}{\partial x_3}, 0, \frac{\vec{e}_3}{h_1 h_2} \frac{\partial \psi}{\partial x_1} \right] \quad (\text{A.3})$$

which identically satisfies the continuity equation for steady flow.

Substituting (A.2) and (A.3) into (A.1) and using vector algebra, the

\vec{e}_1 component of the momentum equation can be written down

as

$$\begin{aligned} & \frac{1}{g^2 h_1 h_2 h_3} \left\{ \frac{1}{h_1 h_2} \frac{\partial \psi}{\partial x_1} \left(\frac{h_3}{h_1} \frac{\partial \psi}{\partial x_1} \frac{\partial g}{\partial x_1} + \frac{h_1}{h_3} \frac{\partial \psi}{\partial x_3} \frac{\partial g}{\partial x_3} \right) - \frac{g}{h_1} \frac{\partial \psi}{\partial x_1} \left(\frac{\partial}{\partial x_1} \frac{h_3}{h_1 h_2} \frac{\partial \psi}{\partial x_1} + \frac{\partial}{\partial x_3} \frac{h_1}{h_1 h_3} \frac{\partial \psi}{\partial x_3} \right) - \right. \\ & - h_2 h_3 \frac{\partial g}{\partial x_1} \left[\left(\frac{1}{h_1 h_2} \frac{\partial \psi}{\partial x_1} \right)^2 + \left(\frac{1}{h_1 h_3} \frac{\partial \psi}{\partial x_3} \right)^2 \right] + g \left[\frac{\partial \psi}{\partial x_3} \frac{\partial}{\partial x_1} \frac{1}{h_2 h_3} \frac{\partial \psi}{\partial x_3} + \frac{h_3}{h_1} \frac{\partial \psi}{\partial x_1} \frac{1}{h_2 h_3} \frac{\partial \psi}{\partial x_1} \right] + \\ & + g^2 h_2 h_3 \frac{\partial p}{\partial x_1} \left. \right\} = \frac{4}{3} \frac{1}{h_1} \frac{\partial}{\partial x_1} \frac{\mu}{g^2 h_1 h_2 h_3} \left[\frac{\partial \psi}{\partial x_3} \frac{\partial g}{\partial x_1} - \frac{\partial \psi}{\partial x_1} \frac{\partial g}{\partial x_3} \right] + \frac{1}{h_1} \frac{\partial}{\partial x_1} \frac{1}{g h_1 h_2 h_3} \left(\frac{\partial \psi}{\partial x_1} \frac{\partial h}{\partial x_3} - \right. \\ & \left. - \frac{\partial \psi}{\partial x_3} \frac{\partial h}{\partial x_1} \right) + \frac{1}{h_2 h_3} \frac{\partial \psi}{\partial x_3} \frac{1}{g h_1 h_2 h_3} \left[\frac{\partial}{\partial x_1} \frac{h_2 h_3}{h_1} \frac{\partial h}{\partial x_1} + \frac{\partial}{\partial x_3} \frac{h_1 h_2}{h_3} \frac{\partial h}{\partial x_3} \right] + \\ & + \frac{1}{h_3} \frac{\partial \mu}{\partial x_3} \frac{1}{h_2 h_3} \left[\frac{\partial}{\partial x_3} \frac{h_1}{h_2 h_3 g} \frac{\partial \psi}{\partial x_3} + \frac{\partial}{\partial x_1} \frac{h_3}{h_1 h_3 g} \frac{\partial \psi}{\partial x_1} \right] + \frac{1}{h_1} \frac{\partial \mu}{\partial x_1} \frac{1}{g^2 h_1 h_2 h_3} \left[\frac{\partial \psi}{\partial x_1} \frac{\partial g}{\partial x_3} - \frac{\partial \psi}{\partial x_3} \frac{\partial g}{\partial x_1} \right] - \\ & - \frac{1}{h_2 h_3} \frac{\partial}{\partial x_3} \frac{h_2}{h_1 h_3} \left[\frac{\partial}{\partial x_3} \frac{\mu h_1}{g h_2 h_3} \frac{\partial \psi}{\partial x_3} + \frac{\partial}{\partial x_1} \frac{\mu h_3}{g h_1 h_2} \frac{\partial \psi}{\partial x_1} \right] \end{aligned} \quad (A.4)$$

Similarly, the \vec{e}_3 component becomes

$$\begin{aligned} & \frac{1}{g^2 h_1 h_2 h_3} \left\{ \frac{1}{h_2 h_3} \frac{\partial \psi}{\partial x_3} \left(\frac{h_3}{h_1} \frac{\partial \psi}{\partial x_1} \frac{\partial g}{\partial x_1} + \frac{h_1}{h_3} \frac{\partial \psi}{\partial x_3} \frac{\partial g}{\partial x_3} \right) - \frac{g}{h_3} \frac{\partial \psi}{\partial x_3} \left(\frac{\partial}{\partial x_1} \frac{h_3}{h_1 h_2} \frac{\partial \psi}{\partial x_1} + \right. \right. \\ & \left. \left. + \frac{\partial}{\partial x_3} \frac{h_1}{h_2 h_3} \frac{\partial \psi}{\partial x_3} \right) - h_1 h_2 \frac{\partial g}{\partial x_3} \left[\left(\frac{1}{h_1 h_2} \frac{\partial \psi}{\partial x_1} \right)^2 + \left(\frac{1}{h_1 h_3} \frac{\partial \psi}{\partial x_3} \right)^2 \right] + \right. \\ & \left. + g \left[\frac{\partial \psi}{\partial x_1} \frac{\partial}{\partial x_3} \frac{1}{h_1 h_2} \frac{\partial \psi}{\partial x_1} + \frac{h_1}{h_3} \frac{\partial \psi}{\partial x_3} \frac{\partial}{\partial x_3} \frac{1}{h_2 h_3} \frac{\partial \psi}{\partial x_3} \right] + g^2 h_1 h_2 \frac{\partial p}{\partial x_3} \right\} = \\ & = \frac{4}{3} \frac{1}{h_3} \frac{\partial}{\partial x_3} \frac{\mu}{g^2 h_1 h_2 h_3} \left[\frac{\partial \psi}{\partial x_3} \frac{\partial g}{\partial x_1} - \frac{\partial \psi}{\partial x_1} \frac{\partial g}{\partial x_3} \right] + \frac{1}{h_3} \frac{\partial}{\partial x_3} \frac{1}{g h_1 h_2 h_3} \left(\frac{\partial \psi}{\partial x_1} \frac{\partial h}{\partial x_3} - \right. \\ & \left. - \frac{\partial \psi}{\partial x_3} \frac{\partial h}{\partial x_1} \right) - \frac{1}{h_1 h_2} \frac{\partial \psi}{\partial x_1} \frac{1}{g h_1 h_2 h_3} \left[\frac{\partial}{\partial x_1} \frac{h_2 h_3}{h_1} \frac{\partial h}{\partial x_1} + \frac{\partial}{\partial x_3} \frac{h_1 h_2}{h_3} \frac{\partial h}{\partial x_3} \right] - \\ & - \frac{1}{h_1 h_3} \frac{\partial \mu}{\partial x_1} \left[\frac{\partial}{\partial x_3} \frac{h_1}{g h_2 h_3} \frac{\partial \psi}{\partial x_3} + \frac{\partial}{\partial x_1} \frac{h_3}{g h_1 h_2} \frac{\partial \psi}{\partial x_1} \right] - \frac{1}{g^2 h_1 h_2 h_3} \frac{\partial \mu}{\partial x_3} \left[\frac{\partial \psi}{\partial x_1} \frac{\partial g}{\partial x_3} - \right. \\ & \left. - \frac{\partial \psi}{\partial x_3} \frac{\partial g}{\partial x_1} \right] + \frac{1}{h_1 h_2} \frac{\partial}{\partial x_1} \frac{h_2}{h_1 h_3} \left[\frac{\partial}{\partial x_3} \frac{\mu h_1}{g h_2 h_3} \frac{\partial \psi}{\partial x_3} + \frac{\partial}{\partial x_1} \frac{\mu h_3}{g h_1 h_2} \frac{\partial \psi}{\partial x_1} \right] \end{aligned} \quad (A.5)$$

For the special case of a "polar" coordinate system the coordinates and metric functions are

$$x_1 = r, \quad x_2 = (1-n)z + n\varphi, \quad x_3 = \theta$$

$$h_1 = 1, \quad h_2 = (r \sin \theta)^n, \quad h_3 = r$$

(A.6)

where $n = 0$ is the plane two-dimensional, and $n = 1$ the axially symmetric case. (These are the conventional cylindrical and spherical polar coordinate systems respectively). Using (A.6) in (A.4) and (A.5), and performing all the algebra, the two momentum equations become

$$\frac{1}{s (r \sin \theta)^{2n}} \left\{ \frac{\psi_r \psi_{\theta} s_{\theta}}{r^2 s} - \frac{\psi_r^2}{r} - \frac{\psi_r \psi_{\theta\theta}}{r^2} + \frac{n \cos \theta \psi_r \psi_{\theta}}{r^2 \sin \theta} - \frac{\psi_{\theta}^2 s_r}{s r^2} + \right.$$

$$\left. + \frac{\psi_{\theta} \psi_{\theta r}}{r^2} - \frac{(1+n) \psi_{\theta}^2}{r^3} \right\} + P_r = \frac{1}{(r \sin \theta)^n s r} \left\{ \frac{4}{3} \frac{\psi_{\theta} \mu_r s_r}{s} - \frac{8}{3} \frac{\psi_{\theta} \mu s_r^2}{s^2} - \right.$$

$$\left. - \frac{4}{3} \frac{(1+n) \psi_{\theta} \mu s_{\theta}}{s r} + \frac{2}{3} \frac{\psi_r \mu_r s_{\theta}}{s} + \frac{2}{3} \frac{\psi_r \mu s_r s_{\theta}}{s^2} + \frac{7+n}{3} \frac{\psi_r \mu s_{\theta}}{s r} + \frac{2(1+n) \psi_{\theta} \mu_r}{r} - \right.$$

$$\left. - \frac{\psi_r \mu_r s_r}{s} - \frac{(1+n) \psi_r \mu_{\theta}}{r} + \psi_{rr} \mu_{\theta} - 2 \psi_{r\theta} \mu_r + \frac{n \cos \theta \psi_{\theta} \mu_r}{r^2 \sin \theta} - \frac{\psi_{\theta r} \mu_r}{r^2} + \right.$$

$$\left. + \frac{\psi_{\theta} \mu_r s_{\theta}}{s r^2} + \frac{n \cos \theta \psi_{\theta r} \mu}{r^2 \sin \theta} - \frac{n \cos \theta \psi_{\theta} \mu}{r^2 \sin^2 \theta} - \frac{n \cos \theta \psi_{\theta} \mu s_{\theta}}{s r^2 \sin \theta} - \frac{\psi_{\theta r} \mu}{r^2} + \right.$$

$$\left. + \frac{2 \psi_{\theta r} \mu s_{\theta}}{s r^2} - \frac{n \psi_{\theta} \mu}{r^2} + \frac{\psi_{\theta} \mu s_{\theta r}}{s r^2} - \frac{2 \psi_{\theta} \mu s_{\theta}^2}{s^2 r^2} - \psi_{rr} \mu - \right.$$

$$\left. - \frac{(1-n) \psi_{\theta} \mu}{r} + \frac{\psi_{\theta r} \mu s_{\theta}}{s} + \frac{\psi_{\theta r} \mu s_r}{s} + \frac{\psi_{\theta} \mu s_{\theta r}}{s} \right\} \quad (\text{A.7})$$

in the r direction, and

$$\begin{aligned}
 & \frac{1}{r g(r \sin \theta)^2 n} \left\{ \frac{\psi_0 \psi_r s r}{s} - \frac{(1-n) \psi_0 \psi_r}{r} - \psi_0 \psi_{rr} - \frac{\psi_r^2 s r}{s} + \psi_r \psi_{r\theta} - \frac{n \cos \theta \psi_r^2}{\sin \theta} \right\} + \\
 & + \frac{P_r}{r} = \frac{1}{s(r \sin \theta)^2 n} \left\{ \frac{4}{3} \frac{\psi_0 \mu_0 s r}{s^2 r^2} - \frac{n \cos \theta \psi_0 \mu_0 s r}{3 s^2 \sin \theta} - \frac{10}{3} \frac{\psi_0 \mu_0 s r}{s r^2} + \right. \\
 & + \frac{8}{3} \frac{\psi_0 \mu_0 s r^2}{s^2 r^2} + \frac{4}{3} \frac{n \cos \theta \psi_0 \mu_0 s r}{s r^2 \sin \theta} + \frac{1}{3} \frac{\psi_{0r} \mu_0 s r}{s r^2} + \frac{1}{3} \frac{\psi_0 \mu_{0r} s r}{s r^2} - \\
 & - \frac{7}{3} \frac{\psi_{0\theta} \mu_0 s r}{s r^2} - \frac{4}{3} \frac{\psi_r \mu_{0\theta} s r}{s r^2} - \frac{\psi_{0r} \mu_{r\theta} s r}{s r^2} + \frac{n \cos \theta \psi_0 \mu_r}{r^2 \sin \theta} - \\
 & - \frac{2 n \cos \theta \psi_r \mu_{r\theta}}{r^2 \sin \theta} + \frac{2 \psi_{0r} \mu_{r\theta}}{r^2} - \frac{\psi_{0r} \mu_{r\theta}}{r^2} - \frac{(1+n) \psi_r \mu_r}{r} + \psi_{rr} \mu_r - \\
 & - \frac{\psi_r \mu_{r s r}}{s} - \frac{2 \psi_{0r} \mu_{r\theta}}{r^3} + \frac{\psi_{0\theta} \mu_r}{r^2} - \frac{2 \psi_{0\theta} \mu_r}{r^3} - \frac{n \cos \theta \psi_{0r} \mu_r}{r^2 \sin \theta} + \\
 & + \frac{2 n \cos \theta \psi_0 \mu_r}{r^3 \sin \theta} + \frac{2 \psi_{0r} \mu_{r\theta}}{s r^3} + \psi_{0r r} \mu_r - \frac{2 \psi_{0r} \mu_{r\theta} s r}{s} + \frac{(1-n) \psi_{0r} \mu_r}{r} - \\
 & \left. - \frac{(1-n) \psi_r \mu_{r s r}}{s r} - \frac{(1-n) \psi_r \mu_r}{r^2} - \frac{\psi_r \mu_{r s r}}{s} + \frac{2 \psi_r \mu_{r s r}^2}{s^2} \right\} \quad (A.8)
 \end{aligned}$$

in the θ direction. The subscripts r and θ denote the respective partial derivatives.

Now the energy equation for steady flow can be considered.

In vector notation

$$\begin{aligned}
 s \rho \vec{q} \cdot \text{grad} T - \vec{q} \cdot \text{grad} p &= \text{div } k \text{ grad} T + \mu \left[\nabla^2 (q^2) + \right. \\
 & \left. + (\text{curl } \vec{q})^2 - 2 \text{div} (\vec{q} \times \text{curl } \vec{q}) - 2 \vec{q} \cdot \text{grad} (\text{div } \vec{q}) - \frac{2}{3} (\text{div } \vec{q})^2 \right]
 \end{aligned}$$

(A.9)

Expanding in terms of the general coordinate system of

(A.2), the energy equation (A.9) becomes

$$\begin{aligned}
 & \frac{4}{h_1 h_2 h_3} \left[\frac{\partial \Psi}{\partial x_1} \frac{\partial T}{\partial x_3} - \frac{\partial \Psi}{\partial x_3} \frac{\partial T}{\partial x_1} \right] - \frac{1}{h_1 h_2 h_3 s} \left[\frac{\partial \Psi}{\partial x_1} \frac{\partial \rho}{\partial x_3} - \frac{\partial \Psi}{\partial x_3} \frac{\partial \rho}{\partial x_1} \right] = \\
 & = \frac{1}{h_1 h_2 h_3} \left[\frac{\partial}{\partial x_1} \frac{h_2 h_3}{h_1} k \frac{\partial T}{\partial x_1} + \frac{\partial}{\partial x_3} \frac{h_2 h_1}{h_3} k \frac{\partial T}{\partial x_3} \right] + \mu \left\{ \frac{1}{h_1 h_2 h_3} \left[\frac{\partial}{\partial x_1} \frac{h_2 h_3}{h_1} \frac{\partial}{\partial x_1} + \right. \right. \\
 & + \frac{\partial}{\partial x_3} \frac{h_1 h_2}{h_3} \frac{\partial}{\partial x_3} \left. \right] \frac{1}{h_1^2 s^2} \left[\left(\frac{1}{h_3} \frac{\partial \Psi}{\partial x_3} \right)^2 + \left(\frac{1}{h_1} \frac{\partial \Psi}{\partial x_1} \right)^2 \right] + \left(\frac{1}{h_1 h_3} \right)^2 \left[\frac{\partial}{\partial x_3} \frac{h_1}{s h_2 h_3} \frac{\partial \Psi}{\partial x_3} + \right. \\
 & + \frac{\partial}{\partial x_1} \frac{h_2}{s h_1 h_2} \frac{\partial \Psi}{\partial x_1} \left. \right]^2 - \frac{2}{h_1 h_2 h_3} \left[\frac{\partial}{\partial x_1} \frac{h_2}{s h_1} \frac{\partial \Psi}{\partial x_1} \frac{1}{h_1 h_3} \left(\frac{\partial}{\partial x_3} \frac{h_1}{s h_2 h_3} \frac{\partial \Psi}{\partial x_3} + \right. \right. \\
 & + \frac{\partial}{\partial x_1} \frac{h_2}{s h_1 h_2} \frac{\partial \Psi}{\partial x_1} \left. \right) + \frac{\partial}{\partial x_3} \frac{h_1}{s h_3} \frac{\partial \Psi}{\partial x_3} \frac{1}{h_1 h_2} \left(\frac{\partial}{\partial x_3} \frac{h_1}{s h_2 h_3} \frac{\partial \Psi}{\partial x_3} + \frac{\partial}{\partial x_1} \frac{h_2}{s h_1 h_2} \frac{\partial \Psi}{\partial x_1} \right) \left. \right] - \\
 & - \frac{2}{h_1 h_2 h_3 s} \left[\frac{\partial \Psi}{\partial x_1} \frac{\partial}{\partial x_3} - \frac{\partial \Psi}{\partial x_3} \frac{\partial}{\partial x_1} \right] \frac{1}{h_1 h_2 h_3} \left[\frac{\partial}{\partial x_3} \frac{1}{s} \frac{\partial \Psi}{\partial x_1} - \frac{\partial}{\partial x_1} \frac{1}{s} \frac{\partial \Psi}{\partial x_3} \right] - \\
 & \left. - \frac{2}{3} \frac{1}{(h_1 h_2 h_3)^2 s^4} \left[\frac{\partial \Psi}{\partial x_3} \frac{\partial s}{\partial x_1} - \frac{\partial \Psi}{\partial x_1} \frac{\partial s}{\partial x_3} \right]^2 \right\} \quad (A.10)
 \end{aligned}$$

Expanding in the "polar" coordinates of (A.6), the equation

becomes

$$\begin{aligned}
 & \rho (\Psi_r T_\theta - \Psi_\theta T_r) + \frac{1}{3} (\Psi_r P_r - \Psi_r P_\theta) = (\sin \theta)^n \left[r^{1+n} k T_{rr} + r^{1+n} k_r T_r + \right. \\
 & + (1+n) r^n k T_r + r^{n-1} k T_{\theta\theta} + r^{n-1} k_\theta T_\theta + \frac{n \cos \theta}{\sin \theta} r^{n-1} k T_\theta \left. \right] + \mu \Phi \quad (A.11)
 \end{aligned}$$

where Φ is the dissipation function.

For future reference, the expression for vorticity in the general coordinate system is

$$\begin{aligned}\Omega_2 \equiv \text{curl } \vec{q} &= \text{curl } \frac{1}{s} \text{curl } \vec{e}_2 \frac{\Psi}{h_2} = -\frac{1}{s^2} (\text{grad } s) \times (\text{curl } \vec{e}_2 \frac{\Psi}{h_2}) + \frac{1}{s} \text{curl } \text{curl } \vec{e}_2 \frac{\Psi}{h_2} = \\ &= \frac{1}{s^2} \frac{1}{h_1 h_2 h_3} \left[\frac{h_3}{h_1} \frac{\partial \Psi}{\partial x_1} \frac{\partial s}{\partial x_1} + \frac{h_1}{h_3} \frac{\partial \Psi}{\partial x_3} \frac{\partial s}{\partial x_3} \right] - \frac{1}{s h_1 h_3} \left[\frac{\partial}{\partial x_3} \frac{h_1}{h_2 h_3} \frac{\partial \Psi}{\partial x_3} + \frac{\partial}{\partial x_1} \frac{h_3}{h_1 h_2} \frac{\partial \Psi}{\partial x_1} \right] \\ &\hspace{15em} \text{(A.12)}\end{aligned}$$

For the special case of the "polar" coordinate system of

(A.6)

$$\begin{aligned}\Omega &= \frac{1}{s^2 (r \sin \theta)^n} \left[\Psi_r s_r + \frac{\Psi_\theta s_\theta}{r^2} - \frac{s \Psi_{\theta\theta}}{r^2} + \frac{n \cos \theta s \Psi_\theta}{r^2 \sin \theta} - \right. \\ &\quad \left. - s \Psi_{rr} + (n-1) \frac{s \Psi_r}{r} \right]\end{aligned}$$

(A.13)

APPENDIX B

Derivation of Boundary Conditions at the Solid-Gas Interface.

The boundary conditions for a gas flowing along a solid body can be derived from the kinetic theory of gases, and are given by many authors, e.g. Schaaf and Chambre⁽³⁶⁾ as

$$u(0) = \frac{2-\delta}{\delta} \lambda \left. \frac{\partial u}{\partial y} \right|_{y=0} + \frac{3}{4} \frac{\mu}{sT} \left. \frac{\partial T}{\partial x} \right|_{y=0} \quad (\text{B.1})$$

$$T(0) - T_w = \frac{2-\alpha_w}{\alpha_w} \frac{2T}{\delta+1} \frac{1}{\lambda} \left. \frac{\partial T}{\partial y} \right|_{y=0} \quad (\text{B.2})$$

where the same reference gives the mean free path in terms of the fluid properties, as follows:

$$\lambda = \sqrt{\frac{\pi}{2}} \sqrt{\delta} \frac{\mu}{s a} = \sqrt{\frac{\pi}{2Q}} \frac{\mu}{s \sqrt{T}} \quad (\text{B.3})$$

In addition, the no-through-flow boundary condition can be used

$$v(0) = 0 \quad (\text{B.4})$$

These expressions can be applied to the stagnation-point flow that is being considered by substituting into them changes of variables and expansions (2.1) through (2.7). To find u (2.2) and (2.4) can be substituted into (1.4).

$$u = A \times \left\{ \frac{f_0'}{f_0} + \frac{1}{R \sqrt{A}} \left[\frac{f_1'}{f_0} - \frac{n \eta f_0'}{f_0} - \frac{f_0' f_1'}{f_0^2} \right] + \dots \right\} \quad (\text{B.5})$$

Differentiating once one obtains

$$\frac{\partial u}{\partial y} = \frac{A_x}{R} \left\{ R \sqrt{\frac{A}{\nu_s}} \left[\frac{t_0''}{t_0} - \frac{t_0' t_0'}{t_0^2} \right] + \frac{t_1''}{t_0} - \frac{t_1' t_0'}{t_0^2} - \frac{n(t_0' + \eta t_0'')}{t_0} + \right. \\ \left. + \frac{n \eta t_0' t_0'}{t_0^2} - \frac{t_0'' t_1 + t_0' t_1'}{t_0^2} + \frac{2 t_0' t_0' t_1'}{t_0^3} + \dots \right\}$$

(B.6)

Similarly, the expression for v becomes

$$v = -(1+n) \sqrt{\nu_s A} \left\{ \frac{t_0}{t_0} + \frac{1}{R} \sqrt{\frac{\nu_s}{A}} \left[\frac{t_1}{t_0} - \frac{(1+n) \eta t_0}{t_0} - \frac{t_0 t_1}{t_0^2} \right] + \dots \right\}$$

(B.7)

The $\frac{\partial T}{\partial x}$ term in the slip velocity is of order ν_s , and hence, will not contribute to the order 1 and order $\sqrt{\nu_s}$ that are being considered. Equation (2.3) can now be used to find

$$\frac{\partial T}{\partial y} = \frac{T_s}{R} \left[R \sqrt{\frac{A}{\nu_s}} H_0' + H_1' + \dots \right]$$

(B.8)

and finally equations (2.3), (2.4) and (2.7) to express

$$\lambda = \sqrt{\frac{\pi}{2Q}} \frac{\nu_s}{\sqrt{T_s}} \left\{ \frac{h_0}{h_s} \frac{1}{t_0 H_0^{3/2}} + \frac{1}{R} \sqrt{\frac{\nu_s}{A}} \left[\frac{h_0}{h_s} T_s \frac{H_1}{t_0 H_0^{3/2}} - \right. \right. \\ \left. \left. - \frac{h_0}{h_s} \left(\frac{t_1}{t_0^2} H_0^{3/2} + \frac{1}{2} \frac{H_1}{t_0 H_0^{3/2}} \right) \right] + \dots \right\}$$

(B.9)

Using (B.5), (B.6) in (B.1), and equating like powers of Reynolds-number parameter $\frac{1}{R} \sqrt{\frac{\nu_s}{A}}$, one obtains

$$\frac{f_0'(0)}{f_0(0)} = 0$$

(B.10)

and (using this result)

$$f_1'(0) = \frac{2-d}{\delta} \frac{\sqrt{\pi}}{\sqrt{2}} \frac{AR}{\sqrt{RT_s}} \frac{\mu_0(0)}{\mu_s} \frac{f_0''(0)}{f_0(0) \sqrt{H_0(0)}}$$

(B.11)

Similarly, using (B.7) in (B.4)

$$f_0(0) = 0$$

$$f_1(0) = 0$$

(B.12)

Finally, (B.8) and (B.9) are used in (B.2)

$$H_0(0) = \frac{T_w}{T_s} \equiv W$$

$$H_1(0) = \frac{2-\alpha_a}{\alpha_a} \frac{\sqrt{\pi}}{\sqrt{2}} \frac{AR}{\sqrt{RT_s}} \frac{2\tau_w}{\tau_w+1} \frac{1}{\tau_w} \frac{\mu_0(0)}{\mu_s} \frac{H_0'(0)}{f_0(0) \sqrt{H_0(0)}}$$

(B.13)

Since (B.13) shows that $\mu_0(0) = \mu_w$, the last expression can be rewritten as

$$H_1(0) = \frac{2-\alpha_a}{\alpha_a} \frac{\sqrt{\pi}}{\sqrt{2}} \frac{AR}{\sqrt{RT_s}} \frac{2\tau_w}{\tau_w+1} \frac{1}{\tau_w} \frac{k_w}{k_s} \frac{c_s}{c_w} \frac{1}{W} \frac{H_0'(0)}{f_0(0)}$$

(B.14)

APPENDIX C

Numerical Solution of Inviscid Hypersonic Flow Near Stagnation Points of Sphere and Cylinder.

The first step in the numerical solution is the solution of equation (3.7), which relates $\frac{\Delta}{R}$ to e . For the case of the cylinder, the solution can be obtained graphically by writing the equation in the form

$$\frac{C_I}{C_K}(e) = \frac{K_I}{I_I} \left[\frac{e-1}{e \left(1 + \frac{\Delta}{R}\right)} \right] \quad (C.1)$$

The functions on the two sides of (C.1) were found numerically as functions of their respective arguments with the aid of Bessel-function tables and then plotted on the same graph. Corresponding values of the two arguments were then found graphically, from which the corresponding values of $\frac{\Delta}{R}$ and e were computed. These results were then used in (3.10a) to calculate the velocity-gradient parameter.

For the sphere a similar procedure was followed, except here a graphical solution was not necessary since (3.7) is a quadratic in e , and can be solved analytically

$$e = \frac{6 - 20\left(1 + \frac{\Delta}{R}\right)^2 + 14\left(1 + \frac{\Delta}{R}\right)^5 + \left(1 + \frac{\Delta}{R}\right) \sqrt{400\left(1 + \frac{\Delta}{R}\right)^2 + 100\left(1 + \frac{\Delta}{R}\right)^8 - 320\left(1 + \frac{\Delta}{R}\right)^5 - 180}}{6 + 24\left(1 + \frac{\Delta}{R}\right)^5} \quad (C.2)$$

The result of this solution was again used in (3.10b) to obtain $\frac{AR}{V}$ and VR for the sphere.

APPENDIX D

Calculations of Flow Parameters at Various Flight Speeds and Altitudes in the Atmosphere.

In order to calculate the flow parameters that are of interest, the following three quantities have to be calculated at various flight speeds and altitudes; kinematic viscosity ν_s and mean free path λ_s , both at the (inviscid) stagnation point, and (for supersonic flight) e , the shock density ratio. The altitudes were chosen at 50,000 ft. intervals, starting at 150,000 up to and including 400,000 ft. The flight speeds were grouped into three regimes: (1) perfect-gas regime, 10, 100, 1,000 ft/sec., (2) non-dissociated regime, 3,000 ft/sec., and (3) real-gas regime, 7,000, 10,000, 20,000 ft/sec. The ARDC model atmosphere⁽⁴²⁾ was used to find the free-stream density, temperature, and speed of sound (the latter by extrapolation at the two highest altitudes). The standard reference temperatures and densities of $T_{\text{standard}} = 518.69^\circ\text{R}$ and $\rho_{\text{standard}} = 2.3769 \times 10^{-3} \frac{\text{lb sec}^2}{\text{ft}^4}$ were used. Different calculation procedures were used in each of the three regimes, as follows.

In the perfect-gas regime, the free-stream Mach number was determined first; then, using $\gamma = 1.4$, standard compressible-flow tables (e.g. reference 1) were used to find stagnation thermodynamic properties.

At 3,000 ft/sec. Kaufman's⁽¹⁸⁾ tables (based on the Beattie-Bridgeman equation) were used to determine the quantities of interest. The tables give shock density, temperature, and pressure ratios, shock Mach number, stagnation temperature, and pressure directly as functions of free-stream Mach number and altitude. Perfect-gas relations were then used behind the shock to determine the stagnation density from the known shock thermodynamic properties and the stagnation pressure and temperature.

In the real-gas regime, Hochstim's⁽¹²⁾ chart was used to find the temperature behind the shock, and the density ratio across, and hence density behind, the shock at the various flight conditions. Feldman's⁽⁷⁾ Mollier diagram for air was used to determine the effect on these thermodynamic quantities of the isentropic compression behind the shock. The enthalpy change during this compression could be determined since the velocity after the shock was known from continuity considerations. (Some care had to be exercised in using this multiplicity of charts, since both Hochstim's and Feldman's reference conditions are slightly different from those of the ARDC atmosphere). Compressibility factor Z at the stagnation point could also be determined from the Mollier diagram.

Hansen's⁽¹⁰⁾ calculations were used to determine the viscosity at the stagnation point as a function of temperature and (at high temperatures) of pressure. (A graph of stagnation pressures at various flight velocities and altitudes is given in the same reference). Schaaf⁽³⁷⁾, and also Maslen⁽²⁵⁾ use the following expression to calculate the mean free path

$$\lambda = 1.255 \frac{v}{\sqrt{RT}} = 0.0303 \frac{v}{\sqrt{2T}} \quad \text{for air}$$

where v and T are in units of $\text{ft}^2/\text{sec.}$ and $^{\circ}\text{R}$ respectively.

Constant $1.255 = \sqrt{\frac{R}{2}}$ above is less than 2% different
 from $1.278 = \frac{16}{5 \sqrt{2\pi}}$, which is used by Hansen⁽¹⁰⁾ and
 Patterson⁽³⁰⁾.

Using the above procedures to determine v_s , λ_s ,
 and ϵ ; and using Figures 1 and 2, all the parameters given
 in equation (3.14) could now be calculated at the various altitudes
 and flight speeds. The curves of Figure 3 were then obtained by
 means of cross plots.

APPENDIX E

Calculation of Power Laws for Variable Fluid Properties.

Hansen's⁽¹⁰⁾ tables were used to determine the specific heat, viscosity, and heat conductivity as functions of temperature. These results were plotted on log-log graph paper, and tangents to the curves were drawn at various temperatures. The results were as follows:

$$\text{For specific heat, } c_p \propto T^\alpha$$
$$\alpha = 0.144$$

$$\text{For viscosity, } \mu \propto T^\omega$$

at 500°K	$\omega = 0.661$
at 1000°K	$\omega = 0.608$
at 2000°K	$\omega = 0.562$

$$\text{For heat conductivity, } k \propto T^\epsilon$$

at 500°K	$\epsilon = 0.785$
at 1000°K	$\epsilon = 0.702$
at 1500°K	$\epsilon = 0.674$

The Prandtl number at four representative temperatures is given as

T°K	Pr
500	0.738
1000	0.756
1500	0.767
2000	0.773

Considering 1200°K as the desirable median temperature for the range under consideration, and neglecting the small variation in Prandtl number, the following properties represent an optimum "fit;"

$$\text{Pr} = 0.76$$

$$\alpha = 0.11, \quad \omega = 0.58 \quad \varepsilon = 0.69$$

APPENDIX F

Derivation of Equations for Constant Fluid Properties

For the case of constant fluid properties, the analysis of Chapter I and II is modified. The perfect-gas equation of state is replaced by $\rho = \text{constant}$, and the temperature-dependent viscosity, heat conductivity, and specific heat are replaced by constants. Thus there will be no coupling between the momentum and energy equations; the momentum equation can then be solved first, and, using this solution, the energy equation subsequently.

In the inviscid-flow solution of Chapter I result (1.9) was derived from the energy equation only, and hence remains unchanged; likewise results (1.13) through (1.20) are all derived from the momentum equations only, and therefore also remain unchanged. The former determines the first term in the temperature expansion, the latter all the terms that were considered in the stream-function and pressure expansions. These results can then be used unchanged, as they are presented in equations (1.22), (1.24), and (1.25); these furnish all the boundary conditions that are necessary for solution of the viscous flow

$$\psi = \rho A x^{1+n} \left[y + \left(\frac{n-1}{R} + nV \right) \frac{y^2}{2} + \dots \right]$$

$$T = T_s - \frac{A^2}{\rho} \left[\sigma(y^2) + \sigma(x^2) \dots \right]$$

$$p = p_s - \rho A^2 \left[(1+n)^2 \frac{y^2}{2} + \frac{x^2}{2} - \frac{x^2 y}{R} + \dots \right]$$

(F.1)

For the viscous flow the differential equations have to be modified in accordance with the constancy of fluid properties

$$f_0 = 1, \quad f_{r_1} = 0, \quad g_{r_0} = 0, \quad \text{etc.}$$

$$\frac{\mu_0}{\mu_s} = 1, \quad \frac{\lambda_0}{\lambda_s} = 0, \quad \frac{k_0}{k_s} = 1, \quad \text{etc.}$$

(F.2)

These results can be used throughout the analysis of Chapter

II; e.g. (2.9) through (2.12) become

$$f_0' = 0$$

$$f_{r_1}' = 0$$

$$g_{r_0}' = 0$$

$$\frac{\rho_0}{s A^2} g_{r_1}' = f_0'^2$$

(F.3)

The first three of these equations can be integrated immediately as in (2.27), since the boundary conditions given by (F.1) remain unchanged

$$f_0 = 1$$

$$f_{r_1} = 0$$

$$\frac{\rho_0}{s A^2} g_{r_0} = -1$$

(F.4)

Using (F.2) and (F.4), boundary-layer equations (2.14) and (2.17) become

$$(1+n) f_0 f_0'' - f_0'^2 + 1 + f_0''' = 0$$

$$2r(1+n) f_0 f_0' + f_0'' = 0$$

(F.5)

The boundary conditions at the wall were obtained from kinetic theory, and remain unchanged, as given in (2.20). Since the inviscid flow, given by (F.1), is unchanged, (2.25) is equally applicable. Summarizing the boundary conditions then

$$\begin{aligned}
 f_0(0) &= 0 \\
 f_0'(0) &= 0 \\
 H_0(0) &= W \\
 \eta \rightarrow \infty \quad & \begin{aligned} H_0(\eta) &\rightarrow 1 \\ f_0'(\eta) &\rightarrow 1 \end{aligned}
 \end{aligned} \tag{F.6}$$

The solution of (F.5) subject to (F.6) can be performed in two steps; the momentum solution is Hiemenz's and Homann's classical result for the two-dimensional and axially symmetric cases respectively, as given for example by Schlichting⁽³⁸⁾. The energy equation is linear, and can be normalized with respect to the arbitrary temperature ratio, by setting

$$f_0(\eta) = W + (1 - W) \vartheta_0(\eta) \tag{F.7}$$

so that

$$\begin{aligned}
 \text{Pr} (1+n) f_0 \vartheta_0' + \vartheta_0'' &= 0 \\
 \vartheta_0(0) &= 0 \\
 \eta \rightarrow \infty \quad \vartheta_0(\eta) &\rightarrow 1
 \end{aligned} \tag{F.8}$$

The solutions of (F.8) can be written down in the form of the following integral

$$f_0(\eta) = \frac{\int_0^\eta e^{-(1+n)\eta} \int_0^\xi f_0(\xi) d\xi dt}{\int_0^\infty e^{-(1+n)\eta} \int_0^\xi f_0(\xi) d\xi dt} \quad (F.9)$$

Tabulated values for $f_0(\eta)$ are given for a range of Prandtl numbers by Goldstein (8) and Yih (44) for the two-dimensional and axially symmetric cases respectively.

The equations for the correction terms are obtained by using (F.2) in (2.15) and (2.18). Considering momentum equation (2.15) first

$$(1+n)f_0 f_1'' + (1+n)f_0'' f_1 - 2f_0' f_1' + f_1''' = \eta \left\{ (2n+1) \left[(1+n) f_0 f_0'' - f_0'^2 \right] + 1 + n f_0''' \right\} + (n-1) f_0 f_0' + (n-1) f_0'' + \frac{2P_2}{S A^2} \eta^2$$

Using (2.47) and (2.49), the above expression becomes

$$\begin{aligned} M_{inc}(f_1) &\equiv (1+n)f_0'' f_1 - 2f_0' f_1' + (1+n)f_0 f_1'' + f_1''' = M_{Cinc}(f_0, \eta) - 2C_D \equiv \\ &\equiv \eta \left[\frac{2-6n}{2+n} - (n+1) f_0''' \right] + \frac{2}{2+n} \left[n f_0'' + 2n f_0 f_0' + (1+n) \eta^* \right] - 2C_D \end{aligned}$$

(F.10)

which defines operators M_{inc} and M_{Cinc} .

The remark made above concerning the boundary conditions for the boundary-layer terms is equally applicable to the first-order correction terms f_1 and f_1' ; but the wall and "outer" boundary conditions are unchanged from the variable-fluid-property case. At the wall, from (2.35)

$$\begin{aligned} f_1(0) &= 0 \\ f_1'(0) &= K_1 \frac{AR}{\sqrt{RT_s}} \frac{h_w}{\lambda_s} \sqrt{W} f_0''(0) \\ f_1''(0) &= K_2 \frac{AR}{\sqrt{RT_s}} \frac{h_w}{\lambda_s} \sqrt{W} f_0'(0) \end{aligned} \quad (\text{F.11})$$

As for the variable-fluid-property case, the linearity of the equations can be used to separate the various "effects," implied by the arbitrary constants appearing in the boundary conditions. Using the results of Chapter II then, the equation and boundary conditions for the curvature term are

$$M_{ime}(f_{ic}) = M_{Lme}$$

$$f_{ic}(0) = 0$$

$$f_{ic}'(0) = 0$$

(F.12)

$$\eta \rightarrow \infty \quad (\eta) \rightarrow (n-1)\eta$$

For the slip term

$$M_{inc}(f_{1SL}) = 0$$

$$f_{1SL}(0) = 0$$

$$f'_{1SL}(0) = f''_0(0)$$

$$\eta \rightarrow \infty \quad f'_{1SL}(\eta) \rightarrow 0$$

(F.13)

The solution of (F.13) is

$$\frac{1}{\eta} = \frac{1}{\eta_0}$$

(F.14)

The displacement effect is determined by

$$M_{inc}(f_{1D}) = -2$$

$$f_{1D}(0) = 0$$

$$f'_{1D}(0) = 0$$

$$\eta \rightarrow \infty$$

(F.15)

which has the solution

$$f_{1D} = \frac{1}{2} (f_0 + \eta f'_0)$$

(F.16)

Finally, for the vorticity effect one can write

Finally, for the vorticity effect one can write

$$M_{inc}(f_{iv}) = 0$$

$$f_{iv}(0) = 0$$

$$f'_{iv}(0) = 0$$

$$\eta \rightarrow \infty, \quad f_{iv}(\eta) \rightarrow n(\eta - \eta^*) \quad (\text{F.17})$$

The correction term for the stream function can then be written

$$f_1 = f_{1c} + \frac{AR}{\sqrt{RT_s}} \frac{\mu_w}{\mu_s} \sqrt{W} K_1 f'_0 + \frac{G}{2} (f_0 + \eta f'_0) + nRV f_{iv} \quad (\text{F.18})$$

The equation for the temperature-function correction term is obtained by using (F.2) in (2.18)

$$Pr(1+n) f_0 \theta_1' + \theta_1'' = -(1+n) [\eta \theta_0'' + \theta_0' + Pr \theta_0' f_1]$$

where the function f_1 , as given by (F.18), is now a known function obtained from the solution of the momentum equation. Defining

$$(1-W) \theta_1 = \theta_1 \quad (\text{F.19})$$

and using (F.7), the following differential equation is obtained for

$$\theta_1, \quad (\text{permitting solution for all values of } W)$$

$$Pr(1+n) f_0 \theta_1' + \theta_1'' \equiv E_{inc}(\theta_1) = -(1+n) [\eta \theta_0'' + \theta_0' + Pr \theta_0' f_1]$$

(F.20)

which defines operator E_{inc} . The boundary conditions for \mathcal{D}_1 , are obtained from (F.11)

$$\mathcal{D}_1(0) = \frac{AR}{\sqrt{K_1}} \frac{\mu_w}{\mu_s} \sqrt{W} K_2 \mathcal{D}'_0(0)$$

$$\eta \rightarrow \infty, \quad \mathcal{D}_1(\eta) \rightarrow 0$$
(F.21)

Due to the linearity of (F.20), the four "effects" can again be separated. The equation and boundary conditions for the curvature term are

$$E_{inc}(\mathcal{D}_{1c}) = -(1+n) [\eta \mathcal{D}_{1c}'' + \mathcal{D}'_{1c} + Pr \mathcal{D}'_{1c}]$$

$$\mathcal{D}_{1c}(0) = 0$$

$$\eta \rightarrow \infty, \quad \mathcal{D}_{1c}(\eta) \rightarrow 0$$
(F.22)

For the slip and temperature-jump effects

$$E_{inc}(\mathcal{D}_{1s}) = -Pr(1+n) K_1 \mathcal{D}'_{1s}$$

$$\mathcal{D}_{1s}(0) = K_2 \mathcal{D}'_0(0)$$

$$\eta \rightarrow \infty, \quad \mathcal{D}_{1s}(\eta) \rightarrow 0$$
(F.23)

The solution of (F.23) can be written down by inspection

$$\mathcal{D}_{1s} = K_1 \mathcal{D}'_0 + (K_2 - K_1) \mathcal{D}'_0(0) (1 - \mathcal{D}_0)$$
(F.24)

The equation and boundary conditions for the displacement effect term are

$$E_{inc}(\theta_{1D}) = -Pr(1+n)\theta'_0 \frac{\eta t'_0 + t_0}{2}$$

$$\theta_{1D}(0) = 0$$

$$\eta \rightarrow \infty, \theta_{1D}(\eta) \rightarrow 0 \quad (F.25)$$

which has the solution

$$\theta_{1D} = \frac{\eta \theta'_0}{2} \quad (F.26)$$

Finally, for the vorticity term

$$E_{inc}(\theta_{1V}) = -2nPr\theta'_0 \frac{1}{2} \eta$$

$$\theta_{1V}(0) = 0$$

$$\eta \rightarrow \infty, \theta_{1V}(\eta) \rightarrow 0 \quad (F.27)$$

The entire temperature-function correction term can then be written

$$\theta_1 = (1-W) \left\{ \theta_{1c} + \frac{AR}{12T_s} \frac{k_w}{k_s} \sqrt{W} \left[K_1 \theta'_0 + (K_2 - K_1) \theta'_0(0)(1-\theta_0) \right] + \frac{S_2}{2} \eta \theta'_0 + nRV\theta_{1V} \right\} \quad (F.28)$$

This completes the presentation of the differential equations and boundary conditions for the constant-fluid-property case. It is of interest to observe that these constant-fluid property solutions are actually identical to the variable-fluid-property solutions for the special case of $W = 1$. This is observable by inspecting (2.66), and noting that $\theta_0 = 1$ is the solution for this special case.

Using this result in the equations of Chapter II reduces these equations to those of the present appendix.

APPENDIX G

Machine-Computation Procedure

The differential equations with boundary conditions that were solved by the Burroughs 220 computer can be described as a two-point boundary-value problem. For the boundary-layer case the equations are nonlinear, for the correction terms linear. The computer's first-order simultaneous-differential-equations routine (which uses the Runge-Kutta method) was applied to the problem. Three pairs of starting values (for $f''(0)$ and $f'(0)$) were assumed, and then the (inviscid asymptotic) behavior of the functions at $\eta = 7$ was used to obtain successively better and final starting values by means of double interpolation, which was programmed on the machine. This procedure was then successively repeated with the decrements of η halved, until the final starting values did not change.

APPENDIX H

Comparison of Theory with Experiments of Tewfik and Giedt^{(40), (41)}

The two references that describe the above experiments are (40) and (41); in this appendix they will be referred to as Parts I and II respectively. The following calculation procedure was used to compare the present theory with the experimental Nusselt numbers presented in Table XI, p. 55, Part I. First, the velocity gradient at the stagnation point had to be determined. This was done by using the experimentally determined values given in Table A6, Part II. Using the definitions given on p. 9, Part II, the relation between the nomenclature of the present analysis, and of Tewfik and Giedt is the following

$$\frac{AR}{U} = \frac{\epsilon}{2} \tilde{U}'_e(0)$$

(H.1)

where ϵ is the density ratio across the shock. In the Mach-number range considered (1.3) to 5.7), and around free-stream pressures of 10^{-5} atmospheres (in agreement with the "low" stagnation pressures of 80-120 microns, mentioned on p. 14 Part I) Kaufman⁽¹⁸⁾ indicates that the perfect-gas formulae are sufficiently accurate to calculate the flow. For air $\gamma = 1.4$ can be assumed, and then

ϵ and the Mach number after the shock can be obtained from

M_2 . Furthermore after the shock an isentropic compression takes place, for which $\rho \propto T^{\frac{1}{\gamma-1}} = T^{2.5}$, and the variation of viscosity with temperature can be assumed to be $\mu \propto T^{0.8}$

Then the Reynolds number that is of interest in the present analysis can be related to Re_1 given by Tewfik and Giedt as follows:

$$\frac{AR^2}{\lambda} = AR^2 \frac{R_{e1}}{2ReV} \frac{\mu_{SHOCK}}{\mu_s} \frac{\rho_s}{\rho_{SHOCK}} = \frac{\tilde{U}_e'(0) Re_1}{4} \left(\frac{T_s}{T_{SHOCK}} \right)^{1.7} = \frac{\tilde{U}_e'(0) Re}{4} \left(1 + 0.2 M_{SHOCK}^2 \right)^{1.7} \quad (H.2)$$

Table V of Part I shows that the recovery factor is always almost exactly 1.0 at the stagnation point, indicating that the adiabatic wall temperature, T_{aw} , which forms the basis of the experimental Nusselt numbers that are presented, is almost exactly the same as the stagnation temperature, T_s , which forms the basis of the heat-transfer formulae of the present analysis. Then the non-dimensional heat-transfer rate of the present analysis can be related to Nu_1 of Tewfik and Giedt as follows:

$$\frac{Q_{exp}}{(1-w) h_s T_s / \sqrt{\frac{\lambda}{h}}} = \frac{Nu_1 b_1 (T_s - T_w)}{2 R (1-w) b_s T_s / \sqrt{\frac{\lambda}{h}}} = \frac{Nu_1}{2} \frac{1}{R \sqrt{A}} \frac{1}{(1 + 0.2 M_{SHOCK}^2)^{0.85}} \quad (H.3)$$

where it was assumed that during the isentropic compression from the shock to the stagnation condition $h \propto T^{0.85}$. The experimental result obtained in (H.3) can then be compared to the theory of the present analysis, as given in Chapter IV. The displacement-correction term will not have to be considered because the experimentally measured velocity gradients already include this effect. The parameter defining the magnitude of the curvature correction is the inverse square root of the Reynolds number given in (H.2). For the slip and temperature-jump correction term, the parameter that is significant is the ratio of the mean free path at the wall to the boundary-layer thickness:

$$\begin{aligned} \frac{\lambda_w}{\sqrt{x_s/A}} \frac{z-3}{\delta} &= \sqrt{\frac{\pi}{2}} \frac{\mu_w}{s_w \sqrt{RT_w}} \frac{z-3}{\delta} \frac{1}{\sqrt{x_s/A}} = \frac{1}{R} \sqrt{\frac{x_s}{A}} \frac{\mu_w}{\mu_s} \frac{s_s}{s_w} \sqrt{\frac{T_s}{T_w}} \frac{AR}{\sqrt{RT_s}} K_1 = \\ &= \frac{1}{R} \sqrt{\frac{x_s}{A}} \frac{\mu_w}{\mu_s} \sqrt{W} \sqrt{T} M_\infty \frac{AR}{U} \sqrt{\frac{T_s}{T_s}} K_1 = \frac{1}{R} \sqrt{\frac{x_s}{A}} \frac{\mu_w}{\mu_s} \sqrt{W} \frac{AR}{U} \frac{M_\infty \sqrt{\delta} K_1}{\sqrt{1+0.2M_\infty^2}} \end{aligned} \quad (\text{H.4})$$

Temperature ratio W in the above expressions is tabulated in Table A5, p. 56, Part II. Viscosity ratio $\frac{\mu_w}{\mu_s}$ was related to W by using the viscosity vs temperature variation given by Hansen⁽¹⁰⁾ and (at the low temperatures) by Jakob⁽¹⁷⁾. For a stagnation temperature of $T_s = 300^\circ\text{K}$ (p 3, Part I) a good approximation for this viscosity variation is $\mu \sim T^{0.73}$ near $W = 0.3$ and $\mu \sim T^{0.79}$ near $W = 0.7$. Now all quantities in (H.4) are known except K_1 . A reasonable guess (e.g. references (36) and (27)) is

$$\begin{aligned} K_1 &= \sqrt{\frac{\pi}{2}} \quad (\text{i.e. } \delta = 1) \\ \frac{K_2}{K_1} &= 1.8 \end{aligned} \quad (\text{H.5})$$

Now all quantities that are necessary to apply the theoretical results of Chapter IV have been determined. Using the results of this theory (Table III), the heat-transfer rate at the stagnation point can be written for the constant-fluid-property case

$$\begin{aligned} \frac{Q}{(1-w)k_s T_s \sqrt{x_s/A}} &= \frac{Q_{o,inc}}{(1-w)Q_{ref}} + \frac{1}{R} \sqrt{\frac{x_s}{A}} \frac{Q_{o,inc}}{(1-w)Q_{ref}} + \frac{\lambda_w}{\sqrt{x_s/A}} 0.8 \frac{Q_{o,inc}}{(1-w)Q_{ref}} = \\ &= 0.5123 - \frac{1}{R} \sqrt{\frac{x_s}{A}} 0.135 - \frac{\lambda_w}{\sqrt{x_s/A}} 0.8 = 0.2624 \end{aligned}$$

(H.6)

The corresponding numbers for the variable-fluid-property case can be determined as functions of W by using the graphs of Figure 7. The results of these calculations are presented in terms of the difference between the calculated result and the heat-transfer rate based on constant-fluid-property boundary-layer theory, as a fraction of the latter. The experimental results, as calculated in (h.3), are presented in the same manner, e.g.

$$\frac{\Delta Q_{c \text{ comp}}}{Q_{o \text{ inc}}} = \frac{\frac{1}{R} \sqrt{\frac{1}{2}} Q_{ic \text{ comp}}}{0.5123 Q_{ref}} \quad \text{or} \quad \frac{\Delta Q_{exp}}{Q_{o \text{ inc}}} = \frac{Q_{exp} - Q_{o \text{ inc}}}{Q_{o \text{ inc}}} \quad (\text{H.7})$$

etc. Finally displacement effect parameter C_D is also tabulated for the sake of reference. The calculation of it is based on an empirical relation between stagnation-point velocity gradients for circular cylinders and Mach number, as presented by Reshotko and Beckwith⁽³³⁾. (This is the "infinite"-Reynolds-number case). Using these and the experimentally determined velocity gradients of Tewfik and Giedt (H.1) in expression (2.22) C_D is determined as follows

$$C_D = \frac{A_{\text{Tewfik \& Giedt}} - A_{\text{Reshotko \& Beckwith}}}{A_{\text{Reshotko \& Beckwith}} \frac{1}{R} \sqrt{\frac{1}{2}}} \quad (\text{H.8})$$

NOMENCLATURE

a	speed of sound
a	(with subscript) constant coefficients (Chapter I only)
A	stagnation-point velocity gradient; $u = Ax$
b	constant coefficients (Chapter I)
C_D	displacement-effect parameter (equation 2.22)
C_1, C_k	combinations of Bessel functions (equation 3.4a)
c_p	specific heat at constant pressure
e	density ratio across (normal) shock;
$\vec{e}_1, \vec{e}_2, \vec{e}_3$	base vectors in orthogonal system (Appendix A)
$E(\)$	energy-equation differential operator (equation 2.40)
$E_c(\)$	inhomogeneous terms in energy equation (equation 2.40)
f, g	functions in expansion of viscous flow about stagnation point, x^0 and x^2 terms respectively. Without adscript stream function, with adscripts p, ρ, τ pressure, density, and temperature respectively. (E.g. ψ_0 is temperature-function, x^0 term, etc., equations 2.2 through 2.5)
h	enthalpy
h_1, h_2, h_3	metric functions in orthogonal coordinate system (Appendix A)
H	altitude, ft.
$I_1(\)$	Bessel function of () (Chapter III and Appendix C)
k	heat conductivity
K	constant of integration (equation 2.35)
K_1, K_2	proportionality constants (equation 2.21)
$K_1(\)$	Bessel function of () (Chapter III and Appendix C)
L	reference length indicative of body size, determines A ; $A = \frac{v}{L}$

M	Mach number
$M(\)$	momentum-equation differential operator (equation 2.40)
$M_c(\)$	inhomogeneous terms in momentum equation (equation 2.40)
n	0 for two-dimensional, 1 for axially symmetric flow
Nu	Nusselt number
$\sigma(\)$	Order of ()
P	pressure
Pr	Prandtl number
\vec{q}	velocity vector
Q	heat-transfer rate normal to surface $Q = h \frac{\partial T}{\partial y}$
r	radial coordinate
R	nose radius of curvature
R	gas constant
Re	Reynolds number
T	absolute temperature
u, v	velocity components in x and y directions respectively
U	free-stream velocity, ft/sec
V	Vorticity parameter for axially symmetric stagnation-point flow (equation 1.19)
W	cooling ratio; $W = \frac{T_w}{T_s}$
x, y	boundary-layer coordinates (equation 1.1)
α	exponent of temperature for specific heat; $c_p \propto T^\alpha$
α_a	accommodation coefficient for energy transfer at solid-gas interface
γ	ratio of specific heats
δ	boundary-layer thickness parameter $\delta = \sqrt{\frac{x}{A}}$
Δ	inviscid shock stand-off distance

- ϵ exponent of temperature for heat conductivity; $k \propto T^\epsilon$
 η boundary-layer coordinate (equation 2.1) $\eta = y\sqrt{\frac{U_\infty}{\nu_0}}$
 η^* displacement number (equation 2.34)
 θ (without subscript) angular coordinate
 θ (with subscripts) temperature function in constant-fluid-property flow (equations F.7 and F.20)
 λ mean free path in gas
 μ viscosity
 ν kinematic viscosity
 ρ density
 δ fraction of diffusely reflected molecules
 τ shear parallel to surface $\tau = \mu \frac{\partial v}{\partial y}$
 ψ compressible stream function
 Φ dissipation function in energy equation
 ω exponent of temperature for viscosity $\mu \propto T^\omega$
 Ω vorticity $\Omega = \text{curl } \vec{v}$
 \propto proportional to

Subscripts;

- $0, 1, 2, \dots$ successive terms in Reynolds-number expansion; boundary-layer 1st order, 2nd order, etc. correction terms; also (in Chapter I) successive coefficients in y expansion of inviscid quantities.
C correction due to curvature effect
comp result of compressible (variable-fluid-property) analysis
D correction due to displacement effect

exp	experimental result
J	correction due to temperature jump ($K_1 \neq K_2$)
inv	result of incompressible (constant-fluid-property) analysis
M	correction due to finite mean free path (equation 2.39)
p	refers to pressure
ρ	refers to density
r	partial derivative with respect to r (Appendix A only)
ref	reference quantities (see Chapter IV), equations (4.1) and (4.3) (except (F.23) and (F.24)).
s	inviscid stagnation value
shock	condition after shock
SL	correction due to velocity slip
std. cond.	standard conditions at standard atmosphere
t	refers to temperature
V	correction due to vorticity effect
W	condition at solid surface ("wall")
x, y	partial derivatives with respect to x and y
\mathcal{D}	partial derivative with respect to \mathcal{D}
∞	free-stream

Superscripts

'	derivative with respect to η
.	derivatives with respect to temperature

Reference Index

1. Ames Research Staff: "Equations, Tables, and Charts for Compressible Flow." NACA Rep. 1135, 1953.

Beckwith, I.E. see Reshotko and Beckwith.
2. Brown, W.B.: "Exact Solutions of the Laminar Boundary Layer Equations for a Porous Plate with Variable Fluid Properties and a Pressure Gradient in the Main Stream." Proc. 1-st U.S. National Congress of Applied Mech., Chicago, June 1951.
3. Brown, W.B. and Donoughe, P.L.: "Tables of Exact Laminar Boundary Layer Solutions when the Wall is Porous and Fluid Properties are Variable." NACA TN 2479, Sept. 1951.
4. Brown, W.B., and Livingood, J.W.B.: "Solutions of Laminar Boundary Layer Equations which Result in Specific Weight Flow Profiles Locally Exceeding Free Stream Values." NACA TN 2800, Sept. 1952.

Chambre, P.L. see Schaaf and Chambre

Chan, K.K., see Neice Rutowski, and Chan.
5. Cohen, C.B. and Reshotko, E.: "Similar Solutions for the Compressible Laminar Boundary Layer with Heat Transfer and Pressure Gradient." NACA Rep. 1293, 1956.

Cole, J.D. see Lagerstrom and Cole
6. Crawford, D.H., and McCauley, W.D.: "Investigations of the Laminar Aerodynamic Heat-Transfer Characteristics of a Hemisphere-Cylinder in the Langley 11 Inch Hypersonic Tunnel at a Mach Number of 6.8." NACA TN 3706, July 1956.

Donoughe, P.L. see Brown and Donoughe.
7. Feldman, S.: "Hypersonic Gas Dynamic Charts for Equilibrium Air." AVCO Res. Rep. #40, Jan. 1957.

Giedt, W.H. see Tewfik and Giedt
8. Goldstein, S. (Editor): "Modern Developments in Fluid Dynamics." Oxford Press, 1938.
9. Hayes, W.D., Probst, R.F.: "Hypersonic Flow Theory." Academic Press, New York, 1959.
10. Hansen, C.F.: "Approximations for the Thermodynamic and Transport Properties of High Temperature Air." NACA TN 4150, March 1958.

11. Herring, T.K.: "The Boundary Layer near the Stagnation Point in Hypersonic Flow Past a Sphere." *Journal of Fluid Mechanics*, v.7, Part 2, p. 257, Feb. 1960.

Ho, H.T. see Probststein and Ho.
12. Hochstim, A.R." "Gas Properties behind Shocks at Hypersonic Velocities. I. Normal Shocks in Air." Convair, San Diego Rep # Z ph (GP)-002. Jan. 30, 1957.
13. Hoshizaki, H." "Shock Generated Vorticity Effects at Low Reynolds Numbers." Lockheed Technical Report LMSD 48381, pp. 9-43, Jan. 1959.
14. Hoshizaki, H.: "The Effect of Shock Generated Vorticity, Surface Slip, and Temperature Jump on Stagnation Point Heat Transfer Rates." *J.Aero.Sc.* v. 27 #2, Feb. 1960; also Lockheed Technical Report LMSD 288139 Vol. I, Part 1, #5. Jan. 1960.
15. Hoshizaki, H." "On Mass Transfer and Shock Generated Vorticity." Lockheed Technical Report LMSD 288139, Vol. I, Part 1, #4, Jan. 1960.
16. Howe, J.T. and Mersman, W.A.: "Solutions of the Laminar Compressible Boundary Layer Equations with Transpiration which are Applicable to the Stagnation Regions of Axisymmetric Blunt Bodies." NASA TN #12, Aug. 1959.
17. Jakob, M.: "Heat Transfer." Vol. I. John Wiley & Sons, 1949.
18. Kaufman, L.G. II.: "Real Gas Flow Tables for Nondissociated Air." WADC Tech Rep #59-4, Jan. 1959.
19. Kemp, N.H.: "Vorticity Interaction at an Axisymmetric Stagnation Point in a Viscous Incompressible Fluid." *J.Ae.Sc.* vo. 26 #8, Aug. 1959.

Kemp, N.H. see Probststein and Kemp
20. Lagerstrom, P.A. and Cole, J.D.: "Examples Illustrating Expansion Procedures for the Navier Stokes Equation." *Jour. of Rational Mech. and Analysis*, v. 4, #6, 1955.
21. Lees, L.: "Laminar Heat Transfer over Blunt Nosed Bodies at Hypersonic Flight Speeds." *Jet. Prop.* v. 26 #4, p. 259, Apr. 1956.

Lenard, M. see Rott and Lenard
22. Lighthill, M.J.: "Dynamics of a Dissociating Gas, Part I, Equilibrium Flow." *J. of Fluid Mech.* v. 2, Jan. 1957.
23. Lin, T.C. and Schaaf, S.C.: "Effect of Slip on Flow near a Stagnation Point and in a Boundary Layer." NACA TN 2568, Dec. 1951.

Livingood, J.N.B. see Brown and Livingood.

24. Mangler, K.W.: "Ein Equivalenzsatz für Laminare Grenzschichten bei Hyperschallströmung." ZAMM v. 36, Sonderheft pp. 522-525, 1956.
25. Maslen, S.H.: "Second Approximation to Laminar Compressible Boundary Layer on Flat Plate in Slip Flow." NACA TN 2818, Nov. 1952.
- McCauley, W.D. see Crawford and McCauley.
- Mersman, W.A. see Howe and Mersman.
26. Neice, S.E., Rutowski, R. W., Chan, K.K.: "Stagnation Point Heat Transfer Measurements in Hypersonic Low Density Flow." Lockheed Technical Report LMSD 288139, Vol. I, Part II, #7, Jan. 1960.
27. Nonweiler, T.: "The Laminar Boundary Layer in Slip Flow." College of Aeronautics, Cranfield, Rep #62, Nov. 1952.
28. Oguchi, H.: "Hypersonic Flow near the Forward Stagnation Point of a Blunt Body of Revolution." J.Aer.Sc. v. 25, #12, pp. 789-790, Dec. 1958; also Aero.Res.Inst. Tokyo, Rep. #337, 1958.
29. Oguchi, H.: "The Blunt Body Viscous Layer Problem with and without an Applied Magnetic Field." Brown Univ. WADD TN 60-57, Feb. 1960.
30. Patterson, G.N.: "molecular Flow of Gases." John Wiley & Sons, 1956.
31. Probst, R.F., Kemp, N.H.: "Viscous Aerodynamic Characteristics in Hypersonic Rarefied Gas Flow." J.Aer.Sc. v. 27, #3, pp. 174-192, March 1960; also AVCO Res.Rept. #48, March 1959.
32. Probst, R.F., Ho, H.T.: "The Compressible Viscous Layer in Rarefied Hypersonic Flow." Second International Symp. on Rarefied Gas Dyn. Abstracts, Berkeley Cal., Aug.3-6, 1960. Detailed report to be published later.
- Probst, R.F. see also Hayes and Probst
33. Reshotko, E., Beckwith, I.E.: "Compressible Laminar Boundary Layer over a Yawed Infinite Cylinder with Heat Transfer and Arbitrary Prandtl Number." NACA Rep 1379, 1958.
- Reshotko, E. see also Cohen and Reshotko
34. Rowig, M.F.: "Stagnation Point Heat Transfer for Hypersonic Flow." Jet Prop. v. 26, #12, p. 1098, Dec. 1956.
35. Rott, N., and Lenard, M.: "Vorticity Effect on the Stagnation Point Flow of a Viscous Incompressible Fluid." J.Aer.Sc. v. 26, #8, Aug. 1959.
- Rutowski, R.W. see Neice, Rutowski, and Chan.

36. Schaaf, S.A. and Chambre, P.L.: "Flow of Rarefied Gases. Vol. 3, Section H., High Speed Aerodynamics and Jet Propulsion." Princeton Univ. Press, 1959.
37. Schaaf, S.A.: "Theoretical Considerations in Rarefied Gas Dynamics." Heat Transfer Symposium 1952. Univ. of Michigan 1953.

Schaaf, S.A. see also Lin and Schaaf.
38. Schlichting, H.: "Boundary Layer Theory." Pergamon Press.
39. Sherman, F.S.: "Transport Phenomena in Low Density Gases." from "Transport Properties in Gases." Proc. of the 2nd Biennial Gas Dyn. Symp. ARS and Northw. Univ.; A. B. Cambel and J. B. Fenn Edit. Northw. Univ. Press 1958.
40. Tewfik, O.K., Gledt, W.H.: "Heat Transfer, Recovery Factor, and Pressure Distribution around a Cylinder Normal to a Supersonic Rarefied Air Stream. Part I." Univ. of Cal. Tech. Rep. HE-150-162, Jan. 30 1959.
41. Tewfik, O.K.: "Heat Transfer, Recovery Factor, and Pressure Distributions around a Cylinder normal to a Supersonic Rarefied Air Stream. Part II." Univ. of Cal. Tech. Rep. HE-150-169, May 15, 1959.
42. USAF Cambridge Research Ctr., Geophysics Research Directorate: "Handbook of Geophysics for Air Force Designers." Cambridge Mass. 1957.
43. Whitham, G.B.: "A Note on the Stand-Off Distance of the Shock in High Speed Flow past a Circular Cylinder." Comm. on Pure and Appl. Math. v 10 #4, p. 531, November, 1957.
44. Yih, C.S.: "Temperature Distribution in Laminar Stagnation Point Flow with Axisymmetry." J.Aer.Sc. v 21, #1, p. 37, Jan. 1954.

Additional References:

- Ferri, A., Zakay, V., Ting, Lu: "Blunt Body Heat Transfer at Hypersonic Speed and Low Reynolds Numbers." Polyt. Ins. Brooklyn A.L. Rept #611, June, 1960.
- Lunkin, Y.N.: "Boundary Layer Equations and their Boundary Conditions in the Case of Motion at Supersonic Velocities in a Moderately Rarefied Gas." NASA TT F-28, May 1960.
- Cheng, H.K.: "Hypersonic Shock Layer Theory of the Stagnation Region at Low Reynolds Number." Cornell Aero. Lab. Rep. #AF-1285-A-7, April 1961.

Inviscid Hypersonic Stagnation Point Flow Parameters for Cylinder.

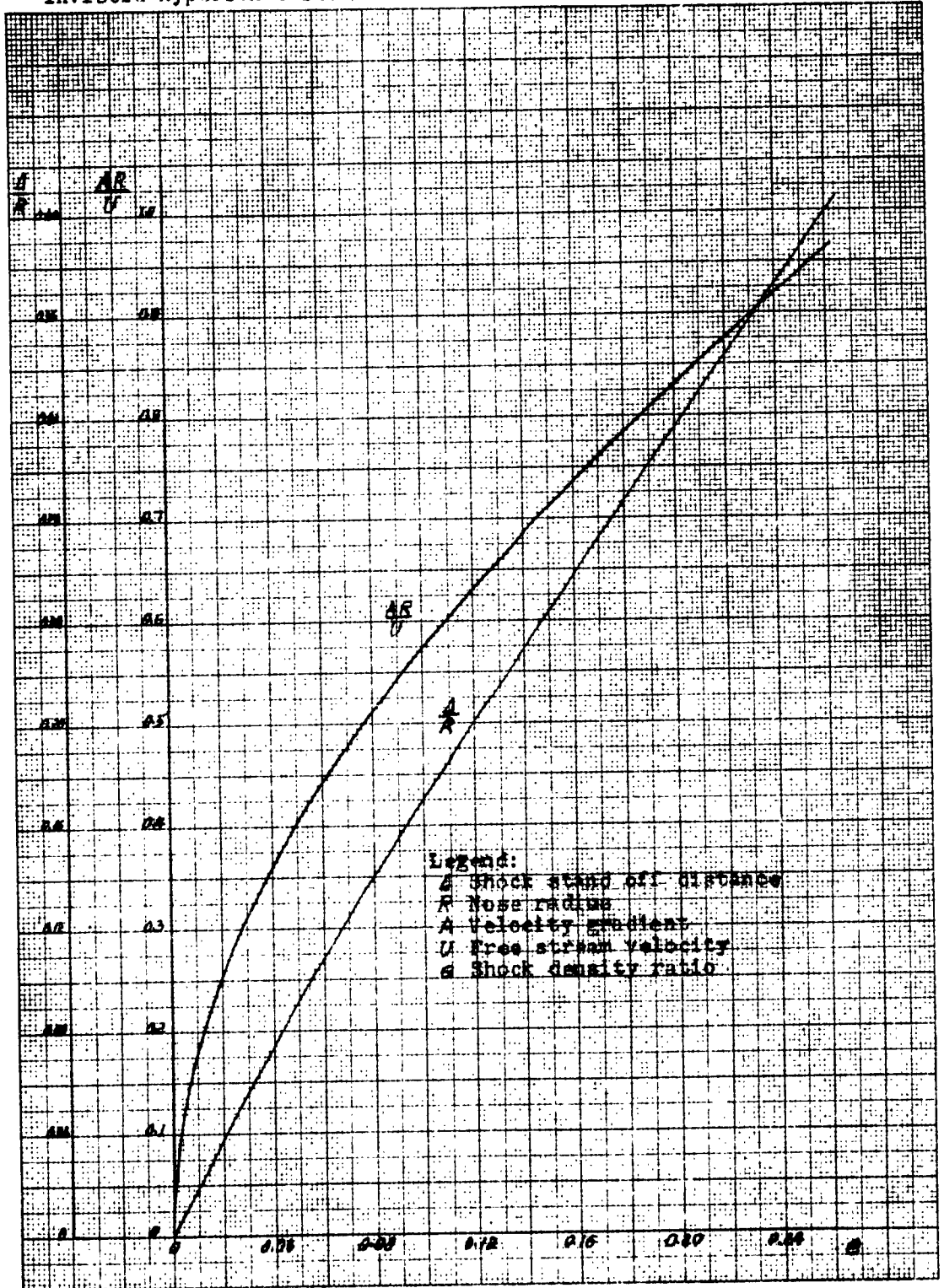


FIGURE 1.

Inviscid Hypersonic Stagnation Point Flow Parameters for Sphere 119

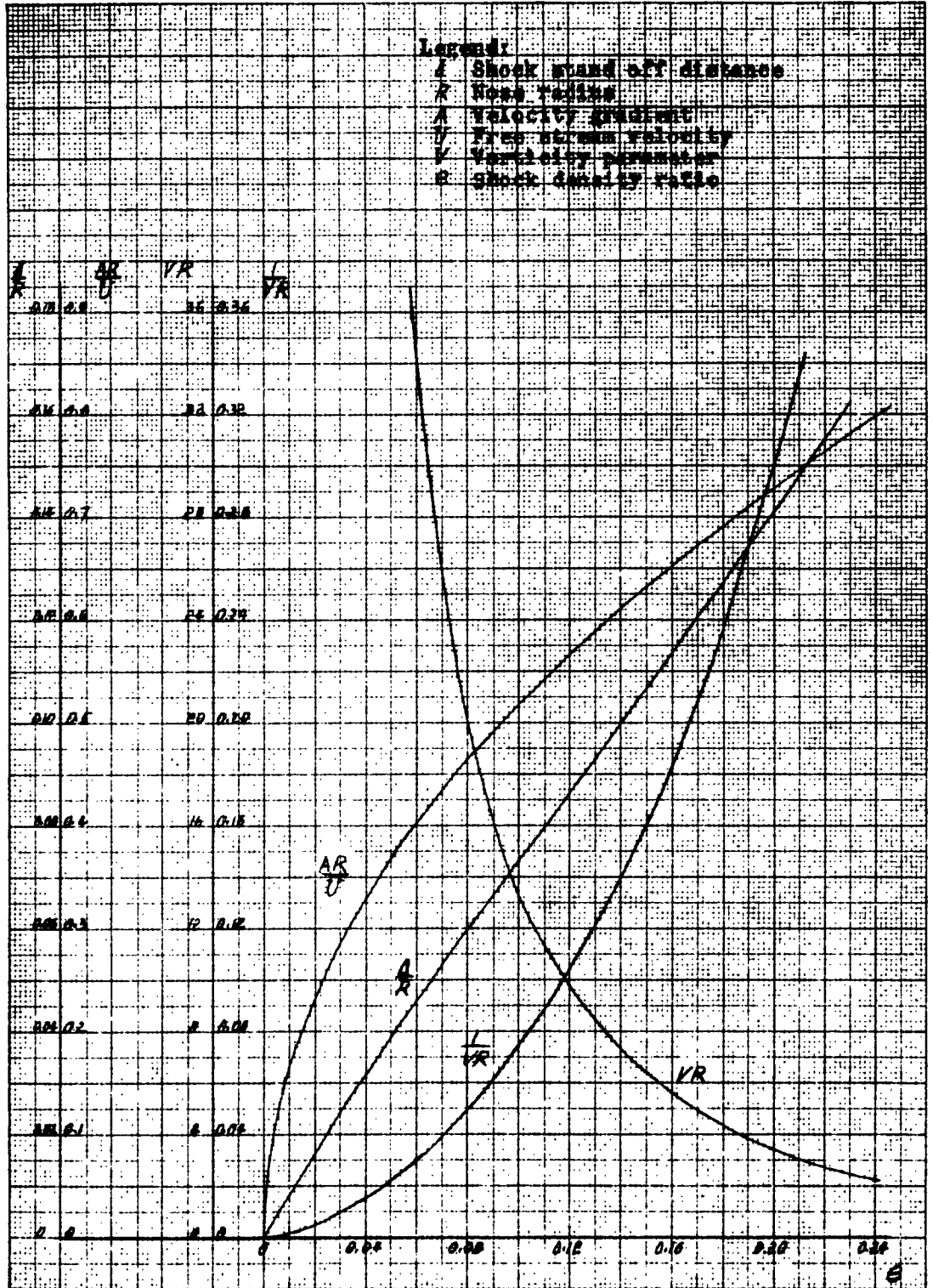


FIGURE 2.

10⁵

BLUNT BODY STAGNATION POINT FLOW

$$\frac{\sum V_R}{\rho c} \sim \sqrt{V_{SE}} = .0316$$

0.1

0.316

$$\frac{V_S}{\sqrt{R}} = \frac{\rho c}{\sqrt{V_{SE}}} \sqrt{V_R} \sim \sqrt{V_{SE}} = .0316$$

0.1

0.316

$$\frac{\sum V_R}{\rho c} \sim \sqrt{V_{SE}} = .01$$

0.0316

0.1

10⁴

$$\lambda_{STAG} \sim \frac{V_{SE}}{\rho c} = .00001$$

$$\frac{\sum V_R}{R} \sim \sqrt{V_{SE}} = .00316$$

10³

FLIGHT SPEED IN FT/SEC

$$\frac{\sum V_R}{R} \sim \sqrt{V_{SE}} = .01$$

$\lambda_{STAG} \sim \frac{V_{SE}}{\rho c} = .001$

100

10

REF: SEMI-LOGARITHMIC 359 81LG
NATIONAL INSTRUMENT CO.

10²

10¹

10⁰

10⁻¹

10⁻²

10⁻³

10⁻⁴

10⁻⁵

10⁻⁶

10⁻⁷

10⁻⁸

10⁻⁹

10⁻¹⁰

10⁻¹¹

10⁻¹²

10⁻¹³

10⁻¹⁴

10⁻¹⁵

10⁻¹⁶

10⁻¹⁷

10⁻¹⁸

10⁻¹⁹

10⁻²⁰

10⁻²¹

10⁻²²

10⁻²³

10⁻²⁴

10⁻²⁵

10⁻²⁶

10⁻²⁷

10⁻²⁸

10⁻²⁹

10⁻³⁰

10⁻³¹

10⁻³²

10⁻³³

10⁻³⁴

10⁻³⁵

10⁻³⁶

10⁻³⁷

10⁻³⁸

10⁻³⁹

10⁻⁴⁰

10⁻⁴¹

10⁻⁴²

10⁻⁴³

10⁻⁴⁴

10⁻⁴⁵

10⁻⁴⁶

10⁻⁴⁷

10⁻⁴⁸

10⁻⁴⁹

10⁻⁵⁰

10⁻⁵¹

10⁻⁵²

10⁻⁵³

10⁻⁵⁴

10⁻⁵⁵

10⁻⁵⁶

10⁻⁵⁷

10⁻⁵⁸

10⁻⁵⁹

10⁻⁶⁰

10⁻⁶¹

10⁻⁶²

10⁻⁶³

10⁻⁶⁴

10⁻⁶⁵

10⁻⁶⁶

10⁻⁶⁷

10⁻⁶⁸

10⁻⁶⁹

10⁻⁷⁰

10⁻⁷¹

10⁻⁷²

10⁻⁷³

10⁻⁷⁴

10⁻⁷⁵

10⁻⁷⁶

10⁻⁷⁷

10⁻⁷⁸

10⁻⁷⁹

10⁻⁸⁰

10⁻⁸¹

10⁻⁸²

10⁻⁸³

10⁻⁸⁴

10⁻⁸⁵

10⁻⁸⁶

10⁻⁸⁷

10⁻⁸⁸

10⁻⁸⁹

10⁻⁹⁰

10⁻⁹¹

10⁻⁹²

10⁻⁹³

10⁻⁹⁴

10⁻⁹⁵

10⁻⁹⁶

10⁻⁹⁷

10⁻⁹⁸

10⁻⁹⁹

10⁻¹⁰⁰

10⁻¹⁰¹

10⁻¹⁰²

10⁻¹⁰³

10⁻¹⁰⁴

10⁻¹⁰⁵

10⁻¹⁰⁶

10⁻¹⁰⁷

10⁻¹⁰⁸

10⁻¹⁰⁹

10⁻¹¹⁰

10⁻¹¹¹

10⁻¹¹²

10⁻¹¹³

10⁻¹¹⁴

10⁻¹¹⁵

10⁻¹¹⁶

10⁻¹¹⁷

10⁻¹¹⁸

10⁻¹¹⁹

10⁻¹²⁰

10⁻¹²¹

10⁻¹²²

10⁻¹²³

10⁻¹²⁴

10⁻¹²⁵

10⁻¹²⁶

10⁻¹²⁷

10⁻¹²⁸

10⁻¹²⁹

10⁻¹³⁰

10⁻¹³¹

10⁻¹³²

10⁻¹³³

10⁻¹³⁴

10⁻¹³⁵

10⁻¹³⁶

10⁻¹³⁷

10⁻¹³⁸

10⁻¹³⁹

10⁻¹⁴⁰

10⁻¹⁴¹

10⁻¹⁴²

10⁻¹⁴³

10⁻¹⁴⁴

10⁻¹⁴⁵

10⁻¹⁴⁶

10⁻¹⁴⁷

10⁻¹⁴⁸

10⁻¹⁴⁹

10⁻¹⁵⁰

10⁻¹⁵¹

10⁻¹⁵²

10⁻¹⁵³

10⁻¹⁵⁴

10⁻¹⁵⁵

10⁻¹⁵⁶

10⁻¹⁵⁷

10⁻¹⁵⁸

10⁻¹⁵⁹

10⁻¹⁶⁰

10⁻¹⁶¹

10⁻¹⁶²

10⁻¹⁶³

10⁻¹⁶⁴

10⁻¹⁶⁵

10⁻¹⁶⁶

10⁻¹⁶⁷

10⁻¹⁶⁸

10⁻¹⁶⁹

10⁻¹⁷⁰

10⁻¹⁷¹

10⁻¹⁷²

10⁻¹⁷³

10⁻¹⁷⁴

10⁻¹⁷⁵

10⁻¹⁷⁶

10⁻¹⁷⁷

10⁻¹⁷⁸

10⁻¹⁷⁹

10⁻¹⁸⁰

10⁻¹⁸¹

10⁻¹⁸²

10⁻¹⁸³

10⁻¹⁸⁴

10⁻¹⁸⁵

10⁻¹⁸⁶

10⁻¹⁸⁷

10⁻¹⁸⁸

10⁻¹⁸⁹

10⁻¹⁹⁰

10⁻¹⁹¹

10⁻¹⁹²

10⁻¹⁹³

10⁻¹⁹⁴

10⁻¹⁹⁵

10⁻¹⁹⁶

10⁻¹⁹⁷

10⁻¹⁹⁸

10⁻¹⁹⁹

10⁻²⁰⁰

10⁻²⁰¹

10⁻²⁰²

10⁻²⁰³

10⁻²⁰⁴

10⁻²⁰⁵

10⁻²⁰⁶

10⁻²⁰⁷

10⁻²⁰⁸

10⁻²⁰⁹

10⁻²¹⁰

10⁻²¹¹

10⁻²¹²

10⁻²¹³

10⁻²¹⁴

10⁻²¹⁵

10⁻²¹⁶

10⁻²¹⁷

10⁻²¹⁸

10⁻²¹⁹

10⁻²²⁰

10⁻²²¹

10⁻²²²

10⁻²²³

10⁻²²⁴

10⁻²²⁵

10⁻²²⁶

10⁻²²⁷

10⁻²²⁸

10⁻²²⁹

10⁻²³⁰

10⁻²³¹

10⁻²³²

10⁻²³³

10⁻²³⁴

10⁻²³⁵

10⁻²³⁶

10⁻²³⁷

10⁻²³⁸

10⁻²³⁹

10⁻²⁴⁰

10⁻²⁴¹

10⁻²⁴²

10⁻²⁴³

10⁻²⁴⁴

10⁻²⁴⁵

10⁻²⁴⁶

10⁻²⁴⁷

10⁻²⁴⁸

10⁻²⁴⁹

10⁻²⁵⁰

10⁻²⁵¹

10⁻²⁵²

10⁻²⁵³

10⁻²⁵⁴

10⁻²⁵⁵

10⁻²⁵⁶

10⁻²⁵⁷

2 3 4 5
POINT FLOW PARAMETERS FOR FLIGHT THROUGH ATMOSPHERE

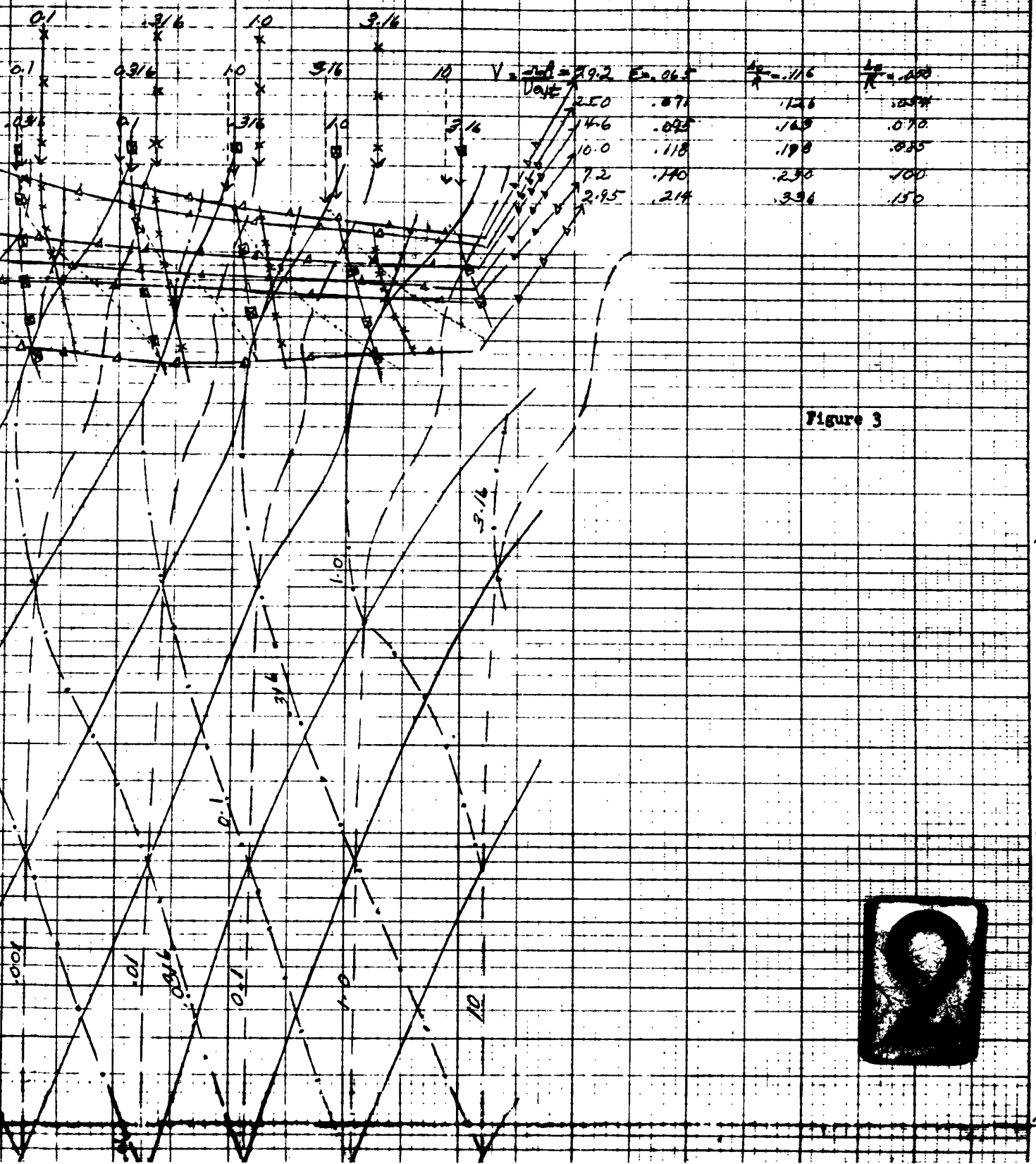
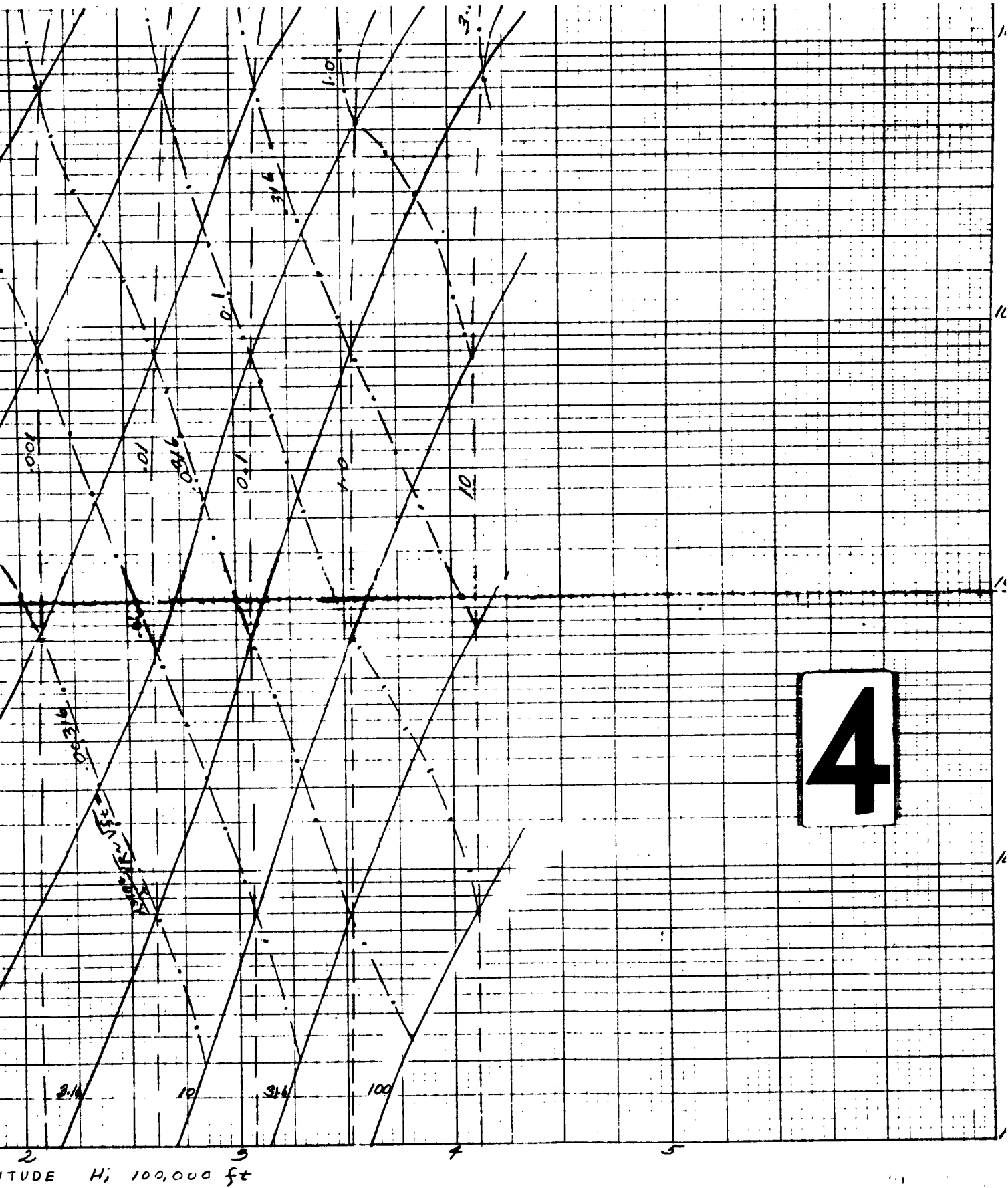


Figure 3





4

ITUDE H; 100,000 ft

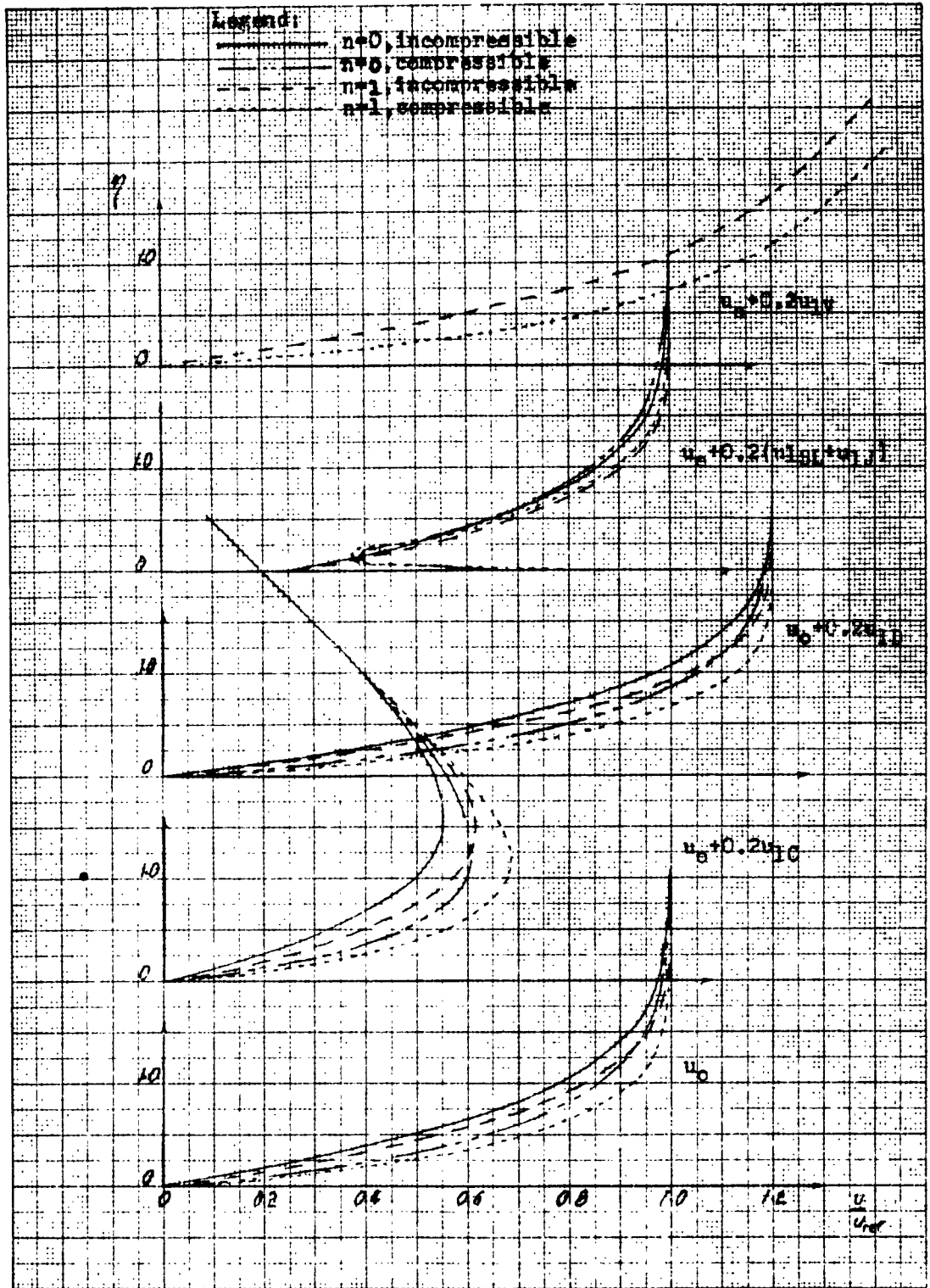


FIGURE 4a.

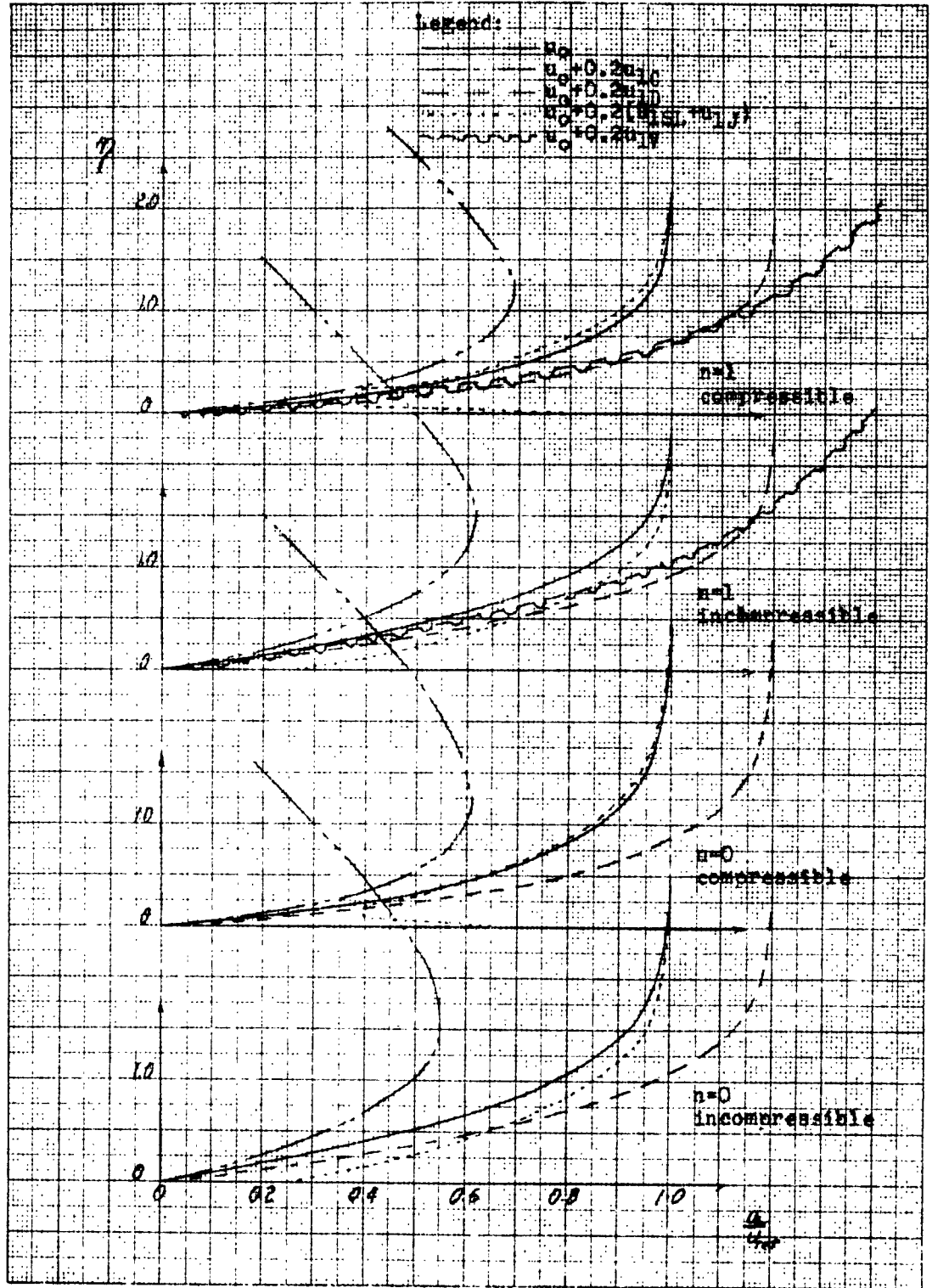


FIGURE 4b.

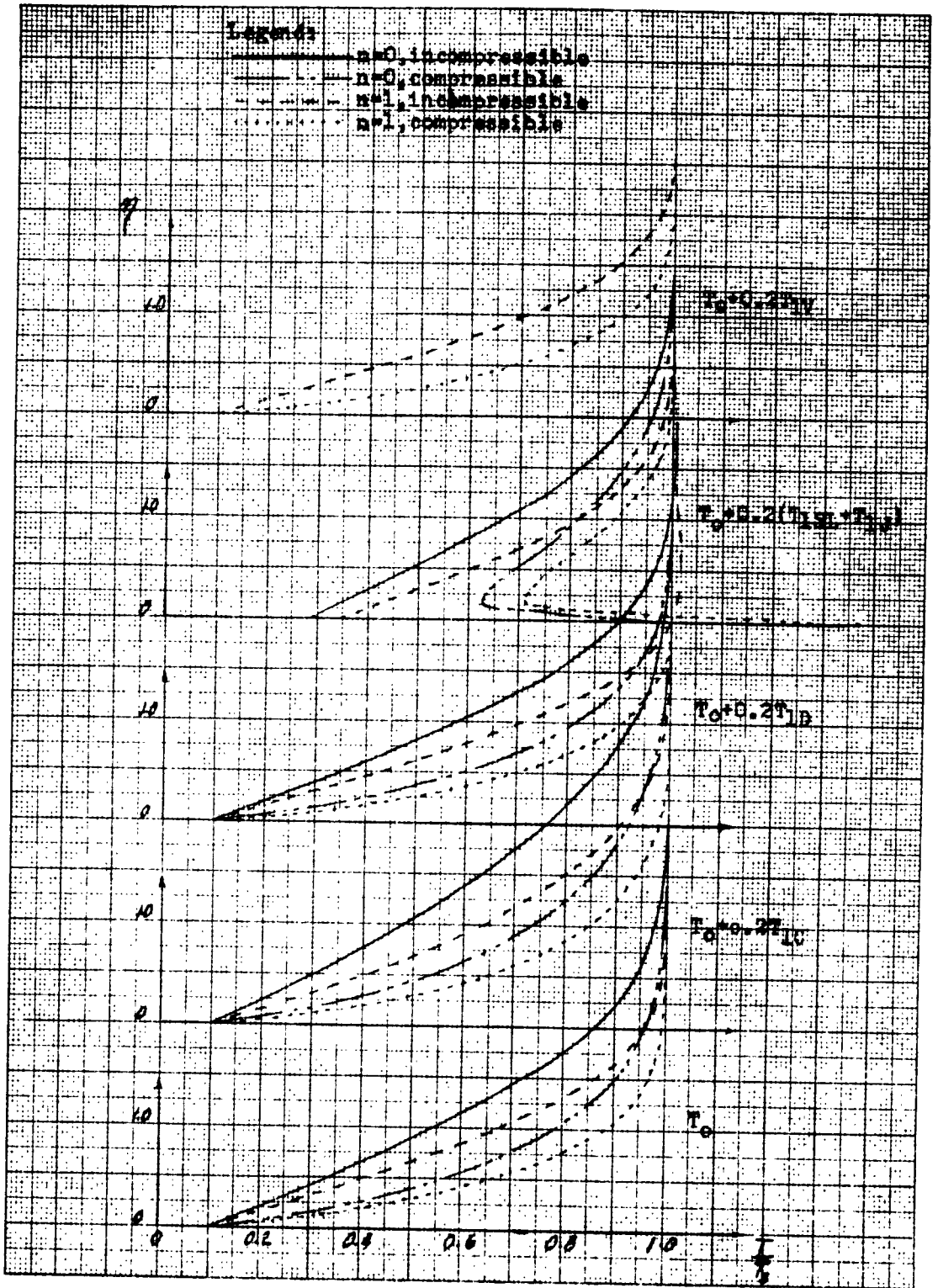


FIGURE 5a.

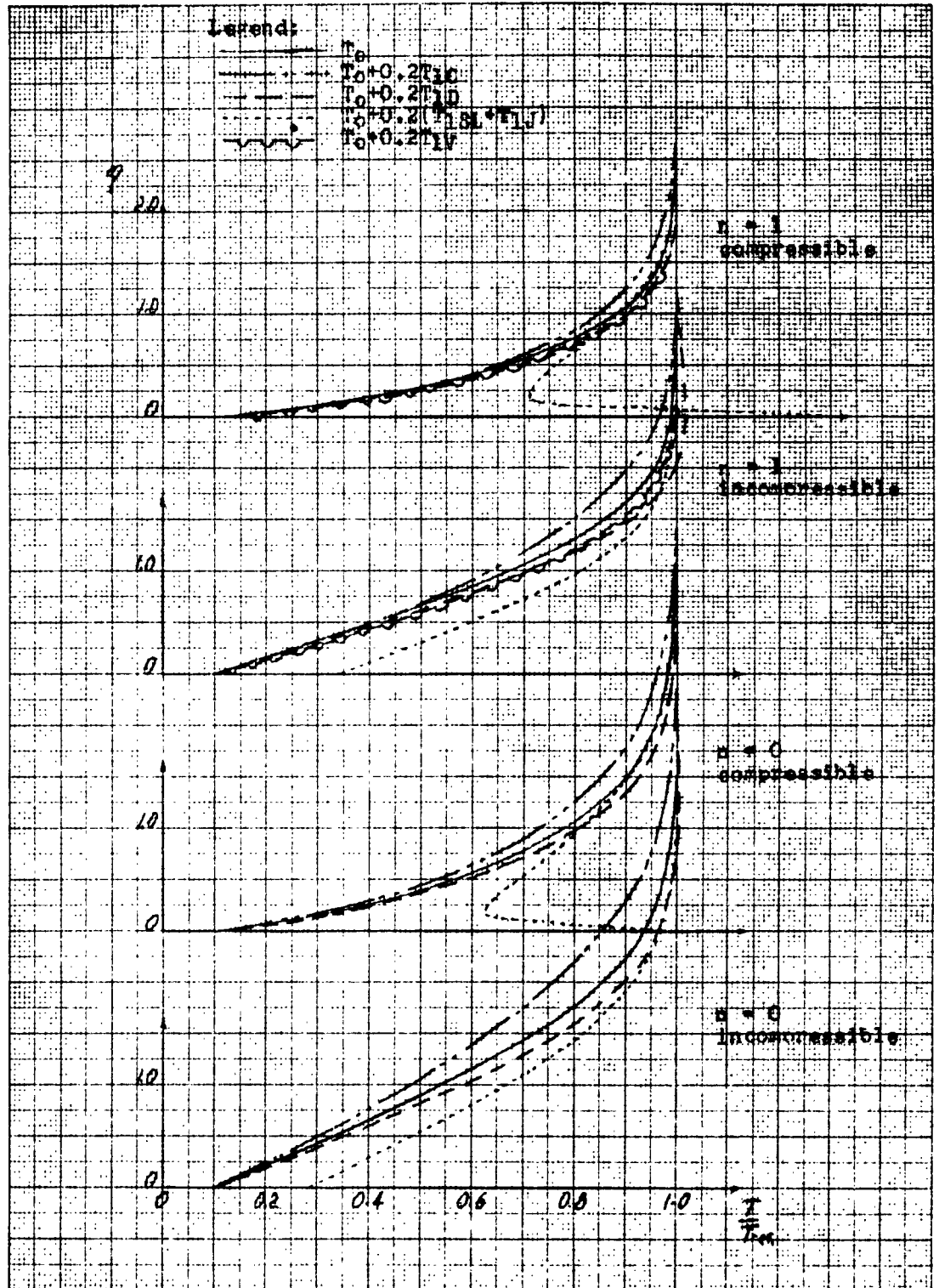


FIGURE 5b.

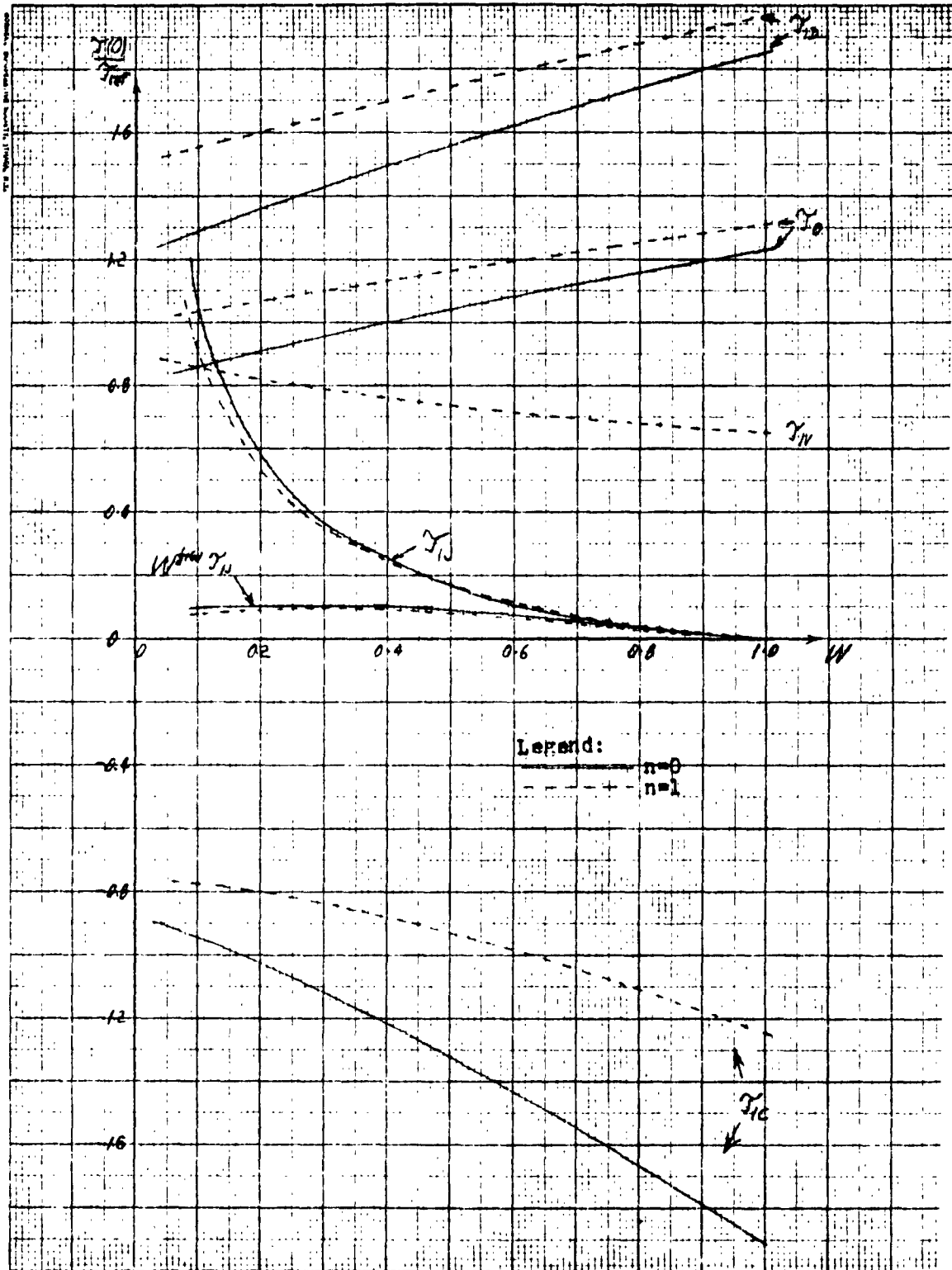


FIGURE 6.

Wall Heat Transfer Rate Parameters.

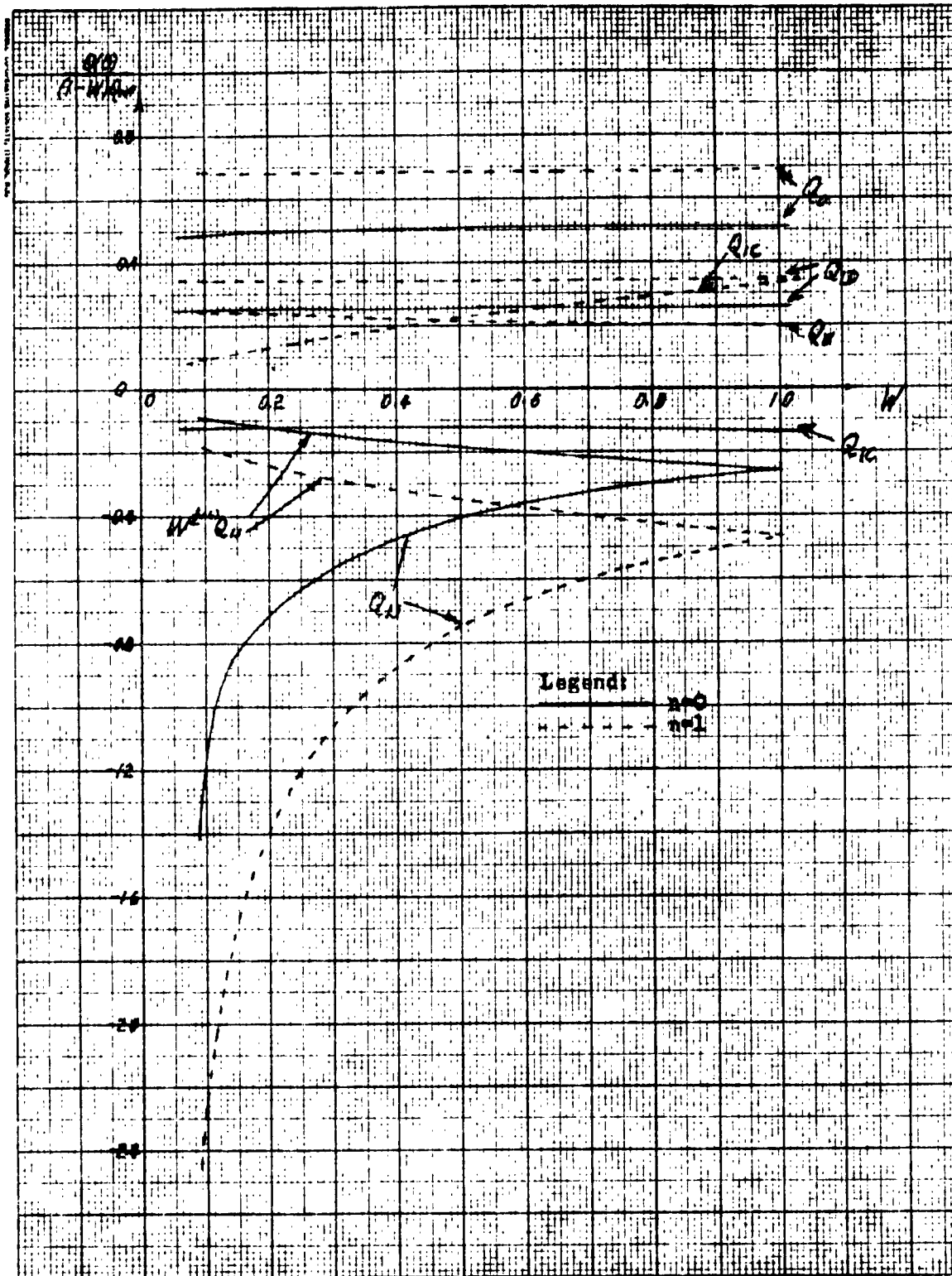


FIGURE 7.

TABLE I. CONSTANT-FLUID-PROPERTY SOLUTIONS
Incompressible Boundary-Layer Solution. Two-Dimensional Case ($n=0$).

$$f_0 f_0'' - f_0'^2 + 1 + f_0''' = 0$$

$$0.76 f_0 g_0' + g_0'' = 0$$

$$f_0(0) = f_0'(0) = g_0(0) = 0 \quad ; \quad \eta \rightarrow \infty, \quad f_0(\eta) \rightarrow 1, \quad g_0(\eta) \rightarrow 1$$

η	f_0	f_0'	f_0''	f_0'''	g_0	g_0'	g_0''
0	0	0	1.2326	-1.0000	0	0.5123	0
0.5	0.1336	0.4946	0.7583	-0.8565	0.2550	0.5034	-0.0611
1.0	0.4592	0.7779	0.3980	-0.5775	0.4960	.04518	-0.1576
1.5	0.8873	0.9162	0.1770	-0.3175	0.6983	0.3505	-0.2364
2.0	1.3620	0.9732	0.0658	-0.1423	0.8431	0.2288	-0.2368
2.5	1.8544	0.9929	0.0202	-0.0517	0.9301	0.1242	-0.1750
3.0	2.3526	0.9984	0.0051	-0.0150	0.9735	0.0559	-0.0998
3.5	2.8522	0.9997	0.0010	-0.0035	0.9915	0.0208	-0.0450
4.0	3.3521	0.0000	0.0002	-0.0006	0.9977	0.0064	-0.0163
4.5	3.8521	1.0000	0.0000	-0.0001	0.9995	0.0016	-0.0047
5.0	4.3521	1.0000	0.0000	0.0000	0.9999	0.0003	-0.0011
5.5	4.8521	1.0000	0.0000	0.0000	1.0000	0.0001	-0.0002
6.0	5.3521	1.0000	0.0000	0.0000	1.0000	0.0000	0.0000

$$\eta^* = 0.6479$$

$$-\frac{v_0}{\sqrt{2}A} = \frac{(sv)_0}{-s_s \sqrt{2}A} = f_0$$

$$\frac{u}{Ax} = \frac{(su)_0}{s_s Ax} = f_0'$$

$$\frac{\Omega_0}{-Ax \sqrt{2}} = \frac{z_0}{A_s Ax \sqrt{2}} = f_0''$$

$$\frac{T_0}{T_s} = W + (1-W)g_0$$

$$\frac{Q_0}{k_s \sqrt{2}} = (1-W)g_0'$$

Incompressible Boundary-Layer Solution, Axially Symmetric Case ($n=1$).

$$2F_0 F_0'' - F_0'^2 + 1 + F_0''' = 0$$

$$1.52 F_0 \theta_0' + \theta_0'' = 0$$

$$F_0(0) = F_0'(0) = \theta_0(0) = 0 \quad ; \quad \eta \rightarrow \infty, F_0(\eta) \rightarrow 1, \theta_0(\eta) \rightarrow 1$$

η	F_0	F_0'	F_0''	F_0'''	θ_0	θ_0'	θ_0''
0	0	0	1.3119	-1.0	0	0.6867	0
0.5	0.1432	0.5316	0.8182	-0.9515	0.3401	0.6614	-0.1439
1.0	0.4924	0.8299	0.3959	-0.7008	0.6418	0.5244	-0.3924
1.5	0.9441	0.9552	0.1357	-0.3431	0.8501	0.3050	-0.4375
2.0	1.4330	0.9919	0.0310	-0.1044	0.9537	0.1237	-0.2692
2.5	1.9313	0.9990	0.0045	-0.0193	0.9897	0.0345	-0.1009
3.0	2.4311	0.9999	0.0004	-0.0022	0.9984	0.0066	-0.0041
3.5	2.9311	1.0000	0.0000	-0.0001	0.9998	0.0009	-0.0038
4.0	3.4311	1.0000	0.0000	0.0000	1.0000	0.0001	-0.0004
4.5	3.9311	1.0000	0.0000	0.0000	1.0000	0.0000	0.0000

$$\eta^* = 0.5689$$

$$\frac{v_s}{-2\sqrt{\frac{\nu}{\rho}} A} = \frac{(sv)_0}{-2s_s \sqrt{\frac{\nu}{\rho}} A} = F_0$$

$$\frac{u_0}{A x} = \frac{(su)_0}{s_s A x} = F_0'$$

$$\frac{\Omega_0}{-A x \sqrt{\frac{\nu}{\rho}}} = \frac{\tau_0}{s_s A x \sqrt{\frac{\nu}{\rho}}} = F_0''$$

$$\frac{T_w}{T_s} = w + (1-w)\theta_0$$

$$\frac{Q_0}{k T_s \sqrt{\frac{\nu}{\rho}}} = (1-w)\theta_0'$$

Incompressible Curvature-Correction Term. Two-Dimensional Case ($n=0$).

$$f_{\theta}'' = -2\beta' f_{\theta}' + f_{\theta}'' + f_{\theta}'' = \eta(1-f_{\theta}') + \eta^2$$

$$0.745\beta_{\theta}'' + \beta_{\theta}'' = -[\eta^2\beta_{\theta}' + \beta_{\theta}'' + 0.143\beta_{\theta}'']$$

$$f_{\theta}(0) = f_{\theta}'(0) = \beta_{\theta}(0) = 0 ; \eta \rightarrow \infty ; f_{\theta}'(\eta) \rightarrow -1 ; \beta_{\theta}(\eta) \rightarrow 0$$

η	f_{θ}	f_{θ}'	f_{θ}''	f_{θ}'''	f_{θ}''''	β_{θ}	β_{θ}'	β_{θ}''	β_{θ}'''	β_{θ}''''	$\frac{\beta_{\theta}''''}{\beta_{\theta}''}$
0	0	0	-1.9133	0.6479	0	0	-0.1390	-0.5123	0	-1.9133	
0.5	-0.2216	-0.8458	-1.4330	1.0989	-0.1286	-0.3660	-0.3598	-0.2884	-0.2884	-0.9384	
1.0	-0.8018	-1.4339	-0.9491	0.7498	-0.3386	-0.4323	0.1320	-1.2610	-1.2610	-0.1712	
1.5	-1.6247	-1.8389	-0.7190	0.1804	-0.5160	-0.2378	0.5972	-2.9557	-2.9557	+0.1972	
2.0	-2.6326	-2.1938	-0.7299	-0.1698	-0.5541	0.0867	0.6128	-5.3565	-5.3565	0.2433	
2.5	-3.8250	-2.5847	-0.8381	-0.2237	-0.4474	0.3083	0.2396	-8.4610	-8.4610	0.1548	
3.0	-5.2264	-3.0287	-0.9307	-0.1387	-0.2803	0.3296	-0.1244	-12.2840	-12.2840	0.0677	
3.5	-6.8595	-3.5076	-0.9779	-0.0567	-0.1367	0.2267	-0.2468	-16.8420	-16.8420	0.0218	
4.0	-8.7364	-4.0016	-0.9947	-0.0166	-0.0548	0.1136	-0.1889	-22.2145	-22.2145	0.0053	
4.5	-10.8618	-4.5003	0.9990	-0.0036	-0.0174	0.0436	-0.0946	-28.1960	-28.1960	0.0010	
5.0	-13.2369	-5.0001	-0.9999	-0.0006	-0.0045	0.0131	-0.0346	-34.9970	-34.9970	0.0001	
5.5	-15.8619	-5.5000	-1.0000	0.0000	-0.0009	-0.0002	0.0031	-42.5479	-42.5479	0.0000	
6.0	-18.7369	-6.0000	-1.0000	0.0000	-0.0002	0.0000	0.0006	-50.8488	-50.8488	0.0000	
6.5	-21.8619	-6.5000	-1.0000	0.0000	0.0000	0.0000	0.0001	-59.8996	-59.8996	0.0000	
7.0	-25.2369	-7.0000	-1.0000	0.0000	0.0000	0.0000	0.0000	-69.7003	-69.7003	0.0000	

$\beta'' = 0.6479$

$$\frac{\beta''}{\beta} = \frac{(3\eta)^2}{-4.1031} = f_{\theta} - \eta^2$$

$$\frac{\beta''}{\beta} = \frac{(3\eta)^2}{5.43\pi} = f_{\theta}'$$

$$\frac{\beta''}{-4.2/\sqrt{\pi}} = f_{\theta} + f_{\theta}'$$

$$\frac{\beta''}{\sqrt{2.85/\sqrt{\pi}}} = f_{\theta}$$

$$\frac{\beta''}{\Gamma_2} = (1-w)\beta_{\theta}$$

$$\frac{\beta''}{(1.5/\sqrt{\pi})} = (1-w)\beta_{\theta}'$$

Incompressible Curvature-Correction Term: Axially Symmetric Case ($n=1$).

$$2\gamma_0 f_{,cc} - 2\gamma_0 f_{,cc} + 2\gamma_0 f_{,cc} + f_{,cc} = -\gamma_0 \left[\frac{1}{2} f_{,cc} + 2\gamma_0 \right] + \frac{1}{2} f_{,cc} + \frac{1}{2} f_{,cc} + \frac{1}{2} f_{,cc}$$

$$1.52 f_{,cc} + f_{,cc} = -2 \left[\gamma_0 \frac{1}{2} + \gamma_0 + 0.16 \gamma_0 f_{,cc} \right]$$

$$f_{,c}(0) = f_{,c}(\infty) = f_{,c}(0) = 0 \quad ; \quad \eta \rightarrow \infty, f_{,c}(\eta) \rightarrow 0, f_{,c}(\eta) \rightarrow 0$$

η	$f_{,c}$	$f_{,c}^I$	$f_{,c}^{II}$	$f_{,c}^{III}$	$f_{,c}^{IV}$	$f_{,c}^V$	$f_{,c}^VI$	$f_{,c}^VII$	$f_{,c}^VIII$	$f_{,c}^IX$	$f_{,c}^{X}$	$f_{,c}^{XI}$	$f_{,c}^{XII}$	$f_{,c}^{XIII}$	$f_{,c}^{XIV}$	$f_{,c}^{XV}$	$f_{,c}^{XVI}$	
0	0	0	0	0	0	0	0	0	0	0	0	0	0	0	0	0	0	0
0.5	-0.1217	-0.4190	1.6332	0	0.0022	0.3362	-1.3734	0	0	0	0	0	0	0	0	0	0	-1.2452
1.0	-0.3549	-0.4985	-0.4353	1.1569	+0.0022	-0.2972	-0.9919	-0.2649	-0.6848	-0.8443	-0.1715	-1.0014	-0.7333	-0.8024	0.1895	0.0637	0.0111	-0.9888
1.5	-0.5422	-0.2740	0.2244	0.9356	-0.2192	-0.4714	0.3718	-1.3398	-1.2884	+0.2219	-1.7069	-2.0814	-2.5184	-3.0024	0.0001	0.0001	0.0001	-0.9999
2.0	-0.6313	-0.0976	0.4253	+0.0971	-0.3638	0.3098	1.0274	-3.3745	-1.7069	-2.0814	-2.5184	-3.0024	-3.5002	-4.0000	0.0000	0.0000	0.0000	-1.0000
2.5	-0.6573	-0.0209	0.2513	-0.4479	-0.2840	0.2669	0.2802	-6.3635	-2.0814	-2.5184	-3.0024	-3.5002	-4.0000	-4.5000	0.0000	0.0000	0.0000	-1.0000
3.0	-0.6619	-0.0027	0.0750	-0.2273	-0.1282	0.1077	-0.3157	-10.3137	-2.5184	-3.0024	-3.5002	-4.0000	-4.5000	-5.0000	0.0000	0.0000	0.0000	-1.0000
3.5	-0.6624	-0.0002	0.0124	-0.0516	-0.0359	0.0250	-0.2601	-15.2485	-3.0024	-3.5002	-4.0000	-4.5000	-5.0000	-5.5000	0.0000	0.0000	0.0000	-1.0000
4.0	-0.6624	0.0000	0.0012	-0.0061	-0.0065	0.0036	-0.0855	-21.1800	-3.5002	-4.0000	-4.5000	-5.0000	-5.5000	-6.0000	0.0000	0.0000	0.0000	-1.0000
4.5	-0.6624	0.0000	0.0001	-0.0004	-0.0008	0.0003	-0.0154	-28.1111	-4.0000	-4.5000	-5.0000	-5.5000	-6.0000	-6.5000	0.0000	0.0000	0.0000	-1.0000
5.0	-0.6624	0.0000	0.0000	0.0000	0.0000	0.0000	-0.0017	-36.0420	-4.5000	-5.0000	-5.5000	-6.0000	-6.5000	-7.0000	0.0000	0.0000	0.0000	-1.0000
5.5	-0.6624	0.0000	0.0000	0.0000	0.0000	0.0000	-0.0001	-44.9733	-5.0000	-5.5000	-6.0000	-6.5000	-7.0000	-7.5000	0.0000	0.0000	0.0000	-1.0000
							0.0000	-54.9043	-5.5000	-6.0000	-6.5000	-7.0000	-7.5000	-8.0000	0.0000	0.0000	0.0000	-1.0000

$$\eta^* = 0.5689$$

$$\frac{\eta^*}{2\sqrt{2}A} = \frac{(5\eta^*)_{cc}}{2\sqrt{2}A} = f_{,cc} - 2\gamma_0$$

$$\frac{\eta^*}{A} = \frac{(5\eta^*)_{cc}}{A} = f_{,cc} - \gamma_0$$

$$\frac{\eta^*}{-A\sqrt{2}} = f_{,cc} - \gamma_0$$

$$\frac{\eta^*}{A\sqrt{2}} = f_{,cc} - \gamma_0$$

$$\frac{\eta^*}{A} = (1-w)\eta^*_{cc}$$

$$\frac{\eta^*}{\sqrt{2}A} = (1-w)\eta^*_{cc}$$

Incompressible Displacement-Correction Term. Two-Dimensional Case ($n=0$).

$$F_D = \frac{1}{2} (F_0 + \gamma F_0')$$

$$T_D = \frac{1}{2} \gamma T_0'$$

γ	F_0	F_0'	F_0''	T_0	T_0'
0	0	0	1.8489	0	0.2561
0.5	0.1905	0.6842	0.9233	0.1258	0.2389
1.0	0.6185	0.9769	0.3082	0.2259	0.1470
1.5	1.1308	1.0489	0.0272	0.2629	-0.0020
2.0	1.1654	1.0390	-0.0438	0.2288	-0.1224
2.5	2.1683	1.0181	-0.0344	0.1553	-0.1567
3.0	2.6739	1.0060	-0.0150	0.0838	-0.1219
3.5	3.1756	1.0015	-0.0046	0.0364	-0.0684
4.0	3.6759	1.003	-0.0011	0.0128	-0.0294
4.5	4.1760	1.0000	-0.0002	0.0036	-0.0099
5.0	4.6760	1.0000	0.0000	0.0009	-0.0027
5.5	5.1760	1.0000	0.0000	0.0002	-0.0006
6.0	5.6760	1.0000	0.0000	0.0000	-0.0001
6.5	6.1760	1.0000	0.0000	0.0000	0.0000

$$\frac{F_D}{-1/2sA} = \frac{(sV)_D}{-s_s \sqrt{s} s A} = F_D$$

$$\frac{U_D}{A\pi} = \frac{(sU)_D}{s_s A \pi} = F_D'$$

$$\frac{\Omega_D}{-A\pi/\sqrt{k}} = \frac{z_D}{k_s A \pi / \sqrt{k}} = F_D''$$

$$\frac{T_D}{T_s} = (1-w) T_0'$$

$$\frac{Q_D}{k_s T_s / \sqrt{k}} = (1-w) T_0'$$

Incompressible Displacement-Correction Term. Axially Symmetric Case ($n=1$).

$$f_{10} = \frac{1}{2} (f_0 + \eta f_0')$$

$$g_{10} = \frac{1}{2} \eta g_0'$$

η	f_{10}	f_{10}'	f_{10}''	g_{10}	g_{10}'
0	0	0	1.9679	0	0.3434
0.5	0.2045	0.7361	0.9893	0.1653	0.2947
1.0	0.6611	1.0278	0.2433	0.2622	0.0659
1.5	1.8885	1.0570	-0.0543	0.2287	-0.1758
2.0	1.7084	1.0228	-0.0584	0.1237	-0.2076
2.5	2.2144	1.0047	-0.0176	0.0431	-0.1092
3.0	2.7154	1.0006	-0.0027	0.0099	-0.0331
3.5	3.2155	1.0000	-0.0002	0.0015	-0.0062
4.0	3.7155	1.0000	0.0000	0.0002	-0.0008
4.5	4.2155	1.0000	0.0000	0.0000	0.0000

$$\frac{v_{10}}{-2\eta/A} = \frac{(sr)_{10}}{-2s_1\eta/A} = f_{10}$$

$$\frac{u_{10}}{Ax} = \frac{(su)_{10}}{s_1 Ax} = f_{10}'$$

$$\frac{\Omega_{10}}{-Ax/\sqrt{2}} = \frac{\tau_{10}}{A_1 Ax/\sqrt{2}} = f_{10}''$$

$$\frac{T_{10}}{T_1} = (1-\eta) g_{10}$$

$$\frac{Q_{10}}{kT_1/\sqrt{2}A} = (1-\eta) g_{10}'$$

**Incompressible Velocity-Slip and Temperature-Jump Correction Terms,
Two-Dimensional Case ($n=0$).**

$$F_{1s_1} = F_0' \quad ; \quad \tilde{q}_{1s_1} = \tilde{q}_0' + \left(\frac{\mu_s}{\mu_1} - 1\right) \tilde{q}_0'(0) [1 - \tilde{q}_0]$$

η	$\tilde{q}_0'(\eta) [1 - \tilde{q}_0]$	$\tilde{q}_0'(0) \tilde{q}_0$
0	0.5123	0.2624
0.5	0.3816	0.2579
1.0	0.2582	0.2314
1.5	0.1546	0.1796
2.0	0.0864	0.1172
2.5	0.0358	0.0636
3.0	0.0136	0.0286
3.5	0.0044	0.0107
4.0	0.0012	0.0033
4.5	0.0003	0.0008
5.0	0.0000	0.0002
5.5	0.0000	0.0001
6.0	0.0000	0.0000

$$\frac{v_{1s_1}}{-\sqrt{\mu_s A}} = \frac{(v\tilde{v})_{1s_1}}{-s_s \sqrt{\nu_s A}} = F_{1s_1}$$

$$\frac{u_{1s_1}}{A x} = \frac{(su)_{1s_1}}{s_s A x} = F_{1s_1}'$$

$$\frac{\Omega_{1s_1}}{-Ax/\sqrt{\mu_s A}} = \frac{\tau_{1s_1}}{\mu_s Ax/\sqrt{\mu_s A}} = F_{1s_1}''$$

$$\frac{T_{1s_1}}{T_s} = (1-w) \tilde{q}_{1s_1}$$

$$\frac{Q_{1s_1}}{k_s T_s/\sqrt{\mu_s A}} = (1-w) \tilde{q}_{1s_1}'$$

Incompressible Velocity-Slip and Temperature-Jump Correction Terms.
Axially Symmetric Case ($n=1$)

$$f_{1s1} = F_0' \quad ; \quad g_{1s1} = g_0' + \left(\frac{\kappa_0}{\mu_1} - 1\right) g_0'(0) [1 - \delta_0]$$

η	$g_0'(0) [1 - \delta_0]$	$g_0'(0) g_0'$
0	0.6867	0.4716
0.5	0.4532	0.4542
1.0	0.2460	0.3601
1.5	0.1029	0.2094
2.0	0.0318	0.0849
2.5	0.0071	0.0237
3.0	0.0011	0.0045
3.5	0.0001	0.0006
4.0	0.0000	0.0001
4.5	0.0000	0.0000

$$\frac{v_{1s1}}{-2\sqrt{\frac{\mu_1}{\rho_1} A}} = \frac{(g_0 v)_{1s1}}{-2g_0 \mu_1 A} = F_{1s1}$$

$$\frac{u_{1s1}}{A x} = \frac{(g_0 u)_{1s1}}{g_0 A x} = F_{1s1}'$$

$$\frac{-\frac{\Omega_{1s1}}{A x \sqrt{\frac{\mu_1}{\rho_1} A}}}{\sqrt{\frac{\mu_1}{\rho_1} A}} = \frac{g_{1s1}}{A_0 \mu_1 \sqrt{\frac{\mu_1}{\rho_1} A}} = F_{1s1}''$$

$$\frac{T_{1s1}}{T_s} = (1-w) g_{1s1}$$

$$\frac{Q_{1s1}}{k_{T,s} \sqrt{\frac{\mu_1}{\rho_1} A}} = (1-w) g_{1s1}'$$

Incompressible Vorticity-Correction Term, Axially Symmetric Case Only ($n=1$).

$$2F_0''F_W - 2F_0'F_W' + 2F_0F_W'' + F_W''' = 0$$

$$1.52 F_0 \varpi_W' + \varpi_W'' = -1.52 \varpi_0' F_{1W}$$

$$F_{1W}(0) = F_W'(0) = \varpi_W(0) = 0 ; \quad \eta \rightarrow \infty, F_W(\eta) \rightarrow 1 ; \varpi_W(\eta) \rightarrow 0$$

η	F_{1W}	F_W'	F_W''	F_W'''	ϖ_W	ϖ_W'	ϖ_W''
0	0	0	0.6491	0	0	0.1956	0
0.5	0.0812	0.3249	0.6523	0.0257	0.0951	0.1748	-0.1196
1.0	0.3262	0.6586	0.6932	0.1521	0.1586	0.0629	-0.3070
1.5	0.7460	1.0298	0.8005	0.2535	0.1516	-0.0841	-0.2249
2.0	1.3661	1.4605	0.9164	0.1862	0.0922	-0.1317	0.0308
2.5	2.2142	1.9368	0.9787	0.0692	0.0365	-0.0830	0.1285
3.0	3.3059	2.4318	0.9968	0.0138	0.0095	-0.0295	0.0762
3.5	4.6466	2.9311	0.9997	0.0015	0.0016	-0.0064	0.0225
4.0	6.2372	3.4311	1.0000	0.0001	0.0002	-0.0009	0.0039
4.5	8.0777	3.9311	1.0000	0.0000	0.0000	-0.0001	0.0004
5.0	10.1683	4.4311	1.0000	0.0000	0.0000	0.0000	0.0000

$$\frac{v_w}{-2\sqrt{s}A} = \frac{(sv)_{1W}}{-2s\sqrt{s}A} = F_{1W}$$

$$\frac{u_w}{Ax} = \frac{(su)_{1W}}{s_s Ax} = F_{1W}'$$

$$\frac{\Omega_w}{-Ax/\sqrt{s}} = \frac{\varpi_w}{A_s Ax/\sqrt{s}} = F_{1W}''$$

$$\frac{T_w}{T_s} = (1-w)J_{1W}$$

$$\frac{Q_w}{k_s T_s/\sqrt{s}} = (1-w)\varpi_{1W}'$$

$n=0$
 $W=0.50$, $\eta^* = 0.2573$

η	f_0	f'_0	f''_0	f'''_0	f_0	f'_0	f''_0	f'''_0	$\frac{f_0}{f'_0}$	$\frac{f_0}{f''_0}$	$\frac{f_0}{f'''_0}$	$\frac{f_0}{f_0}$
0	0	0	0	0	0	0	0	0	0	0	0	0.2517
0.25	0.0768	0.5974	-4.3048	0.50	0.4660	-0.1763	0.0457	1.5540	1.0396	2.0000	1.6802	0.2499
0.50	0.2906	0.8113	-2.1090	0.6791	0.3139	-0.1750	0.1702	1.0788	0.7985	1.6802	1.4725	0.2404
0.75	0.4712	0.9376	-1.0610	0.7521	0.2695	-0.1805	0.3543	0.7418	0.5927	1.4725	1.3297	0.2214
1.0	0.7137	0.9949	-0.5327	0.8136	0.2243	-0.1797	0.5008	0.5056	0.4286	1.3297	1.2288	0.1945
1.5	1.2212	1.0236	-0.1153	0.9042	0.1399	-0.1526	1.1042	0.1971	0.3023	1.2288	1.1059	0.1305
2.0	1.7380	1.0176	-0.0046	0.9570	0.0750	-0.1094	1.6574	0.0578	0.1387	1.1059	1.0450	0.0728
2.5	2.2385	1.0087	0.0161	0.9833	0.0342	-0.0596	2.2011	0.0201	0.0564	1.0450	1.0169	0.0338
3.0	2.7413	1.0034	0.0124	0.9945	0.0131	-0.0275	2.7262	0.0060	0.0199	1.0169	1.0055	0.0131
3.5	3.2423	1.0010	0.0059	0.9985	0.0042	-0.0103	3.2373	0.0015	0.0060	1.0055	1.0015	0.0042
4.0	3.7426	1.0003	0.0021	0.9996	0.0011	-0.0032	3.7413	0.0003	0.0003	1.0015	1.0004	0.0011
4.5	4.2427	1.0000	0.0006	0.9999	0.0002	-0.0008	4.2424	0.0001	0.0001	1.0004	1.0000	0.0000
5.0	4.7427	1.0000	0.0001	1.0000	0.0000	-0.0001	4.7427	0.0000	0.0000	1.0000	1.0000	0.0000
5.5	5.2427	1.0000	0.0000	1.0000	0.0000	0.0000	5.2427	0.0000	0.0000	1.0000	1.0000	0.0000

$W=0.25$, $\eta^* = 0.0337$

η	f_0	f'_0	f''_0	f'''_0	f_0	f'_0	f''_0	f'''_0	$\frac{f_0}{f'_0}$	$\frac{f_0}{f''_0}$	$\frac{f_0}{f'''_0}$	$\frac{f_0}{f_0}$
0	0	0	0	0	0	0	0	0	0	0	0	0.3741
0.125	0.0449	0.6103	-19.9039	0.25	0.9738	-1.1648	0.0160	2.0791	0.9304	4.0000	2.8045	0.3730
0.25	0.1382	0.8514	-7.4120	0.3566	0.7600	-0.7536	0.0613	1.4708	0.8087	2.8045	2.2533	0.3678
0.50	0.3776	1.0256	-1.8116	0.4438	0.6442	-0.4849	0.2809	1.1185	0.6983	2.2533	1.7094	0.3429
0.75	0.6407	1.0680	-0.5801	0.5850	0.4963	-0.3842	0.4454	0.7011	0.6000	1.7094	1.4385	0.3027
1.0	0.9084	1.0702	-0.1870	0.6952	0.3891	-0.3203	0.7096	0.4577	0.4286	1.4385	1.2802	0.2541
1.5	1.4379	1.0459	0.0177	0.8963	0.3014	-0.2170	1.2887	0.3014	0.8359	1.2802	1.1157	0.1555
2.0	1.9947	1.0228	0.0411	0.9568	0.1677	-0.1296	1.8703	0.1269	0.9374	1.1157	1.0451	0.0794
2.5	2.4623	1.0093	0.0295	0.9845	0.0819	-0.0694	2.4442	0.0487	0.9786	1.0451	1.0157	0.0338
3.0	2.9652	1.0031	0.0151	0.9953	0.0342	-0.0273	2.9512	0.0047	0.9936	1.0157	1.0047	0.0120
4.0	3.9662	1.0002	0.0018	0.9998	0.0009	-0.0026	3.9654	0.0002	0.9999	1.0002	1.0002	0.0009
5.0	4.9663	1.0000	0.0000	1.0000	0.0000	0.0000	4.9663	0.0000	0.0000	1.0000	1.0000	0.0000

Compressible Boundary-Layer Solution. Axially Symmetric Case (n=1).

$$2F_0' \frac{d^2 F_0'}{dx^2} + \frac{2F_0'^2}{F_0'} - \frac{F_0'^2}{F_0'} + F_0''' + 2.50 F_0' \frac{F_0'}{F_0} + 0.50 F_0' \frac{F_0'^2}{F_0^2} + F_0' \frac{F_0''}{F_0} = 0$$

$$1.52 F_0' \frac{F_0'}{F_0} + F_0'' + 0.63 \frac{F_0'^2}{F_0} = 0$$

$$F_0(0) = F_0'(0) = 0, F_0(1) = W; \quad \eta \rightarrow \infty, F_0(\eta) \rightarrow 1, F_0'(\eta) \rightarrow 1$$

$$\frac{F_0''}{F_0'} = F_0', \quad \frac{F_0''}{F_0'} = F_0', \quad \frac{d(F_0' / F_0)}{dx} = F_0'$$

$$\frac{F_0''}{F_0'} = F_0' + F_0', \quad \frac{F_0''}{F_0'} = F_0' + F_0', \quad \frac{F_0''}{F_0'} = F_0' + F_0', \quad \frac{F_0''}{F_0'} = F_0' + F_0'$$

W=0.75, $\eta^* = 0.4193$

η	F_0	F_0'	F_0''	F_0'''	$F_0^{(4)}$	$F_0^{(5)}$	$F_0^{(6)}$	$\frac{F_0''}{F_0'}$	$\frac{F_0'''}{F_0''}$	$\frac{F_0^{(4)}}{F_0''}$	$\frac{F_0^{(5)}}{F_0''}$	$\frac{F_0^{(6)}}{F_0''}$	$\frac{F_0''}{F_0}$	$\frac{F_0'''}{F_0}$	$\frac{F_0^{(4)}}{F_0}$	$\frac{F_0^{(5)}}{F_0}$	$\frac{F_0^{(6)}}{F_0}$
0	0	0	1.9526	0.75	0.2086	0	0	0	0	0	0	0	1.4644	1.2394	1.3333	1.3333	0.1710
0.5	0.1981	0.6671	0.8277	0.8484	0.1809	0.1613	-0.0840	0.5659	0.7479	0.8228	0.8527	0.8527	0.8228	0.7479	1.1788	1.1788	0.1615
1.0	0.5988	0.9211	0.2648	0.9258	0.1248	0.5344	-0.1303	0.9629	0.3443	0.0627	0.9629	0.9629	0.3601	0.3443	1.0802	1.0802	0.1183
1.5	1.0810	0.9905	0.0538	0.9721	0.0627	1.0509	-0.1075	0.9933	0.1126	0.0223	0.9933	0.9933	0.1145	0.1126	1.0287	1.0287	0.0615
2.0	1.5799	1.0011	0.0029	0.9923	0.0223	1.5677	-0.0947	0.9999	0.0044	0.0009	0.9999	0.9999	0.0044	0.0044	1.0078	1.0078	0.0222
3.0	2.9907	1.0001	-0.0005	0.9998	0.0009	2.9861	-0.0036	1.0000	0.0004	0.0000	1.0000	1.0000	0.0004	0.0004	1.0002	1.0002	0.0009
4.0	3.9807	1.0000	0.0000	0.9999	0.0000	3.9807	0.0000	1.0000	0.0000	0.0000	1.0000	1.0000	0.0000	0.0000	1.0000	1.0000	0.0000

W=0.50, $\eta^* = 0.2584$

η	F_0	F_0'	F_0''	F_0'''	$F_0^{(4)}$	$F_0^{(5)}$	$F_0^{(6)}$	$\frac{F_0''}{F_0'}$	$\frac{F_0'''}{F_0''}$	$\frac{F_0^{(4)}}{F_0''}$	$\frac{F_0^{(5)}}{F_0''}$	$\frac{F_0^{(6)}}{F_0''}$	$\frac{F_0''}{F_0}$	$\frac{F_0'''}{F_0}$	$\frac{F_0^{(4)}}{F_0}$	$\frac{F_0^{(5)}}{F_0}$	$\frac{F_0^{(6)}}{F_0}$
0	0	0	3.4787	0.5	0.5901	0	0	0	0	0	0	0	1.7393	1.1635	2.0000	2.0000	0.3410
0.25	0.0827	0.9801	1.4057	0.6262	0.4639	0.0518	-0.3135	0.3633	0.9143	0.6639	0.6119	0.6119	1.1995	0.9143	1.5968	1.5968	0.3359
0.5	0.2638	0.8355	0.6652	0.7324	0.3847	0.1932	-0.3242	0.6119	0.4627	0.3024	0.4000	0.4000	0.8685	0.6749	1.3654	1.3654	0.3103
0.75	0.4888	0.9483	0.2847	0.8183	0.3024	0.4000	-0.3295	0.7760	0.2924	0.2225	0.7760	0.7760	0.5197	0.4627	1.2221	1.2221	0.2633
1.0	0.7325	0.9942	0.1051	0.8838	0.2225	0.6474	-0.3048	0.8787	0.1819	0.0951	0.8787	0.8787	0.3141	0.2924	1.1315	1.1315	0.2043
2.0	1.7399	1.0048	-0.0113	0.9903	0.0300	1.7231	-0.0805	0.9951	0.0003	0.0000	0.9951	0.9951	0.0190	0.0189	1.0098	1.0098	0.0298
3.0	2.7415	1.0002	-0.0007	0.9998	0.0010	2.7409	-0.0041	0.9999	0.0003	0.0000	0.9999	0.9999	0.0003	0.0003	1.0002	1.0002	0.0010
4.0	3.7416	1.0000	0.0000	0.9999	0.0000	3.7416	0.0000	1.0000	0.0000	0.0000	1.0000	1.0000	0.0000	0.0000	1.0000	1.0000	0.0000

Compressible Curvature-Correction Term. Two-Dimensional Case ($n = 0$).

$$M(f_{1c}, f_{2c}) = M_c(\eta, t_0, f_{1c}) = E_c(\eta, t_0, f_{1c}) \quad \text{(cf. EQUATIONS (2.64) AND (2.65))}$$

$$f_{1c}(\eta) = f_{1c}(\eta) = f_{1c}(\eta) = 0; \quad \eta \rightarrow \infty \quad f_{1c}(\eta) \rightarrow -1, \quad f_{2c}(\eta) \rightarrow 0$$

$$\frac{\partial f_{1c}}{\partial \eta} = f_{1c} + f_0 f_{2c} - \eta f_0 f_{1c} = f_{1c} f_{2c} + f_0 f_{1c} f_{2c} - \eta f_0 f_{1c} f_{2c} = f_{1c} f_{2c} (1 + f_0 - \eta f_0)$$

$$\frac{\partial f_{2c}}{\partial \eta} = f_{2c} f_{1c} + f_0 f_{1c} f_{2c} - \eta f_0 f_{1c} f_{2c} = f_{1c} f_{2c} (1 + f_0 - \eta f_0)$$

$$\frac{\partial^2 f_{1c}}{\partial \eta^2} = f_{1c} f_{2c} (1 + f_0 - \eta f_0) + f_{1c} f_{2c} (1 + f_0 - \eta f_0) - \eta f_0 f_{1c} f_{2c} (1 + f_0 - \eta f_0)$$

$$\frac{\partial^2 f_{2c}}{\partial \eta^2} = f_{1c} f_{2c} (1 + f_0 - \eta f_0) + f_{1c} f_{2c} (1 + f_0 - \eta f_0) - \eta f_0 f_{1c} f_{2c} (1 + f_0 - \eta f_0)$$

$W = 0.75$

η	f_{1c}	f_{2c}	f_{1c}''	f_{2c}''	f_{1c}'''	f_{2c}'''	$f_{1c}^{(4)}$	$f_{2c}^{(4)}$	$\frac{f_{1c}'''}{f_{1c}''}$	$\frac{f_{2c}'''}{f_{2c}''}$	$\frac{f_{1c}^{(4)}}{f_{1c}'''} - \frac{f_{2c}^{(4)}}{f_{2c}'''}$	$\frac{f_{1c}^{(4)}}{f_{1c}''}$	$\frac{f_{2c}^{(4)}}{f_{2c}''}$	$\frac{f_{1c}^{(4)}}{f_{1c}'''} - \frac{f_{2c}^{(4)}}{f_{2c}'''}$	$\frac{f_{1c}^{(4)}}{f_{1c}''}$	$\frac{f_{2c}^{(4)}}{f_{2c}''}$
0	0	0	-2.5238	0	-0.0397	0	0	0	0	0	-1.8973	-1.6057	0	-0.0325	-0.0325	
0.25	-0.0728	-0.5570	-1.9234	-0.0142	-0.0727	-0.1163	-0.0679	-0.4443	-0.0853	-1.3476	-1.4408	0.0229	0.0229	-0.0633	-0.0633	
0.5	-0.2662	-0.9668	-1.3748	-0.0355	-0.0956	-0.0668	-0.2989	-0.8193	-0.3549	-0.8408	-1.2315	0.0522	0.0522	-0.0873	-0.0873	
1.0	-0.8879	-1.4669	-0.7325	-0.0854	-0.0921	0.0763	-1.3424	-1.3601	-1.4554	-0.1373	-0.8864	0.1080	0.1080	-0.0920	-0.0920	
1.5	-1.7041	-1.7885	-0.6179	-0.1176	-0.0307	0.1504	-3.1834	-1.7933	-3.2626	0.1540	-0.7483	0.1336	0.1336	-0.0361	-0.0361	
2.0	-2.6794	-2.1234	-0.7390	-0.1147	0.0389	0.1119	-5.7554	-2.1749	-5.7510	0.1960	-0.7719	0.1219	0.1219	0.0343	0.0343	
3.0	-5.2202	-2.9977	-0.9719	-0.0492	0.0653	-0.0412	-12.9059	-3.0338	-12.8374	0.0661	-0.9294	0.0497	0.0497	0.0648	0.0648	
4.0	-8.7146	-3.9961	-1.0064	-0.0083	0.0185	-0.0338	-22.8963	-4.0031	-22.8745	0.0085	-0.9913	0.0083	0.0083	0.0185	0.0185	
5.0	-13.2129	-4.9996	-1.0011	-0.0028	0.0018	-0.0051	-35.9154	-5.0001	-35.9131	0.0005	-0.9995	0.0006	0.0006	0.0018	0.0018	
6.5	-21.8377	-6.5000	-1.0000	0.0000	0.0000	0.0000	-61.0980	-6.5000	-61.0980	0.0000	-1.0000	0.0000	0.0000	0.0000	0.0000	

$W = 0.5$

η	f_{1c}	f_{2c}	f_{1c}''	f_{2c}''	f_{1c}'''	f_{2c}'''	$f_{1c}^{(4)}$	$f_{2c}^{(4)}$	$\frac{f_{1c}'''}{f_{1c}''}$	$\frac{f_{2c}'''}{f_{2c}''}$	$\frac{f_{1c}^{(4)}}{f_{1c}'''} - \frac{f_{2c}^{(4)}}{f_{2c}'''}$	$\frac{f_{1c}^{(4)}}{f_{1c}''}$	$\frac{f_{2c}^{(4)}}{f_{2c}''}$	$\frac{f_{1c}^{(4)}}{f_{1c}'''} - \frac{f_{2c}^{(4)}}{f_{2c}'''}$	$\frac{f_{1c}^{(4)}}{f_{1c}''}$	$\frac{f_{2c}^{(4)}}{f_{2c}''}$
0	0	0	-3.9900	0	-0.1022	0	0	0	0	0	-1.9750	-1.3212	0	-0.0634	-0.0634	
0.125	-0.0277	-0.4190	-2.8183	-0.0149	-0.1356	-0.2402	-0.0170	-1.2349	-0.0303	-1.6049	-1.2735	0.0495	0.0495	-0.0944	-0.0944	
0.25	-0.0998	-0.7183	-2.0170	-0.0336	-0.1618	-0.1763	-0.0734	-0.4459	-0.1190	-1.2698	-1.2071	0.0949	0.0949	-0.1228	-0.1228	
0.5	-0.3307	-1.0900	-1.0747	-0.0781	-0.1877	-0.0698	-0.3292	-0.8035	-0.4560	-0.7294	-1.0624	0.1693	0.1693	-0.1628	-0.1628	
0.75	-0.6315	-1.2993	-0.6624	-0.1244	-0.1773	0.1091	-0.7993	-1.0998	-0.9848	-0.3512	-0.9365	0.2200	0.2200	-0.1709	-0.1709	
1.0	-0.9751	-1.4440	-0.5274	-0.1641	-0.1363	0.2107	-1.4914	-1.3384	-1.6888	-0.1027	-0.8489	0.2479	0.2479	-0.1453	-0.1453	
1.5	-1.7632	-1.7152	-0.6014	-0.2019	-0.0107	0.2569	-3.4972	-1.7576	-3.5999	0.1300	-0.7684	0.2469	0.2469	-0.0301	-0.0301	
2.0	-2.7037	-2.0626	-0.7886	-0.3568	0.0926	0.1390	-6.2121	-2.1559	-6.1676	0.1621	-0.9344	0.0658	0.0658	0.0956	0.0956	
3.0	-5.2086	-2.9825	-1.0010	-0.0704	0.0965	-0.0835	-13.5372	-3.0315	-13.4326	0.0606	-0.9344	0.0658	0.0658	0.0956	0.0956	
4.0	-8.6988	-3.9948	-1.0103	-0.0094	0.0224	-0.0449	-23.6941	-4.0028	-23.6673	0.0080	-0.9918	0.0094	0.0094	0.0224	0.0224	
5.0	-13.1947	-4.9996	-1.0012	-0.0026	0.0018	-0.0055	-36.9106	-5.0001	-36.9083	0.0004	-0.9996	0.0006	0.0006	0.0010	0.0010	
6.5	-21.8195	-6.5000	-1.0000	0.0000	0.0000	0.0000	-62.3974	-6.5000	-62.3974	0.0000	-1.0000	0.0000	0.0000	0.0000	0.0000	

Compressible Displacement Correction Term. Two-Dimensional Case ($n=0$).

$$f_{1D} = \frac{1}{2} (F_0 + \gamma F_0') ; \quad E_{1D} = \frac{1}{2} \gamma E_{10}'$$

$$\frac{v_{1D}}{-v_{10}'} = E_{10} f_{1D} + F_0' f_{1D} ; \quad \frac{u_{1D}}{A_x} = f_{10}' F_{10}' + F_0' f_{1D}$$

$$\frac{(s_v)_{1D}}{-s_{v10}'} = f_{1D} ; \quad \frac{(s_u)_{1D}}{s_{u10}'} = f_{10}' ; \quad \frac{\Omega_{1D}}{-\Omega_{10}'} = f_{10}' F_{10}'' + E_{10}' f_{10}' + F_0' E_{10}' + F_0'' E_{10}'$$

$$\frac{z_{1D}}{A_x \Delta x / \sqrt{\frac{2}{\gamma}}} = F_{10}^{0.58} [E_{10}' F_{10}'' + E_{10}' f_{10}' + F_0' f_{10}'' + 1.58 E_{10}' f_{10}' + 0.58 F_0' \frac{E_{10}'}{F_{10}'} f_{10}']$$

$$\frac{s_{1D}}{s_{10}'} = -\frac{E_{1D}}{E_{10}'} ; \quad \frac{T_{1D}}{T_{10}'} = F_{1D} ; \quad \frac{Q_{1D}}{Q_{10}'} = F_{10}^{0.49} [E_{10}' + 0.19 \frac{F_{10}'}{F_{10}'} f_{10}']$$

$W = 0.75$

γ	f_{1D}	f_{10}'	E_{1D}	$\frac{v_{1D}}{v_{10}'}$	$\frac{u_{1D}}{u_{10}'}$	$\frac{\Omega_{1D}}{\Omega_{10}'}$	$\frac{z_{1D}}{z_{10}'}$	$\frac{s_{1D}}{s_{10}'}$	$\frac{Q_{1D}}{Q_{10}'}$
0	0	0	0	0	0	2.0199	1.7094	0	0.0635
0.25	0.0719	0.5297	0.0186	0.0576	0.4244	1.3923	1.2249	-0.0300	0.0626
0.5	0.2498	0.8303	0.0353	0.2089	0.7066	0.8883	0.8109	-0.0519	0.0571
1.0	0.7286	1.0410	0.0577	0.6805	0.9768	0.2720	0.2671	-0.0730	+0.0286
1.5	1.2539	1.0460	0.0606	1.2394	1.0407	+0.0282	+0.0330	-0.0688	-0.0089
2.0	1.7696	1.0175	0.0478	1.7902	1.0350	-0.0327	-0.0304	-0.0508	-0.0322
2.5	2.2736	1.0010	0.0297	2.3059	1.0183	-0.0293	-0.0288	-0.0305	-0.0341
3.0	2.7727	0.9968	0.0148	2.7981	1.0073	-0.0151	-0.0150	-0.0149	-0.0236
3.5	3.2713	0.9977	0.0060	3.2851	1.0023	-0.0058	-0.0058	-0.0060	-0.0121
4.0	3.7704	0.9990	0.0019	3.7761	1.0006	-0.0017	-0.0017	-0.0019	-0.0048
4.5	4.2701	0.9997	0.0005	4.2719	1.0001	-0.0004	-0.0004	-0.0005	-0.0015
5.0	5.2700	1.0000	0.0000	5.2700	1.0000	0.0000	0.0000	0.0000	0.0000

n = 0
W = 0.5

η	f_n	f'_0	$f'_{1,0}$	$\frac{v_{1,0}}{v_{ref}}$	$\frac{u_{1,0}}{u_{ref}}$	$\frac{\Omega_{1,0}}{\Omega_{ref}}$	$\frac{\tau_{1,0}}{\tau_{ref}}$	$\frac{s_{1,0}}{s_1}$	$\frac{Q_{1,0}}{Q_{ref}}$
0	0	0	0	0	0	2.3310	1.5594	0	0.1258
0.25	0.1068	0.7329	0.0447	0.0670	0.4607	1.4185	1.0846	-0.1261	0.1225
0.5	0.3281	0.9906	0.0785	0.2425	0.7364	0.8318	0.7043	-0.1702	0.1059
0.75	0.5872	1.0637	0.1011	0.4892	0.8947	0.4637	0.4264	-0.1787	0.0756
1.0	0.8543	1.0671	0.1121	0.7753	0.9800	0.2372	0.2346	-0.1693	+0.0378
1.5	1.3783	1.0269	0.1049	1.3745	1.0359	+0.0262	+0.0340	-0.1283	-0.0311
2.0	1.8836	0.9983	0.0750	1.9326	1.0317	-0.0278	-0.0246	-0.0819	-0.0619
2.5	2.3801	0.9904	0.0428	2.4362	1.0170	-0.0264	-0.0257	-0.0492	-0.0557
3.0	2.8757	0.9926	0.0197	2.9138	1.0069	-0.0141	-0.0140	-0.0199	-0.0344
3.5	3.3730	0.9964	0.0073	3.3916	1.0022	-0.0055	-0.0055	-0.0073	-0.0159
4.5	4.3715	0.9997	0.0005	4.3735	1.0002	-0.0004	-0.0004	-0.0005	-0.0016
5.5	5.3714	1.0000	0.0000	5.3714	1.0000	0.0000	0.0000	0.0000	0.0000

W = 0.25

0	0	0	0	0	0	3.1187	1.3956	0	0.1871
0.125	0.0606	0.7868	0.0475	0.0237	0.3095	1.9864	1.1547	-0.3736	0.1851
0.25	0.1755	1.0119	0.0805	0.0890	0.5177	1.3933	0.9432	-0.4088	0.1761
0.5	0.4452	1.1076	0.1241	0.3073	0.7752	0.7438	0.6082	-0.3626	0.1379
0.75	0.7204	1.0907	0.1459	0.5946	0.9140	0.3991	0.3683	-0.3019	0.0831
1.0	0.9893	1.0567	0.1507	0.9096	0.9867	0.1996	0.2022	-0.2469	+0.0258
1.5	1.5033	1.0053	0.1258	1.5283	1.0326	+0.0185	+0.0271	-0.1566	-0.0581
2.0	2.0001	0.9862	0.0819	2.0738	1.0273	-0.0261	-0.0231	-0.0894	-0.0813
2.5	2.4927	0.9862	0.0428	2.5595	1.0141	-0.0232	-0.0225	-0.0441	-0.0630
3.0	2.9872	0.9920	0.0181	3.0267	1.0054	-0.0118	-0.0117	-0.0182	-0.0347
4.0	3.9835	0.9989	0.0017	3.9894	1.0004	-0.0012	-0.0012	-0.0017	-0.0048
5.0	4.9832	1.0000	0.0000	4.9832	1.0000	0.0000	0.0000	0.0000	0.0000

$n=0$

$W=0.1$

τ	F_0	F_0'	$F_{1,0}$	$\frac{F_{1,0}}{F_{1,0}}$	$\frac{F_{1,0}}{F_{1,0}}$	$\frac{\Omega_{1,0}}{\Omega_{1,0}}$	$\frac{\Omega_{1,0}}{\Omega_{1,0}}$	$\frac{\Omega_{1,0}}{\Omega_{1,0}}$	$\frac{\Omega_{1,0}}{\Omega_{1,0}}$
0	0	0	0	0	0	4.9039	1.2899	0	0.2233
0.03125	0.0138	0.7038	0.0250	0.0024	0.1246	3.3649	1.2281	-1.0066	0.2231
0.0625	0.0396	0.9182	0.0419	0.0093	0.2185	2.7061	1.1689	-1.0158	0.2221
0.125	0.1029	1.0779	0.0671	0.0343	0.3633	2.0066	1.0580	-0.8716	0.2178
0.1875	0.1723	1.1331	0.0950	0.0937	0.4751	1.5984	0.9561	-0.7033	0.2105
0.25	0.2438	1.1527	0.1026	0.1182	0.5656	1.3145	0.8623	-0.6615	0.2006
0.375	0.3882	1.1515	0.1273	0.2342	0.7041	0.9297	0.6957	-0.5368	0.1750
0.5	0.5310	1.1316	0.1445	0.3718	0.8033	0.6740	0.5537	-0.4521	0.1438
0.75	0.8078	1.0833	0.1613	0.6830	0.9280	0.3547	0.3317	-0.3386	0.0750
1.0	1.0733	1.0427	0.1602	1.0097	0.9919	0.1732	0.1783	-0.2610	+0.0105
1.5	1.5811	0.9958	0.1255	1.6261	1.0302	+0.0117	+0.0195	-0.1592	-0.0719
2.0	2.0748	0.9830	0.0773	2.1571	1.0239	-0.0251	-0.0226	-0.0836	-0.0855
3.0	3.0617	0.9929	0.0153	3.0975	1.0044	-0.0096	-0.0096	-0.0154	-0.0310
4.0	4.0585	0.9993	0.0013	4.0628	1.0005	-0.0008	-0.0008	-0.0013	-0.0037
5.0	5.0583	1.0000	0.0000	5.0583	1.0000	0.0000	0.0000	0.0000	0.0000

Compressible Displacement-Correction Term. Axially Symmetric Case ($n=1$).

$$f_{1,2} = \frac{1}{2} (f_0 + \eta f_0') \quad ; \quad f_{1,2}' = \frac{1}{2} \eta f_0''$$

$$\frac{v_{1,2}}{-2\eta f_{1,2}} = f_{1,2} f_{1,2}' + f_0 f_{1,2}'' \quad ; \quad \frac{v_{1,2}}{Ax} = f_{1,2} f_0' + f_0' f_{1,2}$$

$$\frac{(2v)_{1,2}}{-2\eta f_{1,2} A} = f_{1,2}'' \quad ; \quad \frac{(su)_{1,2}}{s_1 A x} = f_{1,2}' \quad ; \quad \frac{\Omega_{1,2}}{-Ax/\sqrt{1-\eta^2}} = f_{1,2} f_0'' + f_{1,2}' f_0' + f_0' f_{1,2}'' + f_0'' f_{1,2}$$

$$\frac{\tau_{1,2}}{\mu A \eta / \sqrt{1-\eta^2}} = f_{1,2} f_0''' \left[f_{1,2} f_0'' + f_{1,2}' f_0' + f_0' f_{1,2}'' + 1.58 f_0'' f_{1,2} + 0.58 f_0' f_{1,2}'' \right]$$

$$\frac{s_{1,2}}{s_1} = -\frac{f_{1,2}}{f_{1,2}'} \quad ; \quad \frac{T_{1,2}}{T_1} = f_{1,2} \quad ; \quad \frac{Q_{1,2}}{L_1 \eta / \sqrt{1-\eta^2}} = f_{1,2} f_0''' \left[f_{1,2}' + 0.69 \frac{f_{1,2}''}{f_{1,2}'} \right]$$

W = 0.75

η	f_0	f_0'	$f_{1,2}$	$\frac{v_{1,2}}{v_{ref}}$	$\frac{v_{1,2}}{U_{ref}}$	$\frac{\Omega_{1,2}}{\Omega_{ref}}$	$\frac{\tau_{1,2}}{\tau_{ref}}$	$\frac{s_{1,2}}{s_1}$	$\frac{Q_{1,2}}{Q_{ref}}$
0	0	0	0	0	0	2.1967	1.8591	0	0.0855
0.25	0.0773	0.5668	0.0247	0.0633	0.4639	1.5367	1.3687	-0.0385	0.0829
0.5	0.2618	0.8740	0.0452	0.2307	0.7716	0.9946	0.9272	-0.0628	0.0679
1.0	0.7599	1.0535	0.0624	0.7409	1.0327	0.3011	0.3014	-0.0728	+0.0028
1.5	1.2834	1.0309	0.0474	1.2985	1.0488	+0.0389	+0.0414	-0.0498	-0.0463
2.0	1.7911	1.0040	0.0223	1.8124	1.0186	-0.0081	-0.0078	-0.0226	-0.0424
3.0	2.7906	0.9993	0.0014	2.7936	1.0005	-0.0008	-0.0008	-0.0014	-0.0050
4.0	3.7904	1.0000	0.0000	3.7904	1.0000	0.0000	0.0000	0.0000	0.0000

W = 0.5

η	f_0	f_0'	$f_{1,2}$	$\frac{v_{1,2}}{v_{ref}}$	$\frac{v_{1,2}}{U_{ref}}$	$\frac{\Omega_{1,2}}{\Omega_{ref}}$	$\frac{\tau_{1,2}}{\tau_{ref}}$	$\frac{s_{1,2}}{s_1}$	$\frac{Q_{1,2}}{Q_{ref}}$
0	0	0	0	0	0	2.6090	1.7453	0	0.1705
0.25	0.1139	0.7658	0.0580	0.0761	0.5132	1.5891	1.2605	-0.1479	0.1610
0.5	0.3408	1.0017	0.0962	0.2750	0.8140	0.9409	0.8368	-0.1793	0.1179
0.75	0.6000	1.0551	0.1134	0.5464	0.9709	0.5196	0.4997	-0.1694	+0.0492
1.0	0.8634	1.0468	0.1112	0.8495	1.0357	0.2567	0.2603	-0.1424	-0.0200
1.5	1.3760	1.0063	0.0722	1.4117	1.0401	+0.0326	+0.0357	-0.0782	-0.0883
2.0	1.8748	0.9935	0.0300	1.9089	1.0141	-0.0051	-0.0048	-0.0306	-0.0644
3.0	2.8711	0.9991	0.0015	2.8745	1.0004	-0.0005	-0.0005	-0.0015	-0.0057
4.0	3.8709	1.0000	0.0000	3.8709	1.0000	0.0000	0.0000	0.0000	0.0000

n = 1
W = 0.25

τ	F_{10}	F'_{10}	F''_{10}	$\frac{F_{10}}{F_{10}}$	$\frac{F'_{10}}{F_{10}}$	$\frac{F''_{10}}{F_{10}}$	$\frac{F_{10}}{F_{10}}$	$\frac{F'_{10}}{F_{10}}$	$\frac{F''_{10}}{F_{10}}$
0	0	0	0	0	0	3.6364	1.6273	0	0.2553
0.125	0.0639	0.8029	0.0607	0.0278	0.3518	2.2363	1.3820	-0.3991	0.2497
0.25	0.1788	0.9981	0.0995	0.1036	0.5840	1.5767	1.1509	-0.3985	0.2260
0.5	0.4417	1.0730	0.1426	0.3496	0.8609	0.8445	0.7426	-0.3190	0.1372
0.75	0.7082	1.0536	0.1515	0.6557	0.9894	0.4390	0.4265	-0.2429	+0.0286
1.0	0.9677	1.0235	0.1363	0.9677	1.0356	0.2062	0.2122	-0.1786	-0.0590
1.5	1.4693	0.9902	0.0764	1.5219	1.0308	+0.0234	+0.0260	-0.0825	-0.1137
2.0	1.9636	0.9899	0.0278	2.0005	1.0096	-0.0036	-0.0034	-0.0282	-0.0670
3.0	2.9593	0.9993	0.0010	2.9619	1.0002	-0.0003	-0.0003	-0.0010	-0.0043
4.0	3.9592	1.0000	0.0000	3.9592	1.0000	0.0000	0.0000	0.0000	0.0000

W = 0.1

0	0	0	0	0	0	5.9211	1.5574	0	0.3065
0.03125	0.0046	0.7181	0.0318	0.0029	0.1443	3.8128	1.4953	-1.0337	0.3059
0.0625	0.0403	0.9019	0.0522	0.0111	0.2501	3.0446	1.4340	-0.9642	0.3033
0.125	0.1017	1.0348	0.0821	0.0401	0.4125	2.2662	1.3137	-0.7790	0.2925
0.25	0.2362	1.0980	0.1221	0.1357	0.6381	1.5017	1.0828	-0.5644	0.2519
0.5	0.5100	1.0816	0.1598	0.4146	0.8897	0.7640	0.6780	-0.3638	0.1294
0.75	0.7754	1.0414	0.1601	0.7358	0.9985	0.3825	0.3753	-0.2536	+0.0045
1.0	1.0315	1.0100	0.1373	1.0480	1.0339	0.1729	0.1790	-0.1768	-0.0827
1.5	1.5285	0.9057	0.0706	1.5865	1.0254	+0.0178	+0.0197	-0.0754	-0.1175
2.0	2.0221	0.9905	0.0235	2.0568	1.0077	-0.0025	-0.0024	-0.0238	-0.0610
3.0	3.0187	1.0000	0.0007	3.0213	1.0008	-0.0002	-0.0002	-0.0007	-0.0032
4.0	4.0184	1.0000	0.0000	4.0184	1.0000	0.0000	0.0000	0.0000	0.0000

Compressible Velocity-Slip and Temperature Jump Correction Terms. Two-Dimensional Case. ($\eta = 0$).

$$M(f_{1m}, f_{A_{1m}}) = 0 ; E(f_{1m}, f_{A_{1m}}) = 0 \quad \text{C.F. EQUATION (2.64)}$$

$$f_{1m}(0) = f'_{1m}(0) = 0, \quad f_{A_{1m}}(0) = 1 ; \quad \eta \rightarrow \infty, \quad f'_{1m}(\eta) \rightarrow 0, \quad f_{A_{1m}}(\eta) \rightarrow 0$$

$$f'_{12L} = f'_0, \quad f_{A_{12L}} = f_{A_0} ; \quad f_U = f_{A_0}(0) f_{1m}, \quad f_{A_{1U}} = f_{A_0}(0) f_{A_{1m}}$$

$$\frac{v_{12L}}{-\sqrt{s_5 A}} = f'_0 f_{A_0} + f'_0 f_{A_0} ; \quad \frac{(s_5 v)_{12L}}{s_5 \sqrt{s_5 A}} = f'_0 ; \quad \frac{(s_5 v)_{12L}}{s_5 A x} = f'_0 ; \quad \frac{\partial v_{12L}}{\partial x} = f''_0 f_{A_0} + 2 f'_0 f'_{A_0} + f'_0 f''_{A_0}$$

$$\frac{z_{12L}}{A_2 A_2 \sqrt{s_5}} = f_{A_0} \left[f''_0 f_{A_0} + 2.50 f'_0 f'_{A_0} + f'_0 f''_{A_0} + 0.50 f'_0 \frac{f_{A_0}^2}{f_{A_0}} \right] ; \quad \frac{z_{12L}}{s_5} = - \frac{f_{A_0}}{f_{A_0}^2} ; \quad \frac{T_{12L}}{T_2} = f_{A_0} ; \quad \frac{Q_{12L}}{s_5 \sqrt{s_5 A}} = f_{A_0} \left(f_{A_0} + 0.69 \frac{f_{A_0}^2}{f_{A_0}} \right)$$

$$\frac{v_U}{-\sqrt{s_5 A}} = f_{A_0} f'_{1U} + f'_0 f_{A_{1U}} ; \quad \frac{(s_5 v)_U}{s_5 \sqrt{s_5 A}} = f'_{1U} ; \quad \frac{(s_5 v)_U}{s_5 A x} = f'_{1U} ; \quad \frac{\partial v_U}{\partial x} = f_{A_0} f''_{1U} + f'_{A_0} f'_{1U} + f'_0 f''_{1U} + f'_0 f''_{A_{1U}}$$

$$\frac{z_U}{A_2 A_2 \sqrt{s_5}} = f_{A_0} \left[f_{A_0} f''_{1U} + f'_{A_0} f'_{1U} + f_{A_0} f''_{1U} + 1.50 f'_0 f'_{A_{1U}} + 0.50 f'_0 \frac{f_{A_0}^2}{f_{A_0}} \right] ; \quad \frac{z_U}{s_5} = - \frac{f_{A_{1U}}}{f_{A_0}^2} ; \quad \frac{T_U}{T_2} = f_{A_{1U}} ; \quad \frac{Q_U}{s_5 \sqrt{s_5 A}} = f_{A_0} \left(f_{A_{1U}} + 0.69 \frac{f_{A_0}^2}{f_{A_0}} \right)$$

$n = 0$
 $W = 0.5$

γ	f_m	f_{m+}	f_{m-}	f_{m+}^*	f_{m-}^*	f_{m+}^0	f_{m-}^0	f_{m+}^1	f_{m-}^1	f_{m+}^{1*}	f_{m-}^{1*}	$\frac{f_{m+}^{1*}}{f_{m-}^{1*}}$	$\frac{f_{m+}^{1*}}{f_{m-}^{1*}}$	$\frac{f_{m+}^{1*}}{f_{m-}^{1*}}$	$\frac{f_{m+}^{1*}}{f_{m-}^{1*}}$
0	0	0	0	0	0	0	0	0	0	0	0	0	0	0	0
0.125	-0.0501	-0.6909	-0.5746	28.6963	-8.5746	0.8441	1.0000	-1.3576	1.4318	0.3533	1.5540	-2.2267	-1.0000	-1.0000	-1.0000
0.25	-0.1535	-0.9111	-3.1702	13.1494	-3.1702	0.7108	0.8441	-0.9990	1.1504	0.6296	1.0768	-1.5979	-0.9045	-0.9045	-0.9045
0.5	-0.3786	-0.8280	+0.8926	+1.8800	+0.8926	0.4960	0.4960	-0.7411	0.8674	0.8321	0.7418	-1.1238	-0.7389	-0.7389	-0.7389
0.75	-0.5557	-0.5862	0.9480	-0.6936	0.9480	0.3359	0.3359	-0.5468	0.6948	0.9697	0.5056	-0.7859	-0.5771	-0.5771	-0.5771
1.0	-0.6749	-0.3771	0.7122	-1.0282	0.7122	0.2194	0.2194	-0.3914	0.5907	1.0965	0.3406	-0.5476	-0.4376	-0.4376	-0.4376
1.5	-0.7940	-0.1341	0.2994	-0.5818	0.2994	0.0819	0.0819	-0.1786	0.3120	1.1038	0.1471	-0.2593	-0.2321	-0.2321	-0.2321
2.0	-0.8336	-0.0402	0.1047	-0.2368	0.1047	+0.0239	+0.0239	-0.0669	0.1479	1.0338	0.0578	-0.1146	-0.1091	-0.1091	-0.1091
3.0	-0.8468	-0.0014	0.0067	-0.0233	0.0067	-0.0001	-0.0001	-0.0029	+0.0145	1.0041	0.0060	-0.0155	-0.0154	-0.0154	-0.0154
4.0	-0.8469	+0.0001	0.0002	-0.0003	0.0002	-0.0002	-0.0002	+0.0005	-0.0006	1.0000	0.0003	-0.0011	-0.0011	-0.0011	-0.0011
5.5	-0.8468	0.0000	0.0000	0.0000	0.0000	0.0000	0.0000	0.0000	0.0000	1.0000	0.0000	0.0000	0.0000	0.0000	0.0000

γ	$\frac{f_{m+}^{1*}}{f_{m-}^{1*}}$														
0	-1.6240	0	0	0	0	0	0	0	0	0	0	0	0	0	0
0.125	-1.0091	-0.0197	-0.0038	-0.0431	-0.0204	-0.0623	-0.0204	-0.2805	-0.2319	0.1678	-1.6240	0.4060	-0.2007	-0.2007	-0.2007
0.25	-0.6808	-0.0573	-0.0149	-0.0622	-0.0623	-0.0623	-0.0623	-0.3699	-0.0864	0.1606	-1.1366	0.3427	-0.2001	-0.2001	-0.2001
0.5	-0.4764	-0.0935	-0.0539	-0.0649	-0.1537	-0.1537	-0.1537	-0.3362	+0.0382	0.1324	-0.8147	0.2886	-0.1971	-0.1971	-0.1971
0.75	-0.1693	-0.1189	-0.1054	-0.0511	-0.2256	-0.2256	-0.2256	-0.2360	+0.0631	0.0985	-0.4367	0.2014	-0.1812	-0.1812	-0.1812
1.0	-0.1711	-0.1284	-0.1594	-0.0360	-0.2740	-0.2740	-0.2740	-0.1531	0.0557	0.0686	-0.2411	0.1364	-0.1547	-0.1547	-0.1547
1.5	-0.0819	-0.0983	-0.2509	-0.0152	-0.3224	-0.3224	-0.3224	-0.0544	0.0282	0.0296	-0.1345	0.0891	-0.1232	-0.1232	-0.1232
2.0	-0.0132	-0.0273	-0.3071	-0.0057	-0.3384	-0.3384	-0.3384	-0.0163	0.0116	0.0117	-0.0406	0.0332	-0.0644	-0.0644	-0.0644
3.0	-0.0022	-0.0032	-0.3441	-0.0006	-0.3438	-0.3438	-0.3438	-0.0006	0.0015	0.0015	+0.0001	0.0097	-0.0026	-0.0026	-0.0026
4.0	0.0000	0.0000	-0.3441	0.0000	-0.3439	-0.3439	-0.3439	0.0000	0.0001	0.0001	+0.0001	-0.0001	-0.0012	-0.0012	-0.0012
5.5	0.0000	0.0000	-0.3438	0.0000	-0.3438	-0.3438	-0.3438	0.0000	0.0000	0.0000	0.0000	0.0000	+0.0002	+0.0002	+0.0002

n=0
W=0.25

η	f_{in}	f'_{in}	f''_{in}	f'''_{in}	f_{in}	f'_{in}	f''_{in}	f'''_{in}	f_{in}	f'_{in}	f''_{in}	f'''_{in}	$\frac{f_{in}}{f'_{in}}$	$\frac{f''_{in}}{f'''_{in}}$	$\frac{f_{in}}{f'_{in}}$	$\frac{f''_{in}}{f'''_{in}}$
0	0	0	-48.4672	276.1018	1.0000	-3.9510	14.3214	0	2.0791	-6.9316	-1.0000					
0.0625	-0.0600	-1.5361	-9.9494	77.8901	0.8002	-2.6177	8.1316	0.2517	1.4708	-3.5154	-0.9333					
0.125	-0.1671	-1.7923	-0.2442	42.8705	0.6997	-1.9438	3.7655	0.4652	1.1185	-2.2760	-0.8329					
0.25	-0.3781	-1.5187	43.1840	-5.2328	0.4652	-1.2577	1.5374	0.7674	0.7011	-1.2313	-0.6494					
0.5	-0.6844	-0.8206	2.1504	-2.9440	0.2367	-0.6606	0.8560	0.9917	0.4577	-0.7664	-0.5003					
0.75	-0.8145	-0.4218	1.1374	-1.5377	0.1109	-0.3735	0.5199	1.1097	0.3014	-0.5051	-0.3792					
1.0	-0.8999	-0.2124	0.5961	-0.8391	0.0402	-0.2055	0.1849	1.1786	0.1269	-0.2292	-0.2022					
1.5	-0.9466	-0.0455	0.1601	-0.1246	-0.0145	-0.0411	0.0424	1.1386	0.0487	-0.0993	-0.0944					
2.0	-0.9562	-0.0033	0.0344	-0.0001	-0.0193	0.0101	-0.0143	1.0341	0.0047	-0.0125	-0.0125					
3.0	-0.9539	0.0024	0.0038	-0.0020	-0.0047	0.0013	-0.0034	1.0034	0.0002	-0.0008	-0.0008					
4.0	-0.9289	0.0000	-0.0009	0.0000	0.0000	0.0013	-0.0034	1.0000	0.0000	0.0000	0.0000					
5.5	-0.9533	0.0000	0.0000	0.0000	0.0000	0.0000	0.0000	1.0000	0.0000	0.0000	0.0000					

η	$\frac{f_{in}}{f'_{in}}$	$\frac{f''_{in}}{f'''_{in}}$														
0	-15.5805	0	0	0	0	0	-3.7007	0.4459	-15.5805	0.9738	-0.4727					
0.0625	-5.9774	-0.0232	-0.0076	-0.0985	-1.4959	-1.6627	-1.6627	0.4430	-8.2988	0.7792	-0.4714					
0.125	-3.2707	-0.0619	-0.1008	-0.1627	-1.7453	-0.7522	-0.7522	0.4314	-5.0525	0.6424	-0.4624					
0.5	-1.4502	-0.1343	-0.2915	-0.3682	-1.4789	-0.0359	-0.0359	0.3910	-2.2999	0.4530	-0.4391					
0.75	-0.8051	-0.1820	-0.4822	-0.7931	-0.6470	-0.7991	0.2443	0.2964	-0.6733	0.2304	-0.3512					
1.0	-0.4939	-0.2025	-0.6421	-0.7931	-0.4107	-0.2283	0.2283	0.2183	-0.2234	0.1080	-0.2986					
1.5	-0.2088	-0.1811	-0.8465	-0.9217	-0.0493	-0.0493	0.0912	0.1601	0.0642	0.0392	-0.1599					
2.0	-0.0894	-0.1210	-0.9277	-0.9212	-0.0032	-0.0032	0.0428	0.0945	0.0176	-0.0142	-0.0398					
3.0	-0.0122	-0.0271	-0.9582	-0.0023	-0.0023	-0.0023	0.0062	0.0062	0.0047	-0.0046	0.0098					
4.0	-0.0009	-0.0026	-0.9277	0.0000	0.0000	0.0000	0.0004	0.0004	0.0000	0.0000	0.0013					
5.5	0.0000	0.0000	-0.9272	0.0000	0.0000	0.0000	0.0000	0.0000	0.0000	0.0000	0.0000					

Compressible Velocity-Slip and Temperature-Jump Correction Terms. Axially Symmetric Case ($n=1$).

$$M(f_{1m}, f_{1m}) = 0 \quad ; \quad E(f_{1m}, f_{1m}) = 0 \quad \text{cf. EQUATION (2.64)}$$

$$f_{1m}(0) = f'_{1m}(0) = 0, \quad f_{1m}(0) = 1 \quad ; \quad \eta \rightarrow \infty, \quad f'_{1m}(\eta) \rightarrow 0, \quad f_{1m}(\eta) \rightarrow 0$$

$$f_{1cL} = f'_0, \quad f_{1cL} = f'_0 \quad ; \quad f_{1j} = f'_0(0) f_{1m}, \quad f_{1j} = f'_0(0) f_{1m}$$

$$\frac{v_{1j}}{-2\sqrt{1/2}A} = f'_0 f_{1cL} + f'_0 f_{1cL} \quad ; \quad \frac{v_{1j}}{A_x} = f'_0 f_{1cL} + f'_0 f_{1cL} \quad ; \quad \frac{(s_{1j})_{1j}}{-2.3\sqrt{1/2}A} = f'_0 \quad ; \quad \frac{(s_{1j})_{1j}}{s_{1j} A_x} = f'_0 \quad ; \quad \frac{Q_{1j}}{-A_x \sqrt{1/2}} = f'_0 f_{1cL} + 2f'_0 f_{1cL} + f'_0 f_{1cL}$$

$$\frac{z_{1j}}{A_x \sqrt{1/2}} = f_{1cL} \left[f'_0 f_{1cL} + 2.58 f'_0 f_{1cL} + f'_0 f_{1cL} + 0.58 f'_0 f_{1cL} \right] \quad ; \quad \frac{s_{1j}}{s_1} = -\frac{f_{1j}}{f'_0} \quad ; \quad \frac{T_{1j}}{T_1} = f_{1j} \quad ; \quad \frac{Q_{1j}}{kT/\sqrt{1/2}} = f_{1cL} \left(f_{1cL} + 0.69 \frac{f_{1cL}^2}{f_{1cL}} \right)$$

$$\frac{v_{1j}}{-2\sqrt{1/2}A} = f_{1cL} f_{1j} + f'_0 f_{1j} \quad ; \quad \frac{v_{1j}}{A_x} = f_{1cL} f_{1j} + f'_0 f_{1j} \quad ; \quad \frac{(s_{1j})_{1j}}{-2.3\sqrt{1/2}A} = f_{1j} \quad ; \quad \frac{(s_{1j})_{1j}}{s_{1j} A_x} = f_{1j} \quad ; \quad \frac{Q_{1j}}{-A_x \sqrt{1/2}} = f_{1cL} f_{1j} + f'_0 f_{1j} + f'_0 f_{1j}$$

$$\frac{z_{1j}}{A_x \sqrt{1/2}} = f_{1cL} \left[f_{1cL} f_{1j} + f_{1cL} f_{1j} + f'_0 f_{1j} + 1.58 f'_0 f_{1j} + 0.58 f'_0 f_{1j} \right] \quad ; \quad \frac{s_{1j}}{s_1} = -\frac{f_{1j}}{f'_0} \quad ; \quad \frac{T_{1j}}{T_1} = f_{1j} \quad ; \quad \frac{Q_{1j}}{kT/\sqrt{1/2}} = f_{1cL} \left(f_{1j} + 0.69 \frac{f_{1j}^2}{f_{1j}} \right)$$

n=1
W=0.1

η	f_{im}	f'_{im}	f''_{im}	f'''_{im}	$f^{(4)}_{im}$	$f^{(5)}_{im}$	$f^{(6)}_{im}$	$f^{(7)}_{im}$	$f^{(8)}_{im}$	$\frac{U_{im}}{U_{ref}}$	$\frac{T_{im}}{T_{ref}}$	$\frac{Q_{im}}{Q_{ref}}$	$\frac{Z_{im}}{Z_{ref}}$
0	0	0	-612.2595	1.0000	-24.0795	171.8742	0	3.9474	-72.5385	-1.0000	-1.0000	-1.0000	-1.0000
0.03125	-0.0971	-3.8040	+9.2184	0.6078	-7.1201	171.8742	0.1239	2.7634	-21.2709	-0.9726	-0.9726	-0.9726	-0.9726
0.0625	-0.2077	-3.2251	20.6219	0.4428	-4.0062	57.3584	0.2335	2.2723	-11.6442	-0.9363	-0.9363	-0.9363	-0.9363
0.125	-0.3740	-2.1821	12.8118	0.2649	-2.0764	16.6993	0.4168	1.7516	-5.7784	-0.8688	-0.8688	-0.8688	-0.8688
0.25	-0.5722	-1.1395	5.3459	0.0892	-0.9603	4.9153	0.6919	1.2231	-2.6632	-0.7527	-0.7527	-0.7527	-0.7527
0.5	-0.7451	-0.3919	1.5953	0.0499	-0.2836	1.5009	1.0232	0.6915	-1.0989	-0.5562	-0.5562	-0.5562	-0.5562
0.75	-0.8063	-0.1380	0.6094	0.0256	-0.0351	0.6179	1.1692	0.3568	-0.5673	-0.3883	-0.3883	-0.3883	-0.3883
1.0	-0.8265	-0.0388	0.2382	0.0141	+0.0638	+0.2109	1.2030	0.2184	-0.3093	-0.2508	-0.2508	-0.2508	-0.2508
1.5	-0.8296	+0.0087	0.0141	-0.1152	0.0766	-0.0765	1.1289	0.0538	-0.0840	-0.0794	-0.0794	-0.0794	-0.0794
2.0	-0.8254	0.0060	-0.0122	-0.0116	0.0332	-0.0750	1.0460	0.0095	-0.0168	-0.0166	-0.0166	-0.0166	-0.0166
3.0	-0.8233	0.0002	-0.0010	-0.0038	0.0013	-0.0054	1.0020	0.0002	-0.0003	-0.0003	-0.0003	-0.0003	-0.0003
4.0	-0.8233	0.0000	0.0000	0.0000	0.0000	0.0000	1.0000	0.0000	0.0000	0.0000	0.0000	0.0000	0.0000

η	$\frac{p_{im}}{p_a}$	$\frac{Q_{im}}{Q_{ref}}$	$\frac{V_{im}}{V_{ref}}$	$\frac{U_{im}}{U_{ref}}$	$\frac{f^{(2)}_{im}}{f^{(2)}_{ref}}$	$\frac{f^{(3)}_{im}}{f^{(3)}_{ref}}$	$\frac{f^{(4)}_{im}}{f^{(4)}_{ref}}$	$\frac{f^{(5)}_{im}}{f^{(5)}_{ref}}$	$\frac{f^{(6)}_{im}}{f^{(6)}_{ref}}$	$\frac{f^{(7)}_{im}}{f^{(7)}_{ref}}$	$\frac{f^{(8)}_{im}}{f^{(8)}_{ref}}$	$\frac{T_{im}}{T_a}$	$\frac{Z_{im}}{Z_{ref}}$
0	-300.2268	0	0	0	0	0	0	0	0	0	0	3.0023	-2.0496
0.03125	-66.1597	-0.0286	-0.0307	-0.9513	-0.2915	-0.2915	11.4205	-65.3052	0.9026	0.9026	0.9026	1.8248	-2.0351
0.0625	-30.8541	-0.0705	-0.1018	-1.2305	-0.6235	-0.6235	9.6826	-14.1877	0.9053	0.9053	0.9053	1.8248	-1.9900
0.125	-12.4633	-0.1588	-0.2956	-1.3837	-1.1229	-1.1229	6.5511	-5.3920	0.9170	0.9170	0.9170	1.7994	-1.8465
0.25	-4.5155	-0.2889	-0.7423	-1.3118	-1.7178	-1.7178	3.4211	-0.6487	0.9386	0.9386	0.9386	1.7994	-1.7412
0.5	-1.4552	-0.4451	-1.5543	-0.9417	-2.2369	-2.2369	1.1765	+1.2327	1.0227	1.0227	1.0227	+0.2678	-1.4712
0.75	-0.6763	-0.4735	-2.1147	-0.6029	-2.4207	-2.4207	0.4144	1.5013	1.1113	1.1113	1.1113	-0.1497	-0.7161
1.0	-0.3536	-0.4171	-2.4287	-0.3537	-2.4814	-2.4814	0.1165	1.1831	0.9704	0.9704	0.9704	-0.2558	-0.1768
1.5	-0.1005	-0.2180	-2.5981	-0.0938	-2.4905	-2.4905	0.0262	0.8148	0.7952	0.7952	0.7952	-0.2331	+0.1256
2.0	-0.0238	-0.0727	-2.5329	-0.0173	-2.4780	-2.4780	0.0179	0.2827	0.2736	0.2736	0.2736	-0.1170	0.2172
3.0	-0.0005	-0.0083	-2.4748	-0.0003	-2.4719	-2.4719	0.0005	0.0647	0.0642	0.0642	0.0642	-0.0349	0.0987
4.0	0.0000	0.0000	-2.4721	0.0000	-2.4721	-2.4721	0.0000	0.0010	0.0010	0.0010	0.0010	-0.0009	0.0039
												0.0000	0.0000

Compressible Vorticity-Correction Term. Axially Symmetric Case Only ($n=1$).

$$M(F_{IV}, f_{IV}) = 0 ; \quad E(F_{IV}, f_{IV}) = 0 \quad \text{C.F. EQUATION (2.64)}$$

$$f_{IV}(0) = f'_{IV}(0) = f_{IV}(0) = 0 ; \quad \eta \rightarrow \infty, \quad f'_{IV}(\eta) \rightarrow 1, \quad f_{IV}(\eta) \rightarrow 0$$

$$\frac{v_{IV}}{-2\sqrt{3}\pi} = f_{IV} f_{IV} + f_0 f_{IV} ; \quad \frac{u_{IV}}{Ax} = f_{IV} f'_{IV} + f_0' f_{IV} ; \quad \frac{(s_{IV})_{IV}}{-2s_{IV} \sqrt{2}\pi} = f_{IV} ; \quad \frac{(s_{IV})_{IV}}{s_{IV} Ax} = f'_{IV}$$

$$\frac{Q_{IV}}{-Ax \sqrt{2}} = f_{IV} f_{IV} + f_0 f_{IV} + f_0' f_{IV} + f_0'' f_{IV} ; \quad \frac{Q_{IV}}{Ax \sqrt{2}} = f_{IV}^{0.58} [f_{IV} f_{IV} + f_0' f_{IV} + f_0'' f_{IV} + 1.58 f_0''' f_{IV} + 0.58 f_0^{IV} f_{IV}]$$

$$\frac{S_{IV}}{S_0} = -\frac{f_{IV}}{E_0} ; \quad \frac{T_{IV}}{T_0} = f_{IV} ; \quad \frac{Q_{IV}}{Q_0 \sqrt{2}} = f_{IV}^{0.69} [f_{IV} + 0.69 \frac{f_{IV}}{f_{IV}} f_{IV}]$$

W = 0.75

η	f_w	f_w'	f_w''	f_w'''	$f_w^{(4)}$	$f_w^{(5)}$	$f_w^{(6)}$	$f_w^{(7)}$	$f_w^{(8)}$	$f_w^{(9)}$	$f_w^{(10)}$	$f_w^{(11)}$	$f_w^{(12)}$	$f_w^{(13)}$	$f_w^{(14)}$	$f_w^{(15)}$	$f_w^{(16)}$	$f_w^{(17)}$	$f_w^{(18)}$	$f_w^{(19)}$	$f_w^{(20)}$
0	0	0	1.0817	-0.9633	0	0.0627	-0.0179	0	0	0	0.8112	0.6866	0	0.0514							
0.25	0.0311	0.2387	0.8489	-0.6976	0.0149	0.0560	-0.0341	0.0257	0.1972	0.7691	0.6868	0.6868	-0.0232	0.0502							
0.5	0.1157	0.4333	0.7229	-0.3248	0.0276	0.0443	-0.0602	0.1034	0.3860	0.7440	0.6904	0.7347	-0.0382	0.0432							
1.0	0.4191	0.7782	0.6972	+0.1605	0.0404	+0.0049	-0.0852	0.4121	0.7576	0.7578	0.7334	0.7334	-0.0471	+0.0083							
1.5	0.8998	1.1554	0.8212	0.2801	0.0337	-0.0277	-0.0362	0.9111	1.1565	0.8451	0.8338	0.8338	-0.0356	-0.0257							
2.0	1.5856	1.5976	0.9382	0.1692	0.0180	-0.0302	+0.0204	1.6017	1.6032	0.9364	0.9425	0.9425	-0.0183	-0.0298							
3.0	3.6699	2.5802	1.0000	0.0045	0.0015	-0.0049	0.0139	3.6788	2.5813	0.9974	0.9974	0.9974	-0.0015	-0.0049							
4.5	8.6658	4.0807	1.0000	0.0000	0.0000	0.0000	0.0000	8.6658	4.0807	1.0000	1.0000	1.0000	0.0000	0.0000							

W = 0.5

η	f_w	f_w'	f_w''	f_w'''	$f_w^{(4)}$	$f_w^{(5)}$	$f_w^{(6)}$	$f_w^{(7)}$	$f_w^{(8)}$	$f_w^{(9)}$	$f_w^{(10)}$	$f_w^{(11)}$	$f_w^{(12)}$	$f_w^{(13)}$	$f_w^{(14)}$	$f_w^{(15)}$	$f_w^{(16)}$	$f_w^{(17)}$	$f_w^{(18)}$	$f_w^{(19)}$	$f_w^{(20)}$
0	0	0	2.1965	-4.3247	0	0.1755	-0.1931	0	0	0	1.0983	0.7347	0	0.1088							
0.125	0.0146	0.2176	1.3890	-2.1727	0.0201	0.1478	-0.1791	0.0088	0.1302	0.9925	0.7347	0.7347	-0.0638	0.1081							
0.25	0.0515	0.3642	0.9997	-0.5091	0.0371	0.1248	-0.1925	0.0353	0.2496	0.9226	0.7347	0.7347	-0.0947	0.1041							
0.5	0.1696	0.5688	0.7051	+0.2555	0.0626	+0.0786	-0.1565	0.1408	0.4689	0.8426	0.7368	0.7368	-0.1168	+0.0817							
1.0	0.5380	0.9054	0.7012	0.2887	0.0780	-0.0142	-0.0888	0.5326	0.8777	0.8152	0.7738	0.7738	-0.0999	-0.0006							
1.5	1.0844	1.2929	0.8509	0.2887	0.0563	-0.0616	-0.0888	1.1119	1.2995	0.8797	0.8627	0.8627	-0.0610	-0.0562							
2.0	1.8426	1.7488	0.9600	+0.1394	0.0264	-0.0511	+0.0547	1.8707	1.7584	0.9516	0.9465	0.9465	-0.0269	-0.0502							
3.0	4.0845	2.7409	1.0016	-0.0016	0.0017	-0.0060	0.0187	4.0881	2.7420	0.9981	0.9980	0.9980	-0.0017	-0.0059							
4.5	9.3216	4.2416	1.0000	0.0000	0.0000	0.0000	0.0000	9.3216	4.2416	1.0000	1.0000	1.0000	0.0000	0.0000							

TABLE III
EFFECT OF COOLING RATIO ON WALL-SHEAR AND HEAT-TRANSFER-RATE PARAMETERS

W	V	$\frac{z_0(0)}{z_{ref}}$	$\frac{z_c(0)}{z_{ref}}$	$\frac{z_D(0)}{z_{ref}}$	$\frac{z_{11}(0)}{z_{ref}}$	$\frac{z_{12}(0)}{z_{ref}}$	$\frac{z_{13}(0)}{z_{ref}}$	$\frac{Q_0(0)}{(-w)Q_{ref}}$	$\frac{Q_c(0)}{(-w)Q_{ref}}$	$\frac{Q_D(0)}{(-w)Q_{ref}}$	$\frac{Q_{11}(0)}{(-w)Q_{ref}}$	$\frac{Q_{12}(0)}{(-w)Q_{ref}}$	$\frac{Q_{13}(0)}{(-w)Q_{ref}}$	$\frac{Q_{14}(0)}{(-w)Q_{ref}}$	$\frac{Q_{15}(0)}{(-w)Q_{ref}}$	η^*
1.0	1.02	1.2326	-1.9133	1.8489	0	-	0	0.5123	-0.1350	0.2561	0	0.2561	-0.2624	-0.2624	-	0.6479
0.75	0.7329	1.1396	-1.6057	1.7094	0.0596	-	0.0437	0.5080	-0.1300	0.2540	0	0.2540	-0.2884	-0.2884	-	0.4600
0.5	0.4730	1.0396	-1.3212	1.5594	0.1693	-	0.0801	0.5034	-0.1288	0.2516	0	0.2516	-0.4014	-0.1899	-	0.2573
0.25	0.2238	0.9304	-1.0649	1.3956	0.4459	-	0.0998	0.4988	-0.1201	0.2495	0	0.2495	-0.6302	-0.1410	-	0.0337
0.1	0.08317	0.8599	-0.9417	1.2899	1.0502	-	0.0873	0.4896	-0.1275	0.2481	0	0.2481	-1.1677	-0.0971	-	-0.1165
$h-1$																
1.0	1.0	1.3119	-1.2452	1.9679	0	0.6491	0	0.6867	0.3362	0.3434	0	0.3434	-0.4716	-0.4716	0.1956	0.5689
0.75	0.7329	1.2394	-1.0764	1.8591	0.0619	0.6866	0.0454	0.6840	0.2816	0.3420	0	0.3420	-0.5688	-0.4169	0.2056	0.4193
0.5	0.4730	1.1635	-0.9308	1.7453	0.1705	0.7347	0.0807	0.6820	0.2202	0.3410	0	0.3410	-0.7464	-0.3531	0.2176	0.2584
0.25	0.2238	1.0849	-0.8187	1.6273	0.4215	0.8011	0.0943	0.6808	0.1481	0.3404	0	0.3404	-1.2043	-0.2695	0.2329	0.0816
0.1	0.08317	1.0383	-0.7779	1.5574	0.9086	0.8983	0.0751	0.6811	0.0959	0.3405	0	0.3405	-2.2773	-0.1894	0.2446	-0.0368

$\eta=0$

TABLE IV

CHANGE IN STAGNATION-POINT HEAT-TRANSFER RATES DUE TO COMPRESSIBILITY AND LOW-REYNOLDS-NUMBER EFFECTS FOR CIRCULAR CYLINDERS. COMPARISON WITH EXPERIMENTS OF TEMLIK AND GLEZT (46), (41)

M_∞^*	Re_∞^*	W^*	$\frac{AR^2}{\gamma^2}$	$\frac{1}{\gamma} \sqrt{\frac{\rho}{\rho_\infty}}$	$\frac{\Delta V}{VA}$	$\frac{\Delta C_{p,inc}}{C_{p,inc}}$	$\frac{\Delta C_{p,comp}}{C_{p,comp}}$	$\frac{\Delta C_{p,inc}}{C_{p,inc}}$	$\frac{\Delta C_{p,comp}}{C_{p,comp}}$	$\frac{\Delta C_{p,inc}}{C_{p,inc}}$	$\frac{\Delta C_{p,comp}}{C_{p,comp}}$	C_p
1.32	37	0.24	25.3	0.1568	0.0469	-0.0192	-0.0716	-0.0486	-0.0470	-0.1254	-0.1991	-0.217
1.65	56	0.30	35.5	0.1678	0.0488	-0.0200	-0.0642	-0.0411	-0.0430	-0.1095	-0.1568	-1.04
1.98	100	0.33	129.5	0.0698	0.0338	-0.0163	-0.0399	-0.0275	-0.0256	-0.0716	-0.1133	-1.70
3.55	330	0.28	153	0.0608	0.0269	-0.0110	-0.0323	-0.0197	-0.0247	-0.0719	-0.3390	-0.856
3.83	610	0.35	250	0.0632	0.0273	-0.0112	-0.0279	-0.0155	-0.0219	-0.0614	-0.2893	-1.28
4.02	1030	0.37	392	0.0505	0.0230	-0.0094	-0.0287	-0.0124	-0.0179	-0.0531	-0.2113	-1.95
4.19	1870	0.38	668	0.0387	0.0181	-0.0076	-0.0176	-0.0095	-0.0136	-0.0457	-0.1466	-2.40
4.88	840	0.33	240	0.0645	0.0248	-0.0170	-0.0271	-0.0193	-0.0207	-0.0615	-0.2487	-1.98
5.29	1230	0.35	329	0.0551	0.0225	-0.0145	-0.0238	-0.0135	-0.0179	-0.0594	-0.1128	-2.71
5.50	2170	0.37	541	0.0430	0.0185	-0.0113	-0.0189	-0.0105	-0.0144	-0.0477	-0.1109	-3.68
1.65	56	0.70	39.9	0.1583	0.1432	-0.0415	-0.1001	-0.0401	-0.0685	-0.1185	-0.3250	-1.095
1.82	100	0.70	71.7	0.1181	0.1116	-0.0459	-0.0770	-0.0099	-0.0536	-0.0994	-0.2738	-1.285
1.90	210	0.71	134	0.0864	0.0778	-0.0319	-0.0546	-0.0219	-0.0395	-0.0774	-0.1895	-1.77
3.83	610	0.71	251	0.0631	0.0636	-0.0227	-0.0427	-0.0096	-0.0318	-0.0574	-0.2669	-1.77
4.02	1030	0.72	394	0.0504	0.0511	-0.0133	-0.0342	-0.0128	-0.0253	-0.0475	-0.2235	-1.95
4.19	1870	0.74	582	0.0383	0.0406	-0.0101	-0.0287	-0.0096	-0.0197	-0.0360	-0.1138	-2.13
5.29	1230	0.72	335	0.0546	0.0453	-0.0141	-0.0363	-0.0094	-0.0265	-0.0498	-0.2290	-2.73
5.50	2170	0.72	541	0.0430	0.0425	-0.0113	-0.0287	-0.0094	-0.0211	-0.0414	-0.1314	-3.68
5.73	4100	0.74	950	0.0328	0.0305	-0.0087	-0.0213	-0.0086	-0.0148	-0.0318	-0.0829	-6.42

* Tabulated from References 40 and 41.

ADDENDUM

February 1962

Since completion of the research work presented in the foregoing report several new developments in low-Reynolds-number boundary-layer theory came to the author's attention. In particular Van Dyke^(A1,A2) and Maslen^(A3) utilized a Lagerstrom-Cole type expansion procedure to calculate second-order terms (i.e. first-order correction terms) to stagnation-point and other boundary-layer problems. The purpose of this Addendum is to clarify a shortcoming of the foregoing analysis which became apparent in comparison with these new developments, and which was brought to the author's attention by Professor Van Dyke in private conversation. In addition, an important detail regarding the application of the foregoing theory to experimental low-Reynolds-number stagnation-point measurements will also be clarified; this was brought to the author's attention by Prof. Rott^(A4) in a different context.

Let the external flow be described by a streamfunction of the form;

$$\psi = \frac{1}{2} A x^{1+n} \left\{ y + \left(\frac{n-1}{R} + nv \right) \frac{y^2}{2} + \dots + \frac{1}{R} \sqrt{\frac{1}{A}} \left[a_n + \left(\frac{1}{R} y \dots \right) \dots \right] \right\} \quad (\text{Ad.1})$$

where the equation above replaces (1.22). The first-order correction terms appearing in the above expression are not necessarily related to the nose radius, rather (as explained in the introduction to Chapter II.) x is merely a convenient reference length. The pressure, temperature, and density expansions can be related to the streamfunction by means of the procedure described in Chapter I. (This is permissible for the first-order correction terms because the viscous terms in the equations are of

ADDENDUM

February 1962

Since completion of the research work presented in the foregoing report several new developments in low-Reynolds-number boundary-layer theory came to the author's attention. In particular Van Dyke^(A1,A2) and Maslen^(A3) utilized a Lagerstrom-Cole type expansion procedure to calculate second-order terms (i.e. first-order correction terms) to stagnation-point and other boundary-layer problems. The purpose of this Addendum is to clarify a shortcoming of the foregoing analysis which became apparent in comparison with these new developments, and which was brought to the author's attention by Professor Van Dyke in private conversation. In addition, an important detail regarding the application of the foregoing theory to experimental low-Reynolds-number stagnation-point measurements will also be clarified; this was brought to the author's attention by Prof. Rott^(A4) in a different context.

Let the external flow be described by a streamfunction of the form;

$$\psi = \frac{1}{2} A x^{1+n} \left\{ y + \left(\frac{n-1}{R} + nV \right) \frac{y^2}{2} + \dots + \frac{1}{R} \sqrt{\frac{1}{A}} \left[a_n + b_n y + \dots \right] \right\} \quad (\text{Ad.1})$$

where the equation above replaces (1.22). The first-order correction terms appearing in the above expression are not necessarily related to the nose radius, rather (as explained in the introduction to Chapter II.) it is merely a convenient reference length. The pressure, temperature, and density expansions can be related to the streamfunction by means of the procedure described in Chapter I. (This is permissible for the first-order correction terms because the viscous terms in the equations are of

order $\frac{1}{Re}$.) Only the pressure expansion is of interest here;

$$p = p_c - \frac{\rho_\infty}{2} A^2 \left\{ (1+n) \frac{y^2}{2} + \frac{x^2}{2} - \frac{x^2 y}{R} + \dots + \frac{1}{R} \sqrt{\frac{y_2}{A}} \left[(1+n) a_n y + (b_n - n v a_n) x^2 + \dots \right] \right\} \quad (A1.2)$$

The "inner" expansions of the same variables are as given in Chapter 11. Matching the two expansions requires that as $\eta \rightarrow \infty$ the "inner" expansion approach the external flow described by (A1.1) and (A1.2). This implies that the solution for f_{p_0} , g_{p_0} , f_{t_0} , f_{t_0} , f_0 , and f_{p_1} are as given in Chapter 11. Furthermore, using the boundary-layer solution in the matching requirement one obtains that;

$$\lim_{\eta \rightarrow \infty} \psi(\eta) = \frac{\rho_\infty}{2} A x^{1+n} \left\{ y - \sqrt{\frac{y_2}{A}} p^* + \lim_{\eta \rightarrow \infty} \frac{1}{R} \sqrt{\frac{y_2}{A}} f_1(\eta) + \dots \right\} \quad (A1.3)$$

Since any constant that might appear in the limiting behaviour of $f_1(\eta)$ or higher-order corrections would be of order $\frac{y_2}{A}$ or smaller, it is apparent that the constant a_{11} in (A1.1) can be identified by comparison with (A1.3) as;

$$a_{11} = -R \eta^* \quad (A1.4)$$

It is likewise apparent that to determine constant b_{11} the limiting behaviour of $f_1(\eta)$ must be known. However equation (A1.2) shows that b_{11} appears as a boundary condition necessary for the integration of $g_{p_1}(\eta)$, which in turn is necessary for the solution of $f_1(\eta)$. This shows that b_{11} can not be determined within the framework of stagnation-point flow alone; it can then be defined as the undetermined "displacement constant", i.e.;

$$b_{11} = \zeta \quad (A1.5)$$

(For further discussion on the somewhat ambiguous nature of defining the displacement effect reference is made to (A4).)

Using results (A1.4) and (A1.5) in (A1.1) and (A1.2) the "outer"-flow expressions become;

$$\psi = s_s A x^{1+n} \left\{ y + \left(\frac{n-1}{R} + nV \right) \frac{y^2}{2} + \dots + \frac{1}{R} \sqrt{\frac{\mu_s}{A}} \left[-R\eta^* + \zeta y + \dots \right] \dots \right\} \quad (\text{A1.6})$$

$$p = p_s - s_s A^2 \left\{ (1+n)^2 \frac{y^2}{2} + \frac{x^2}{2} - \frac{x^2 y}{R} + \dots + \frac{1}{R} \sqrt{\frac{\mu_s}{A}} \left[-(1+n)^2 R\eta^* y + (\zeta + nRV\eta^*) x^2 + \dots \right] \dots \right\}$$

Corresponding to (A1.6) the constant of integration in integrating $g_{p_1}(\eta)$ (cf. pp. 31-32) becomes;

$$K_{\text{corr}} = \frac{1+n}{2+n} \eta^* - \zeta - nRV\eta^* \quad (\text{A1.7})$$

which now replaces (2.35). Then the corrected form of (2.36) becomes;

$$\frac{p_s}{s_s A^2} g_{p_1, \text{corr}}(\eta) = \frac{1}{2+n} \left[(1+n) f_0' H_0 + (1+n)\eta^* + \eta + \frac{\mu_s}{\mu_0} (f_0' H_0 + f_0'' H_0) \right] - \zeta - nRV\eta^* \quad (\text{A1.8})$$

Thus it is clear that the momentum equation for the vorticity correction term is not homogeneous as given in (2.57), but rather;

$$M(f_{1, \text{corr}}, H_{1, \text{corr}}) = - \frac{2\eta^*}{\mu_0} \frac{\mu_s}{\mu_0} \quad (\text{A1.9})$$

is the correct equation. Now the behaviour of the momentum equation for the correction term as $\eta \rightarrow \infty$ can be observed;

$$\lim_{\eta \rightarrow \infty} M(f_1, H_1) = -2 f_1' + (1+n)(\eta - \eta^*) f_1'' \quad (\text{A1.10})$$

Thus it is clear from (2.57) that;

$$\lim_{\eta \rightarrow \infty} f'_{IV}(\eta) = \eta - \eta^* \quad (\text{Ad.11})$$

On the other hand (A1.6) and (Ad.9) imply that;

$$\lim_{\eta \rightarrow \infty} f'_{IV_{\text{corr}}}(\eta) = \eta \quad (\text{Ad.12})$$

Finally, the limiting behaviour of the displacement correction term consistent with (2.55), (Ad.6) and (A1.10) is;

$$\lim_{\eta \rightarrow \infty} f'_{\text{D}}(\eta) = 1 \quad (2.53)$$

Observing that the energy equation and all the remaining boundary conditions for the displacement and vorticity correction terms are identical;

$$E(f_1, H_1) = f_1(0) = f'_1(0) = H_1(0) = \lim_{\eta \rightarrow \infty} H_1(\eta) = 0 \quad (\text{A1.13})$$

and using the five foregoing expressions, it is easy to see that;

$$f'_{IV_{\text{corr}}}(\eta) = f'_{IV}(\eta) + \eta^* f'_{\text{D}}(\eta) \quad (\text{A1.14})$$

satisfies both the correct momentum equation (A1.9) and boundary condition (Ad.12). The energy equation and the remaining boundary conditions are automatically satisfied by (Ad.14). Equation (Ad.14) is then the correct vorticity term; the temperature function $f_{IV_{\text{corr}}}$ is correspondingly modified. The correction to the vorticity effect described by (A1.14) has become known in the literature as the "vorticity-induced pressure-gradient" effect (e.g. Li ^(A5), Van Dyke ^(A1), etc.); and the present result and the results of the above mentioned investigations are thereby in agreement.

One may now consider an application of the foregoing theory to experimental measurements of low-Reynolds-number stagnation-point flow. Let the velocity gradient A be based on pressure distribution data obtained at a "low" Reynolds number, so that;

$$s_s A_{exp}^2 \equiv - \left. \frac{\partial^2 p}{\partial x^2} \right|_{y=0} \quad (Ad.15)$$

Using (A1.8) and (2.5) in the above expression one obtains;

$$s_s A_{exp}^2 = - \left\{ 2g_{p_0}(0) + \frac{2}{R} \sqrt{\frac{\mu_s}{\rho}} g_{p_1}(0) + \dots \right\} p_s = s_s A^2 \left\{ 1 - \frac{2}{R} \sqrt{\frac{\mu_s}{\rho}} \left[\frac{1}{2+n} \left(f_0''(0) f_0(0) \frac{\mu_s}{\mu_s} + (1+n)\eta^* \right) - C_D - nRV\eta^* \right] + \dots \right\} \quad (Ad.16)$$

where A corresponds to an "infinite" Reynolds number.

Now, considering only the highest-order corrections, A can be expressed in terms of A_{exp} ;

$$A = A_{exp} \left\{ 1 + \frac{1}{R} \sqrt{\frac{\mu_s}{\rho}} \left[K_c - C_D - nRV\eta^* \right] \right\} \quad (Ad.17)$$

where constant K_c is defined by;

$$K_c \equiv \frac{1}{2+n} \left[f_0''(0) f_0(0) \frac{\mu_s}{\mu_s} + (1+n)\eta^* \right] \quad (Ad.18)$$

If now A_{exp} is to be used to predict physical quantities in the boundary layer, and if the Reynolds number is sufficiently low to necessitate consideration of the first-order correction terms, then the change described by (Ad.17) and the effect of this change on the boundary-layer term must also be included for a consistent theoretical prediction to this order. The effect on the boundary-layer quantities of changing A to the first order is already known (cf. pp. 38-39); it is the displacement-effect term. Thus expressions of the form given in Chapter IV.,

e.g. (4.6);

$$\frac{U}{U_{ref}} = \frac{U_0}{U_{ref}} + \frac{1}{R} \sqrt{\frac{y_s}{A}} \frac{U_{ic}}{U_{ref}} + \frac{C_D}{R} \sqrt{\frac{y_s}{A}} \frac{U_{ID}}{U_{ref}} + \frac{2-\delta}{\delta} \frac{\lambda_w}{\sqrt{y_s/A}} \left[\frac{U_{visc}}{U_{ref}} + \left(\frac{K_2}{K_1} - 1 \right) \frac{U_{ID}}{U_{ref}} \right] +$$

$$+ nV \sqrt{\frac{y_s}{A}} \frac{U_{Vcorr}}{U_{ref}} \quad (\text{Ad.19})$$

must now be revised in accordance with (Ad.17);

$$\frac{U}{U_{ref}} = \frac{U_0}{U_{ref}} + \frac{1}{R} \sqrt{\frac{y_s}{A}} \frac{U_{ic}}{U_{ref}} + \frac{C_D + K_c - C_D - nRV_0^*}{R} \frac{U_{ID}}{U_{ref}} + \frac{2-\delta}{\delta} \frac{\lambda_w}{\sqrt{y_s/A}} \left[\frac{U_{visc}}{U_{ref}} + \right.$$

$$\left. + \left(\frac{K_2}{K_1} - 1 \right) \frac{U_{ID}}{U_{ref}} \right] + nV \sqrt{\frac{y_s}{A}} \frac{U_{Vcorr}}{U_{ref}} = \frac{U_0}{U_{ref}} + \frac{1}{R} \sqrt{\frac{y_s}{A}} \frac{U_{ic} + K_c U_{ID}}{U_{ref}} +$$

$$+ \frac{2-\delta}{\delta} \frac{\lambda_w}{\sqrt{y_s/A}} \left[\frac{U_{visc}}{U_{ref}} + \left(\frac{K_2}{K_1} - 1 \right) \frac{U_{ID}}{U_{ref}} \right] + nV \sqrt{\frac{y_s}{A}} \frac{U_{Vcorr} - \tau^* U_{ID}}{U_{ref}} \quad (\text{Ad.20})$$

The two expressions above differ because (Ad.19) uses a velocity gradient A calculated from inviscid theory, or measured at an equivalent "infinite" (i.e. very high) Reynolds number, whereas (Ad.20) is based on A_{exp} obtained from pressure measurements at the particular ("low") Reynolds number corresponding to y_s . The former method must therefore account for an undetermined change in A due to the displacement effect, whereas the latter has already taken this into account, but must also account for the changes in surface pressure gradient due to the centrifugal pressure rise and vorticity interaction effects.

Constant K_c (Ad.18) is a function of W and is tabulated below, as a supplement to Table III.

TABLE A1.1. Values of K_c .

N	K_c	
	$n=0$	$n=1$
1.0	0.9402	0.8166
0.75	0.7998	0.6927
0.5	0.6484	0.5601
0.25	0.4820	0.4160
0.1	0.3717	0.3216

The experimental comparison presented in Chapter IV. and Table IV. and carried out in Appendix H must also be revised in accordance with (A1.20). Values of K_c and $Q_{1D}(0)$ clearly indicate that the theoretical heat-transfer rate will be somewhat higher than the predictions presented in Table IV., thereby making the agreement between experiment and theory less favorable than implied by that Table.

Subscripts:

Corr corrected vorticity term due to induced pressure effect

References.

- A1) VanDyke, M.D. : "Higher Approximations in Boundary Layer Theory."
Lockheed Technical Report LLSJ-703097, Oct. 1960.
- A2) VanDyke, M.D. : "Second Order Boundary Layer Theory for Blunt
Bodies in Hypersonic Flow." ARS Preprint #1900-61, August 1961,
also Stanford University GUDASR Rep. No. 112, July 1961.
- A3) Laslen, S.H. : "Second Order Effects in Laminar Boundary Layers."
ARS Preprint #2208-61, October 1961, also Martin Research Report
RR. - 29, Feb. 1962.
- A4) Rott, N. : "On the Definition of the Displacement Effect in Second
Order Boundary Layer Theory." (To be published.)
- A5) Li, Ting Yi : "Effect of Free Stream Vorticity on the Behaviour of
Viscous boundary Layer on Blunt Body." Rensselaer Poly. Inst.
TR AE 6103, Feb. 1961.